LAPPEENRANTA UNIVERSITY OF TECHNOLOGY
Faculty of Technology
LUT Metal
Laboratory of welding technology and laser processing
Master's Thesis

*Taneli Pokkinen*

# SPECTROSCOPIC MONITORING DURING LASER WELDING OF ALUMINIUM ALLOY

Examiners: Professor Veli Kujanpää
Professor Michael F. Zäh

Supervisor: Dipl. Ing. (FH) Sonja Huber

## ABSTRACT

Lappeenranta University of Technology
Faculty of Technology
LUT Metal

Taneli Pokkinen

**Spectroscopic monitoring during laser welding of aluminium alloy**

Master's Thesis

2011

118 pages, 55 figures and 19 tables

Examiners: Professor Veli Kujanpää
Professor Michael F. Zäh

Keywords: laser welding, spectroscopy, spectrometer, monitoring, aluminium alloy, magnesium, emission, stability, repeatability, sensitivity

The mechanical properties of aluminium alloys are strongly influenced by the alloying elements and their concentration. In the case of aluminium alloy EN AW-6060 the main alloying elements are magnesium and silicon. The first goal of this thesis was to determine stability, repeatability and sensitivity as figures of merit of the in-situ melt identification technique. In this study the emissions from the laser welding process were monitored with a spectrometer. With the information produced by the spectrometer, quantitative analysis was conducted to determine the figures of merit. The quantitative analysis concentrated on magnesium and aluminium emissions and their relation. The results showed that the stability of absolute intensities was low, but the normalized magnesium emissions were quite stable. The repeatability of monitoring magnesium emissions was high (about 90 %). Sensitivity of the in-situ melt identification technique was also high. As small as 0.5 % change in magnesium content was detected by the spectrometer.

The second goal of this study was to determine the loss of mass during deep penetration laser welding. The amount of magnesium in the material was measured before and after laser welding to determine the loss of magnesium. This study was conducted for aluminium alloy with nominal magnesium content of 0-10 % and for standard material EN AW-6060 that was welded with filler wire AlMg5. It was found that while the magnesium concentration in the material changed, the loss of magnesium remained fairly even. Also by feeding filler wire, the behaviour was similar.

Thirdly, the reason why silicon had not been detected in the emission spectrum needed to be explained. Literature research showed that the amount of energy required for silicon to excite is considerably higher compared to magnesium. The energy input in the used welding process is insufficient to excite the silicon atoms.

**TIIVISTELMÄ**

Lappeenrannan teknillinen yliopisto
Teknillinen tiedekunta
LUT Metalli

Taneli Pokkinen

**Spektroskooppinen monitorointi alumiiniseoksen laserhitsauksessa**

Diplomityö

2011

118 sivua, 55 kuvaa ja 19 taulukkoa

Tarkastajat: Professori Veli Kujanpää
Professori Michael F. Zäh

Hakusanat: laser welding, spectroscopy, spectrometer, monitoring, aluminium alloy, magnesium, emission, stability, repeatability, sensitivity

Alumiiniseosten mekaaniset ominaisuudet määrittyvät hyvin pitkälti seosaineiden ja niiden pitoisuuksien mukaan. Alumiiniseoksen EN AW-6060 pääseosaineet ovat magnesium ja pii. Tämän diplomityön ensimmäinen tavoite oli selvittää hitsisulan prosessinaikaisen monitorointitekniikan kvantitatiiviset ansioluvut: stabiliteetti, toistettavuus sekä sensitiivisyys. Tässä tutkimuksessa laserhitsauksen aikana syntyviä emissioita monitoroitiin spektrometrillä. Spektrometrin tuottamalle informaatiolle suoritettiin kvantitatiivinen analyysi näiden ansiolukujen selvittämiseksi. Kvantitatiivinen analyysi keskittyi magnesiumin ja alumiinin emissioihin sekä näiden suhteeseen. Tutkimuksessa havaittiin, että absoluuttisten intensiteettien stabiliteetti oli heikko, mutta normalisoidut intensiteetit olivat melko stabiileja. Magnesiumin emissioiden monitoroinnin toistettavuus oli hyvä, jopa 90 %. Sensitiivisyys oli myös korkealla tasolla. Jopa 0,5 % muutos magnesiumpitoisuudessa pystyttiin havaitsemaan spektrometrillä.

Tutkimuksen toinen tavoite oli selvittää materiaalin menetys avaimenreikähitsauksen aikana. Materiaalin magnesiumpitoisuus mitattiin ennen ja jälkeen hitsauksen menetetyn magnesiumin selvittämiseksi. Tämä tutkimus toteutettiin alumiiniseoksilla, joissa oli nimellisesti 0-10 % magnesiumia sekä standardimateriaalilla EN AW-6060, jonka hitsauksessa käytettiin lisäainetta AlMg5. Tuloksista havaittiin, että magnesiumkato pysyi tasaisena riippumatta hitsin nimellisestä magnesiumpitoisuudesta. Lisäainelankaa syöttämällä päästiin hyvin samanlaisiin tuloksiin, kuin jo valmiiksi suurehkoja määriä magnesiumia sisältävää alumiinia hitsattaessa.

Kolmas tavoite tässä tutkimuksessa oli selvittää syy, miksi piitä ei ole kyetty havaitsemaan hitsauksessa syntyvästä emissiospektristä. Kirjallisuuskatsauksen perusteella voidaan todeta, että piin virittymiseen tarvittava energia on huomattavasti suurempi kuin magnesiumin, eikä laserhitsauksen energiantuonti kykene siis virittämään piiatomeja.

**ACKNOWLEDGEMENTS**

This thesis was written during summer 2010 in Munich at the laboratory of *iwb.* The last writings were finished in Lappeenranta during autumn 2010. During this time I was privileged to be able to work with many important and talented people studying and working at the Munich University of Technology. Also during my work, I've been supported by my family and friends to whom I'm eternally grateful. This thesis would not have been possible without the important and always helpful people around me. Here I would like to present my gratitude to some of my strongest supporters.

All the people at the laboratory of *iwb* have been so helpful and kind towards this Finnish student who was trying to manage with German language. All the students and researchers I've worked with at the laboratory have contributed to my work so much that my words here cannot justify the gratitude I owe them. Especially my supervisor Sonja Huber deserves a special acknowledgement. She had infinite patience and understanding and was always willing and able to help me in difficult situations. I would also like to present my gratitude to Professor Michael F. Zäh for his effort and work as the second examiner of my thesis.

I consider myself very privileged for having Professor Veli Kujanpää as the first examiner of my thesis. Our inspiring conversations and meaningful feedback are held in high esteem.

I would also like to present my sincere gratitude to all my friends in Munich and in Lappeenranta for their patience, support and friendship that have given me the much needed relaxation from the research.

Last, but not least, my deepest gratefulness lies with my family. I could not have done this without my parents, my sister and my dear Eeva.

In Lappeenranta 8.4.2011

Taneli Pokkinen

TABLE OF CONTENTS

SYMBOLS

| | |
|---|---|
| $a_{gap}$ | gap width |
| $A_f$ | area of the filler wire cross-section |
| $a_i$ | mass percentage of *i*:th element |
| $a_{ib}$ | absorption coefficient of inverse Bremsstrahlung |
| $A_{ki}$ | transition probability of energy level *i* |
| $a_{Mg}$ | Mg-content in the base material |
| $a_{Mie}$ | absorption coefficient of Mie-scattering |
| $a_{pi}$ | absorption coefficient of photoionization |
| $A_w$ | area of the weld cross-section |
| $b_{Mg}$ | Mg-content in the filler wire |
| *BPP* | Beam Parameter Product |
| *c* | speed of light |
| $C_{pl}\Delta T_l$ | heat required for a liquid metal to reach a temperature below the boiling temperature |
| $C_{ps}\Delta T_s$ | heat required for a solid metal to reach melting point |
| *D* | diameter of an unfocused beam. |
| $d_f$ | wire diameter |
| $E_n$ | energy level of the level *n* |
| $E_0$ | excitation energy of the lower level |
| $E_1$ | excitation energy of the upper level |
| *F* | superelevation (e.g. 20 % = 1.2) |
| $g_0$ | degeneracy of the lower level |
| $g_1$ | degeneracy of the upper level |
| *h* | the Planck constant |
| $H_f$ | latent heat of fusion |
| $I_{full}$ | intensity of the radiation before the vapour |
| $I_{nm}$ | measured intensities of minimum two energy levels *n* and *m* |
| *I(z)* | intensity of the radiation in the depth of *z* inside the vapour |
| $I_0$ | maximum intensity in the focal spot |
| *k* | the Botzmann constant |
| *K* | K-value to describe quality of a beam |

| | |
|---|---|
| $l_w$ | length of the weld |
| $M^2$ | $M^2$-value to describe quality of a beam |
| $N$ | total number of states |
| $n_0$ | population on the lower level |
| $n_1$ | population on the upper energy level |
| $N_0$ | number of neutral atoms |
| $N_1$ | number of ionized atoms |
| $N(T)$ | total density of neutral atom or ion |
| $q$ | energy needed to heat a solid material above melting point |
| $r$ | distance from the beam axis |
| $s$ | standard deviation |
| $T_e$ | electron temperature |
| $T_M$ | temperature of the vaporized metal |
| $t_w$ | welding time |
| $U(T)$ | partition function |
| $V_f$ | volume of the filler wire |
| $v_f$ | filler wire feeding rate |
| $V_i$ | volume of *i*:th element in one meter of the filler wire |
| $V_m$ | volume of the base material |
| $V_{var}$ | variability index |
| $v_w$ | welding speed |
| $V_w$ | volume of the weld |
| $V_1$ | ionization potential of the species |
| $w_0$ | radius of the beam in the focal spot |
| $w(z)$ | focus size at distance $z$ |
| $x_{Mg}$ | Mg-content in the weld |
| $\bar{x}$ | average of the data |
| $z$ | distance from the focal spot in direction of the beam axis |
| $z_R$ | Rayleigh length |
| $\Theta_{div}$ | divergence angle |
| $\lambda$ | wavelength |
| $\rho$ | density of the material |
| $\rho_i$ | density of *i*:th element |

| | |
|---|---|
| $\rho_{lin}$ | linear density of the filler wire |

# 1 INTRODUCTION

Laser technologies are developing continually and new processes are being studied worldwide. Not only in research facilities, but also in industry, new laser processes and machinery are introduced and integrated into existing production lines. The unceasing need for enhancing productivity has created new requirements for the process equipment. In manufacturing industry, laser technologies can offer many solutions for improving efficiency of the process. Latest discoveries in the field of laser processing have made it possible to process materials that were earlier difficult or even impossible to process. Also new processing techniques and invariably developing machinery have opened up doors to new previously unknown territories of laser processing. (Green, 2001) (Havrilla, 2009)

## 1.1 Problem

The increasing demand for higher quality combined with fast production lines can be a difficult situation. Offline quality inspection after each manufacturing phase requires time. And when the pace of production is fast only limited amount of time is at hand. Therefore, online monitoring of the manufacturing is required. In welding, however, monitoring can be problematic. In case of traditional metal arc welding the quality of the weld is determined after the welding process. The mechanical quality can be determined with non-destructive or destructive testing. Also ocular monitoring is utilized. In laser welding, however, the situation is more complicated. In automated production lines, where in many cases laser welding is utilized, there is no time for offline monitoring. Online monitoring of a welding process can be difficult to accomplish in any welding process. This problem is emphasized in laser welding, since the welding process is usually conducted in a welding cell, restricted for security reasons. Laser welding is a very delicate process, where the smallest changes in parameters have a strong impact on the quality of the weld. (Jäger et al., 2008) (Sibillano et al., 2009)

Aluminium alloys have properties that are greatly influenced by their alloying elements. For instance, the 6000-series of aluminium alloys have magnesium and silicon as main alloying components. These alloys have a tendency towards cracking, which can be

prevented by using filler material consisting of magnesium or silicon in higher composition. Both of these elements have a positive effect on the strength of the alloy by combining together and forming magnesium silicide ($Mg_2Si$). These elements tend to vaporize during laser welding, which can create problems. Welds are typically situated in a place where the structure has a discontinuity. These kinds of places have the highest stresses. Hence, it would be valuable to be able to determine the chemical composition and the possible loss of alloying elements in the weld already during welding. (Mathers, 2002)

## 1.2 Approach

At the laboratory of *iwb* (Institut für Werkzeugmaschinen und Betriebswissenschaften) a special monitoring system for in-situ melt identification (figure 1) has been developed and studied. The main component in this monitoring system is a spectrometer. The spectrometer monitors the welding process and observes the emissions occurring during keyhole welding. The data collected by the spectrometer is then transmitted to a computer that records the data to be analysed. The use of a spectrometer is justified by the high energy input that occurs during keyhole welding. The high amount of energy in a material generates certain physical phenomena including material vaporization, excitement of electrons and ionization of the vaporized material. The purpose of the spectrometer is to detect the emissions occurring as a result of these phenomena and to produce data for analysis. Already in previous researches different elements that are present in the metal vapour have been identified (Glasschröder, 2010).

In this thesis, the main issue of monitoring was to observe and detect changes in alloying compositions. This research was meant to be continuation to the study of Johannes Glasschröder (Glasschröder, 2010). In these previous researches the qualitative analysis was already conducted. Based on these results, the next step would be to find out the possible dependency between emissions and actual elemental composition in the weld. This information would not be useful without some figures of merit, such as stability, sensitivity and repeatability. In this research the quantitative analysis was conducted for aluminium and magnesium emissions to determine these figures of merit. It was observed in the research by Glasschröder that silicon emissions were not visible in the emission

spectra (Glasschröder, 2010). A theoretical research was to be conducted in this thesis to determine the reasons for the absence of silicon emissions.

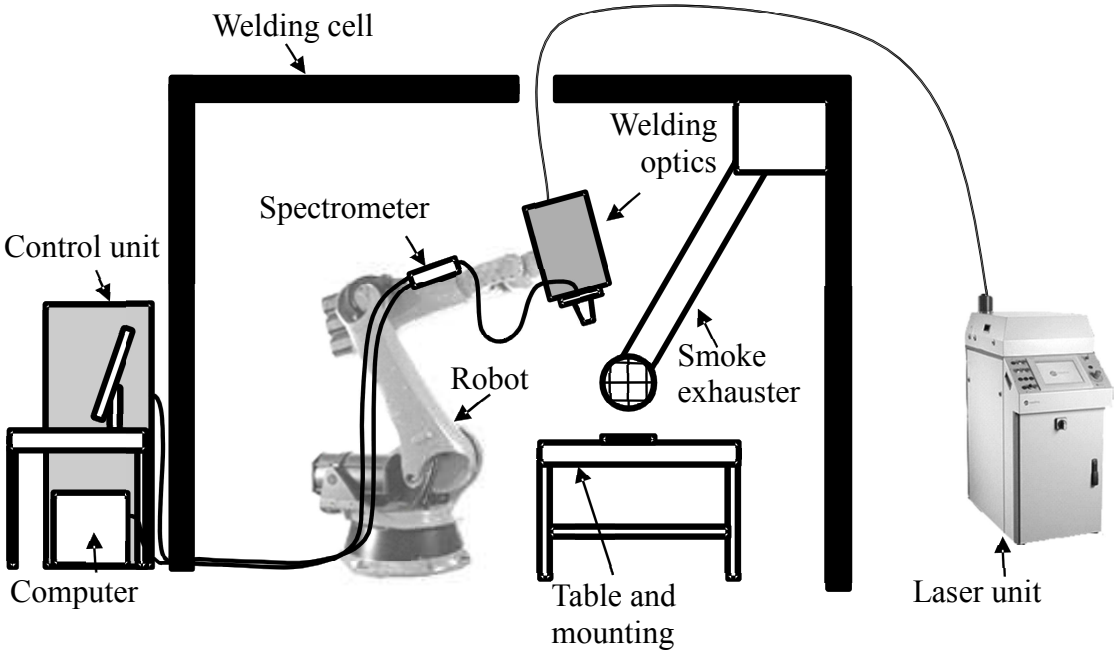


*Figure 1. In-situ melt identification system at the laboratory of iwb. (Glasschröder, 2010)*

## 1.3 Goal setting

The main theme of this Master's Thesis was to analyse emission spectra from laser welding process quantitatively. The basic principal of the quantitative analysis of the emission spectra is that the amount of a certain element and changes in this amount can be detected in the intensities of the emission spectrum. In all of the aspects of the practical studies in this research the analysing of the results was done in respect of magnesium, as it is one of the main and the most important alloying elements of the studied aluminium alloy. Quantitative analysis was done from the point of view of statistics. The goal was to find statistical support for the measuring system. The statistical attributes studied here were stability, sensitivity and repeatability.

Stability describes how reliable the gauge is during one measuring. To study stability of the emissions during one weld, all the detected intensities needed to be processed and analysed. So, in stability research all the emissions during a welding process needed to be

recorded and examined to determine the stability of magnesium emissions. To gain reliable results from the stability research, the magnesium emissions should be examined individually as absolute intensities and also in respect of aluminium intensities to minimize the changes in the intensities of the whole spectrum.

Sensitivity experiments needed to be executed to determine how sensitively the spectrometer detects changes in the chemical composition of the weld. Sensitivity experiments were to be conducted by feeding filler wire into the welding process and thus changing the amount of magnesium in the weld. These welds were monitored with a spectrometer and after welding, the welds were examined with a spark-emission spectrometer to define the actual amount of magnesium in the weld. This way also the loss of magnesium due vaporization could be determined.

Repeatability describes the ability of the gauge and the measuring system to produce identical results with an identical measuring setup. As in stability experiments, also in repeatability experiments the intensities were to be examined as absolute and normalized intensities.

As mentioned above, the loss of magnesium from the sensitivity experiments was to be determined. Previously, welding experiments with aluminium alloy with various contents of magnesium were made. These test pieces had nominal magnesium contents from zero to ten percent by mass. In these experiments no filler wire was used, so the loss of magnesium content could be simply calculated from the difference of the base material and the weld. One of the goals was to determine the loss of magnesium in these test pieces.

The third goal of this thesis was to clarify, with the support of literature research, the reason why there have been difficulties in detecting silicon from the emission spectra. Online monitoring of the welding process is useful if it can produce enough information about the important elemental contents. Silicon is one of the main alloying components in the aluminium alloy EN AW-6060 and the problems occurred formerly needed to be clarified.

# 2 THEORY

Laser processing in manufacturing industry is traditionally considered as an application of high productivity, quality and flexibility. Modern lasers can be used in various branches of manufacturing with an enormous range of materials. Sometimes laser can even be the only process possible. The most important processes are cutting, welding, micro processing, surface treatment, engraving, marking and drilling. All of these processes have certain characteristics in common: laser beam is focused to the processed material, the energy needed for the process comes from the energy of the laser beam and no tools are needed since the laser beam is the only "tool" necessary. The most commonly used processes in modern day industry are cutting, marking and welding. In the following chapters laser welding and its parameters and equipment are studied. (Kujanpää et al., 2005)

## 2.1 Laser welding

Welding is one of many different joining processes. The development of new technologies and productivity has increased the popularity of welding and made it the most used joining process in the modern day's industry. Within welding there are many concepts, but they all have one thing in common: joining energy comes from heat. Laser welding technologies use the purest form of heat energy. Laser beam is coherent electromagnetic radiation which is created in a resonator by exciting gas or solid material. The emitted radiation is then guided via optics and through focusing lenses to the welding process. In the material the laser beam is then absorbed and formed into heat energy melting and partly vaporizing the processed material. (Haferkamp, 2004)

The popularity of laser welding is based on its speed and quality. A coherent laser beam has an almost insignificant divergence angle which makes it possible to focus the beam into an extremely small focal spot. On the other hand welding from relatively long distances is also possible. The small focal spot compresses the energy of the beam into extremely high density, which allows deep welds and high welding speed. (Haferkamp, 2004)

The five main components that usually are found in laser welding systems are the following:

1. Main laser equipment consisting of a resonator, cooling system and shielding gas supply
2. Optics to guide the beam and to focus it on a work piece
3. Equipment to handle the work piece and to move the laser beam on the work piece (whether it is an equipment to move the beam or the work piece) and the process gas equipment
4. An operating system for guiding the whole process
5. Safety equipment to ensure safe processing (Haferkamp, 2004)

Similarly as in traditional gas metal arc welding (GMAW) also in laser welding heat produces certain zones in the work piece. As the laser beam melts the material, it solidifies almost immediately behind the beam. The speed is the metallurgic advantage of this process. Since the melting and solidification happens so quickly, the heat-affected-zone (HAZ) remains really narrow in comparison to GMAW.

### 2.1.1 Process and material parameters

Laser welding process is dependent on several parameters. Welding with wrongly set parameters can decrease the quality of the product. It is most important to understand the meaning and the significance each parameter have on the process. In the next chapters the main parameters for the research in this thesis are examined.

#### 2.1.1.1 Absorption properties of the material

Absorption is the most crucial parameter for laser welding. It determines which materials can be welded with the used laser welding equipment. It also defines other parameters such as focal spot and output power. Absorption describes the ability of a material to transform electromagnetic radiation of a certain wavelength and its energy into different kind of energy. In the case of laser welding materials transform the energy of the radiation into heat. In a perfect case, all of the energy would be absorbed, but in reality this does not happen. Instead, the incoming radiation is partly reflected from the surface of the material, absorbed in the material or goes through the material without interaction. In the case of

metals, the radiation going through the material is insignificant. Therefore, the incoming radiation can either reflect from the surface or be absorbed in the material. (Steen, 2003)

Figure 2 shows the complexity of absorption of different metals as a function of wavelength (µm). It is clearly visible, that with a traditional $CO_2$-laser, welding of some metals can be extremely difficult. For instance, Nd:YAG laser has a wavelength of one tenth of $CO_2$-laser's and a much higher absorption in aluminium.

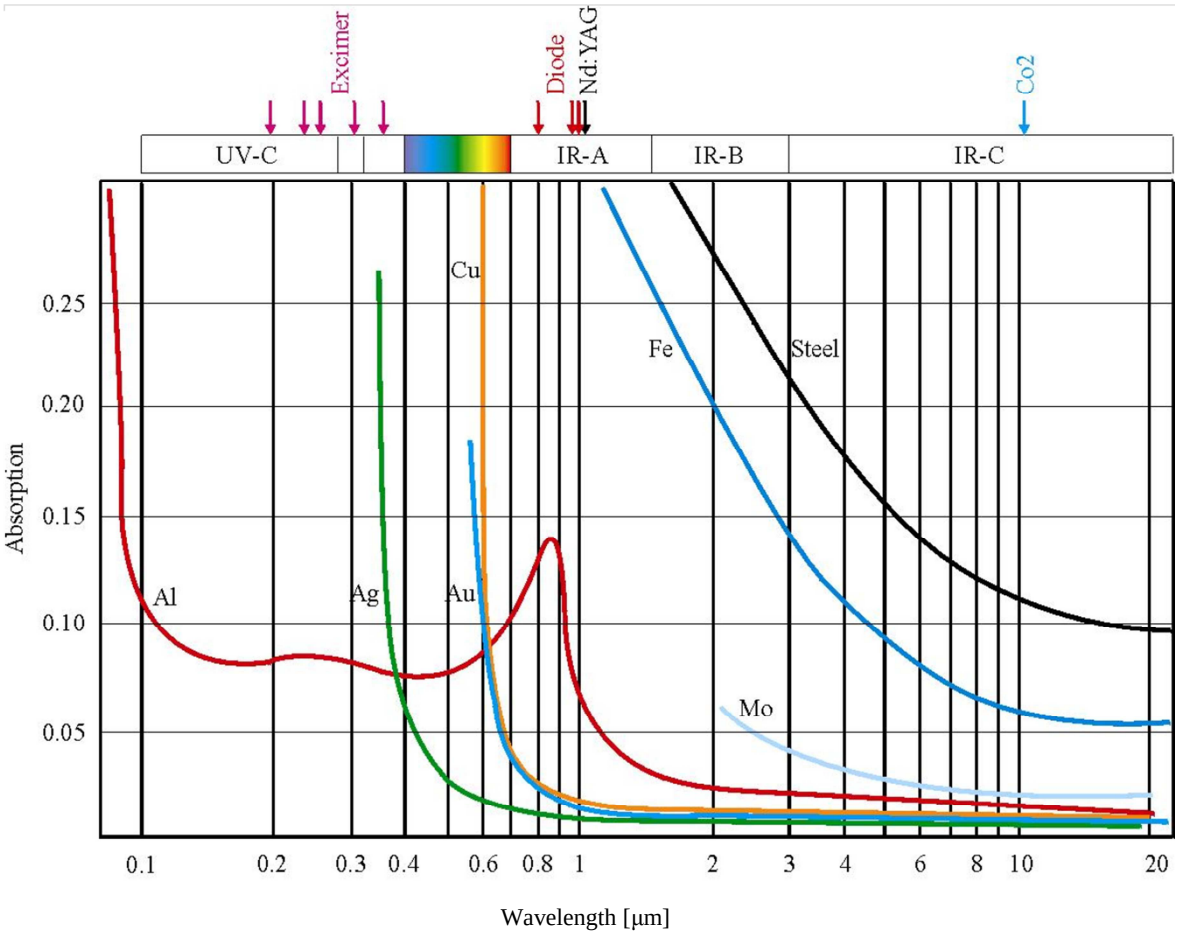


*Figure 2. Absorption coefficient at room temperature as a function of wavelength. (Kujanpää et al., 2005)*

In figure 2 it can also be seen that diode lasers are quite suitable for welding aluminium. The figure shows the three traditional wavelengths of diode lasers, which are achieved by different semiconductor materials. This enables the multiplicity of wavelengths. (Solarz, 2001)

The wavelength determines whether a laser beam is absorbed into material or not. But when the absorption is possible, temperature takes a more controlling role. For example, when normal carbon steel is heated with a $CO_2$-laser, its absorption is about 4 % in room temperature (see figure 2), but the absorption rate increases with temperature reaching 90 % in vaporizing temperature. (Mackwood & Crafer, 2004)

A laser beam is not directly heating up the metal in its full thickness, but in the beginning only from its surface. This absorption is called Fresnel Absorption. At low energy densities only melting occurs, but when the intensity of the beam increases metal starts to vaporize and ionize. This ionized metal vapour is absorbing more efficiently energy directly from the laser beam and thus rising the temperature. This reaction is called inverse Bremsstrahlung and it is always present in penetration welding. In inverse Bremsstrahlung the free electrons, which have come from the ionization of the metal vapour, are absorbing photons, thus increasing their kinetic energy. (Haferkamp, 2004) (Mackwood & Crafer, 2004)

#### 2.1.1.2 Laser beam

Depending on optical configuration of a resonator, intensity distribution of a beam gets a certain form. Also fibre optics after a resonator modifies intensity. Most optimal distribution is the Gaussian distribution, showed in figure 3. In this distribution there is only one intensity maximum, which maximizes the density of intensity and focusability. The number of intensity maximums determines the classification of the distribution according to $TEM_{xx}$-standardization system. For instance the ideal Gaussian distribution with only one circular intensity maximum peak is $TEM_{00}$. The lower index numbering obeys the system illustrated in figure 3. The first digit describes the number of radial zero fields and the second digit describes the number of angular zero fields.

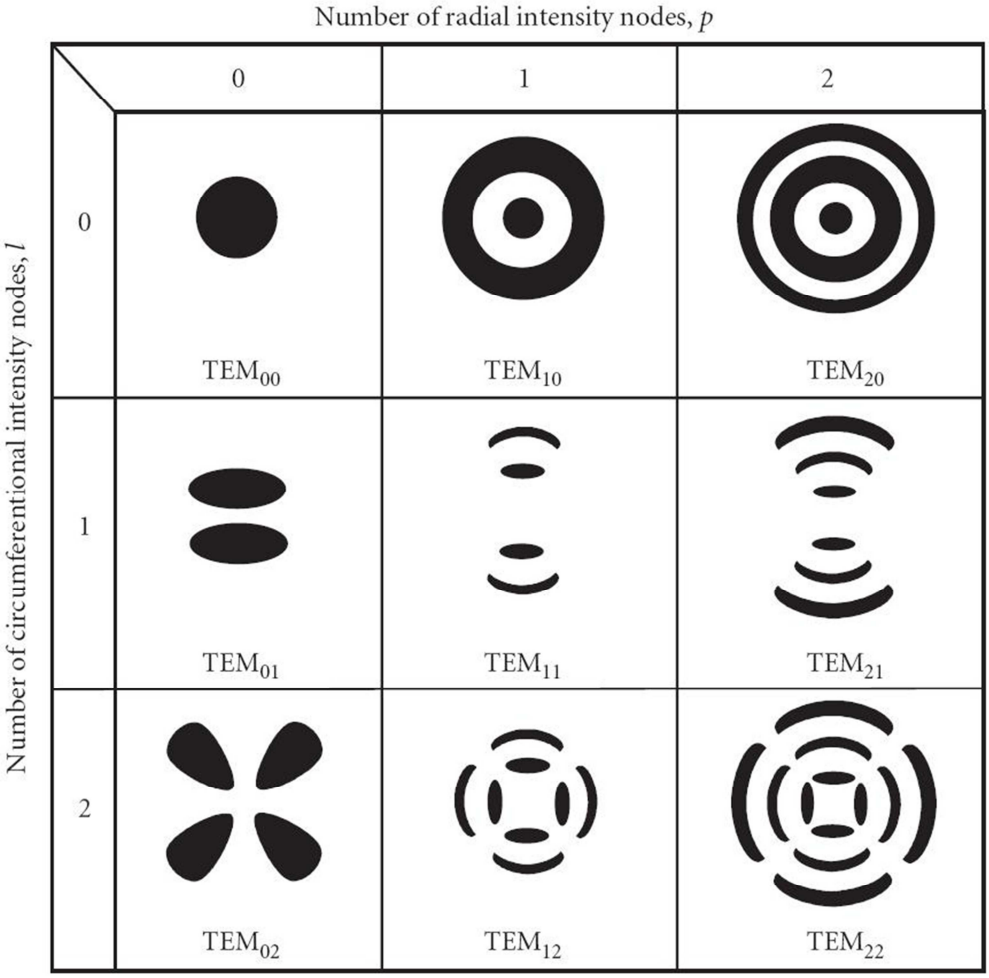


*Figure 3. Intensity distributions with circular optics. (Ion, 2005)*

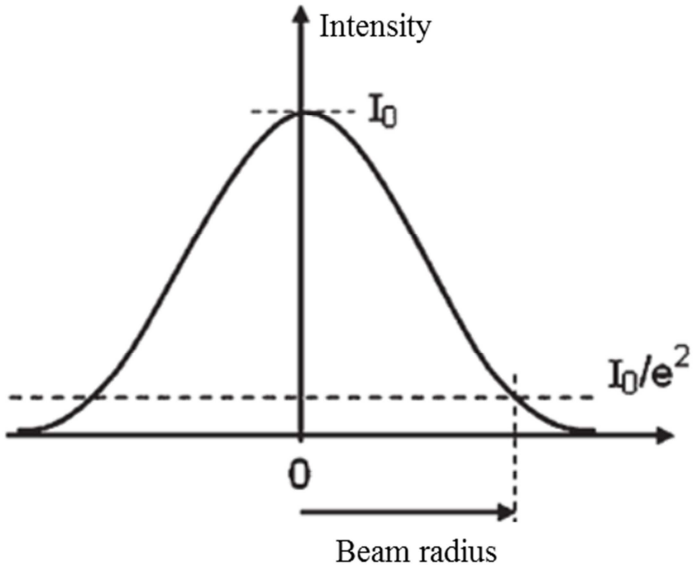


*Figure 4. Gaussian intensity distribution, where $1/e^2$ -part of intensity is illustrated. (Dahotre & Harimkar, 2008)*

Since a Gaussian curve closes asymptotically to the x-axis, to calculate intensities from a Gaussian-shape beam some trimming has to be done. Usually in intensity calculations the curve is trimmed at the point where 13.5 % of the intensity is left out. The point is at the height of $1/e^2$ from the x-axis, which means 0.135 in relative units. In figures 4 and 5 a Gaussian curve is illustrated

The most important variable when comparing different kinds of lasers is the beam quality. The quality of a beam is a product of optical parameters and laser system characteristics. The main variables in focusing a Gaussian type beam are divergence, Rayleigh length and focal spot diameter. Divergence defines the angle in which the beam diverges before and after the focal spot. Rayleigh length is the length in which the beam has diverged to a point where the beam cross section area is doubled (equation (1)). (Paschotta, 2010)

$$z_R = \frac{\pi w_0^2}{\lambda} \tag{1}$$

where

$z_R$ : Rayleigh length

$w_0$ : radius of the beam in the focal spot

$\lambda$ : wavelength.

The divergence angle and Rayleigh length define how the beam diverges, in other words, how long is the focal depth *b*. A long focal depth allows deeper welds and in laser cutting it allows deeper and straighter cuts. If Rayleigh length is long and divergence angle small, processing from long distances is also possible. This has been utilized in scanner technology, where fibre lasers with great beam qualities are used. The Rayleigh length and divergence angle $\Theta_{div}$ have dependence as shown in equation (2). (Kujanpää et al., 2005)

$$\Theta_{div} = 2\frac{w_0}{z_R} \quad , \tag{2}$$

where

$\Theta_{div}$ : divergence angle

Intensity of a laser beam along the waist of the focus can be calculated from the equation given in (3). (Paschotta, 2010)

$$I(r,z) = I_0 \cdot \left(\frac{w_0}{w(z)}\right)^2 \cdot e^{\left[-2\left(\frac{r}{w(z)}\right)^2\right]}, \tag{3}$$

where

$I_0$ : maximum intensity in the focal spot

$r$ : distance from the beam axis

$z$ : distance from the focal spot in direction of the beam axis

$w(z)$ : focus size at distance $z$.

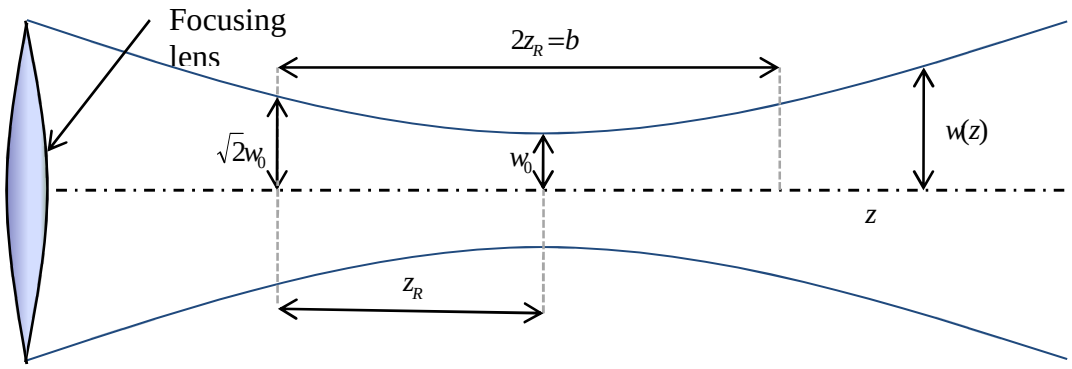


*Figure 5. A waist of a Gaussian beam as a function of axial distance, where b is the focal depth. (Pedrotti et al., 2007)*

To measure the quality of a laser beam, different terms have been developed. These terms are used with different lasers. *K*-value describes normally the quality of a $CO_2$-laser. Another term for $CO_2$-laser is $M^2$. These terms are defined in equations (4) and (5). (Ion, 2005)

$$K = \frac{4\lambda}{\pi\Theta_{div}D} \tag{4}$$

$$M^2 = \frac{\pi\Theta_{div}D}{4\lambda} = \frac{1}{K}, \tag{5}$$

where

$K$: K-value to describe quality of a beam

$M^2$ : $M^2$-value to describe quality of a beam

$D$ : diameter of an unfocused beam.

When optical fibre is used to deliver the laser beam from the resonator to the welding process, beam parameter product (BPP) is generally used unit to compare beam quality. BPP describes divergence and focus size of a beam, as shown in equation (6). (Ion, 2005)

$$BPP = D\frac{\Theta}{4}, \tag{6}$$

where

$BPP$: Beam Parameter Product

#### 2.1.1.3 Other parameters

Laser welding is a very sensitive process, which means that even the smallest changes in everything surrounding the process can have a tremendous effect on the result. Environment can be categorized as one of the process parameters according to Ion. Adjusting the pressure of the atmosphere around the welding process, the behaviour of a plasma plume can be influenced. At low pressures, the impact that plasma would have on the process can be minimized. At high pressures, plasma propagation is stronger and at extremely high pressures, simulation of underwater welding can be accomplished. Plasma propagation defines the density of the plasma. The denser the plasma, the more laser radiation is absorbed. (Ion, 2005)

The most common welding position in laser welding is flat position, since all the other parameters and influential phenomena are in this position easiest to control. If laser welding is done in all three dimensions, the position can naturally change during the process. The same problems of controlling weld pool when welding in overhead position may occur as they do in traditional arc welding. (Ion, 2005)

However, the most important auxiliary process parameter is process gas. The role of process gas is to protect the weld pool from impurities and oxidation, to blow the process plume away from the laser beam and to protect the focusing optics from spatters. Process gas is selected in respect to the processed material and welding technique. Especially for aluminium alloys, inert gas is essential to prevent oxidation of the weld pool. The choice for process gas in laser welding of aluminium is normally done between argon and helium.

When plasma formation needs to be efficiently prevented, the choice for process gas should be helium. Helium has a high first ionization potential, which makes it an ideal gas for removing plasma. Also the high heat conductivity brings positive effects to the welding process. On the other hand, argon is much less expensive choice especially in Europe. Also, the high density of argon enables lower flow rates than helium and more efficient process plume removal, therefore being more economical. When it comes to choosing the process gas according to the welding laser, argon is more suitable for the industrial solid state lasers, because of its transparency for short wavelengths, whereas helium suits better for $CO_2$-lasers. (Ion, 2005)

Other gases used in laser welding are nitrogen and carbon dioxide and mixtures of the previously mentioned. Nitrogen and carbon dioxide are, however, mostly used in welding of steels. Especially for structural steels, nitrogen has a positive impact on the microstructure. The advantage of $CO_2$ is the character of exothermic energy import via oxygen within the gas. This can bring efficiency to the process that is especially used in laser cutting. (Ion, 2005)

Strict groove tolerances in laser welding require also another parameter for the process. To maintain original setup during the whole welding process, fixturing of the work piece is needed. Especially during welding of long joints fixturing has to be taken care of to ensure a stationary groove and air gap. Another pre-process parameter is heat treatment. Especially for high-carbon steels pre-heating may be necessary to prevent cracking and excessive hardening or other unwanted changes in microstructure. (Ion, 2005)

### 2.1.2 Laser welding modes

#### 2.1.2.1 Conduction mode welding

The name of this welding technique comes from the heat conduction behaviour. The focused laser beam heats up the surface of the work piece and the heat is then conducted into the material. The principal difference between conduction mode welding and keyhole welding is that in the first case vaporization is insufficient to create a keyhole and the weld is not as deep as in keyhole welding. The weld is also wider, which reminds more of traditional arc welding. Since the penetration is so small, this process is generally used to weld thin materials. (Ready, 2001)

Conduction mode welding was traditionally the only technique possible, when welding steel or aluminium with diode laser. The power density needed to create a keyhole when welding metals is roughly $10^6$ W/cm$^2$, while traditional high power diode lasers (HPDL) reach a power density of only $10^5$ W/cm$^2$. This power is still adequate to heat the metal above melting point to start the melting process. The usage of diode lasers in welding aluminium is based on its wavelength. As shown in figure 2, diode lasers have great absorption on aluminium. Absorption can also, in addition to temperature and wavelength, be increased by polarization. This phenomenon is generally utilized in diode lasers, since they have a high degree of polarization, approximately 95 %. (Ehlers, 2001)

#### 2.1.2.2 Keyhole welding

The most defining geometrical difference between deep penetration welding, or keyhole welding, and conduction mode welding is the depth-width-relation of the weld. In conduction mode welding this relation is always under and in keyhole welding always above four to one (4:1) (Gnanamuthu, 2001). The focused laser beam heats the material first from the surface to a melting point and then heats up the liquid metal. A function that describes the energy needed to heat a solid metal above melting point is given in the equation (7). For instance, the energy needed for aluminium to reach the melting point is about 2.5 kJ/cm$^2$. (Gnanamuthu, 2001)

$$q = \rho V(C_{ps}\Delta T_s + H_f + C_{p1}\Delta T_1), \tag{7}$$

where

$q$: energy needed to heat a solid material above melting point

$\rho$ : density of the material

$V$ : volume of the material

$C_{ps}\Delta T_s$ : heat required for a solid metal to reach melting point

$H_f$ : latent heat of fusion

$C_{pl}\Delta T_l$ : heat required for a liquid metal to reach a temperature below the boiling temperature.

As mentioned before, absorption increases with temperature, which makes it possible to achieve a reaction where the work piece absorbs continuously more and more energy from the laser beam. When the molten metal reaches boiling point it starts to vaporize. At this point a keyhole phenomenon takes place. For aluminium the energy needed for the vaporization to take place is about 30 kJ/cm$^2$. The boiling temperature for aluminium is 2447 °C (Haferkamp, 2004). The recoil pressure of the vaporized metal forms the keyhole which is surrounded by liquid metal. As the laser beam moves inside the work piece, it melts more material in the front and the liquid then solidifies behind the beam and the metal vapour. A basic principal of keyhole welding is shown in figure 6. If the movement of the beam is too fast, welding is insufficient and the depth of the weld will not be complete. Same happens if the power of the laser is too low. On the other hand, if the power is too high or the welding speed is too slow, the weld can become too deep and have a negative effect on the heat affected zone. (Gnanamuthu, 2001)

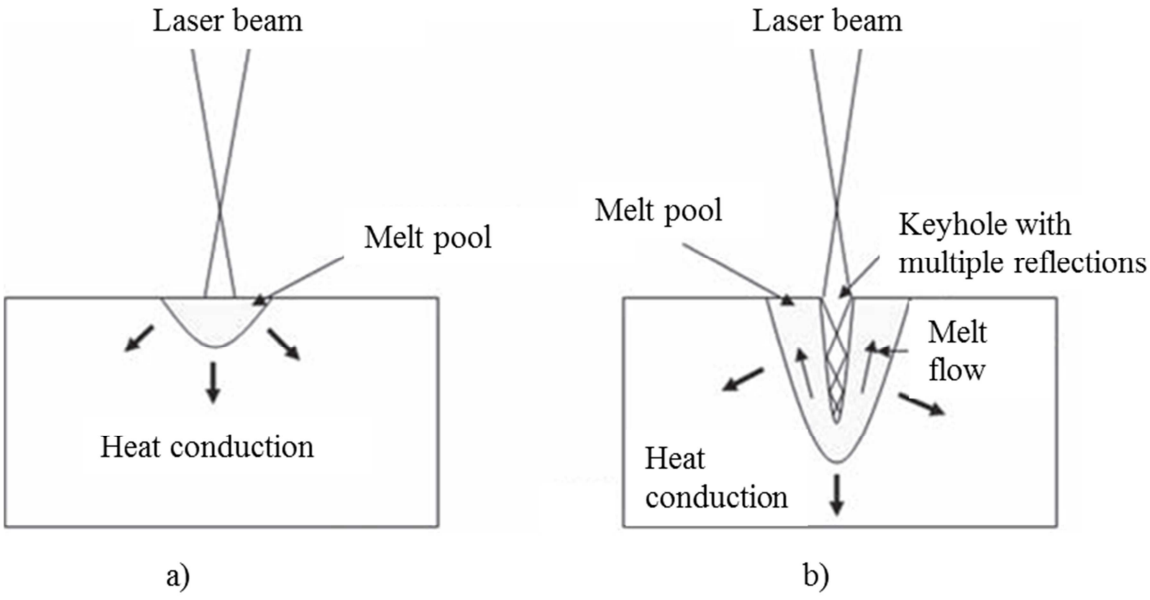


*Figure 6. Basic principle of conduction mode a) and deep penetration welding b). (Dahotre & Harimkar, 2008)*

If welding speed exceeds a limit value for the current process parameters, an unwanted phenomenon called "humping effect" can take place. This can be recognized when drops are forming behind the laser beam. This happens because of a too high welding speed and it creates pores or holes in the weld. During humping effect, the movement of the molten metal in the weld pool is not steady. In a normal case, the liquid metal moves smoothly

over the beam behind it, but in humping effect the currants of the liquid are disordered, which causes the formation of bubbles and drops. (Haferkamp, 2004)

The vaporized metal creates a capillary in the middle of the keyhole surrounded by liquid metal. The pressure of the vapour keeps the keyhole open. The absorption becomes extremely high within the keyhole as the laser beam is absorbed into the walls of the capillary and the reflections cannot escape, but the reflected beams are absorbed again as shown in figure 6. (Gnanamuthu, 2001)

The fluid dynamics have a major influence on the quality of keyhole welding. With stable flow of the molten metal and the keyhole the quality of the weld is high, but an unstable behaviour of the molten material can cause tremendous problems. One of the most difficult problems to prevent is the collapse of the keyhole. A collapsed keyhole causes macro-porosity and insufficient penetration in the weld (Zhai & DebRoy, 2003). As mentioned before, the keyhole is kept open and stable by the pressure of the vaporized metal vapour. If the welding parameters, such as laser power, are insufficient, vaporization is incomplete which results into imperfect keyhole and can cause collapse of the keyhole. The keyhole collapse phenomenon is more frequent in pulsed laser welding. The collapse is then caused by a sudden solidification of the molten metal. (Zhai & DebRoy, 2003) (Kaplan, 2009)

#### 2.1.2.3 Welding with filler wire

One problem with laser welding is that it has strict groove tolerances. If the gap is too wide, the laser beam can go through without any absorption in the work piece. If the laser welding equipment is configured with a filler wire feeding system, groove tolerances can be widened. When welding with a filler wire, the absorption is intensified by the filler wire. Filler wire increases the amount of molten material in the joint, which helps the laser beam to be absorbed in the material. This technique enables also welding of thick materials. Usually root pass is done with normal keyhole welding, and the next passes are done with feeding the filler wire to fill the groove. Figure 7 shows how feeding a filler wire affects the allowed gap width and sheet thickness. When in normal laser welding the gap width must be held as small as possible, feeding filler wire multiplies the permissible gap width. (Gebhardt, 2001)

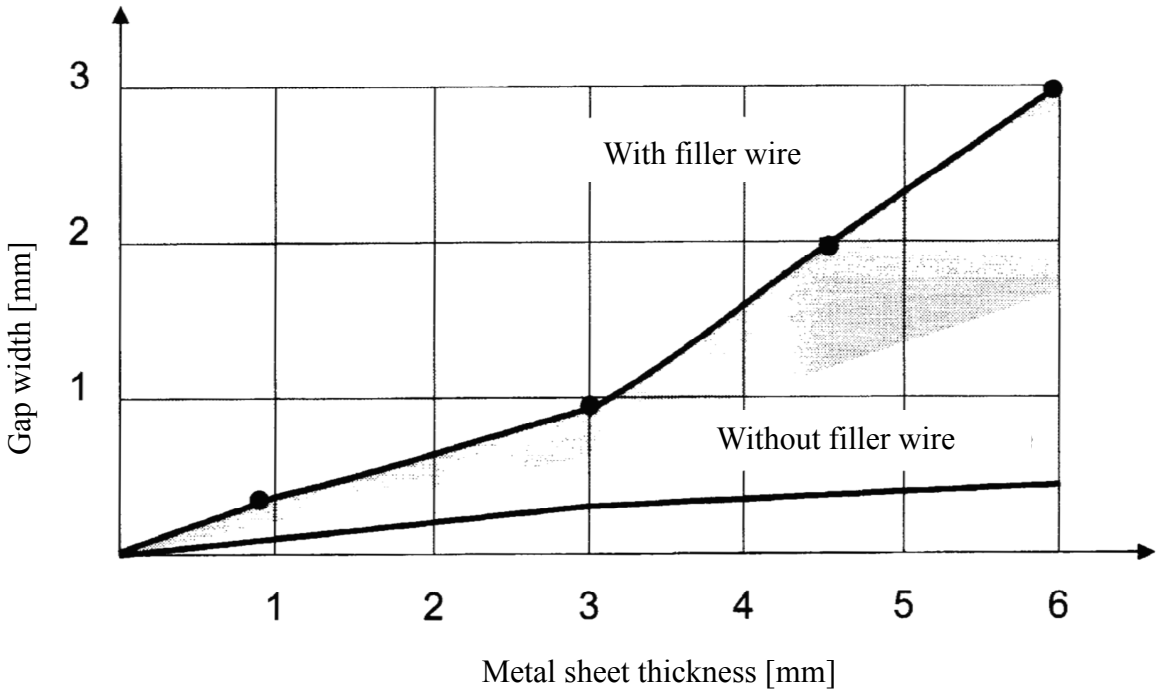


*Figure 7. The effect of filler wire on gap width and sheet thickness. (Gebhardt, 2001)*

The usage of filler wire has also other positive impacts on weld quality. Especially formation of cracks and pores during laser welding of aluminium can be significantly decreased. The vaporization phenomenon during laser welding can cause excess vaporization of important alloying elements. This can result in undesirable mechanical and metallurgical properties. By feeding filler wire consisting of these alloying elements, the loss can be compensated. It has also been observed that filler wire has a positive impact on the weld pool behaviour. The wire seems to calm the fast dynamics of the molten metal and thus contributes to stable and controlled solidification of the weld pool. (Gebhardt, 2001)

The utilization of filler wire does not come without problems. It brings several extra parameters to the process including wire speed, wire material, wire positioning, laser power and wire diameter. The most crucial of these to the process and quality is the positioning of the wire. If the wire is too far away from the beam, the wire melts with droplets, which can have an unwanted effect on quality. On the other hand, if the wire is fed too much under the beam, the filler material vaporizes from its upper surface and may

remain solid from its lower surface. In order to achieve best results, the wire must be fed in front or behind of the beam, but not more than 1 mm away from the centre of the beam, measured form the centreline of the wire. In this case the wire is melted and the molten filler material drops downwards and some of the wire material is vaporized. (Gebhardt, 2001)

The influence of the other parameters in welding with a filler wire should not be underestimated. The melting and vaporizing of the base material and the filler material demands more power from the laser, especially in the case of steel. On the other hand, in the case of aluminium, the need of extra power is not that dramatic, as shown in figure 8. The wire diameter and the wire speed determine the amount of filler material brought to the weld. This depends on the groove geometry. The wire speed can be calculated from a equation given in (8). (Gebhardt, 2001)

$$v_f = F \cdot \frac{v_w 4 s a_{gap}}{\pi d_f^2}, \tag{8}$$

where

$v_f$ : filler wire feeding rate

$F$ : superelevation (e.g.20 % = 1.2)

$v_w$ : welding speed

$s$ : material thickness

$a_{gap}$ : gap width

$d_f$ : wire diameter

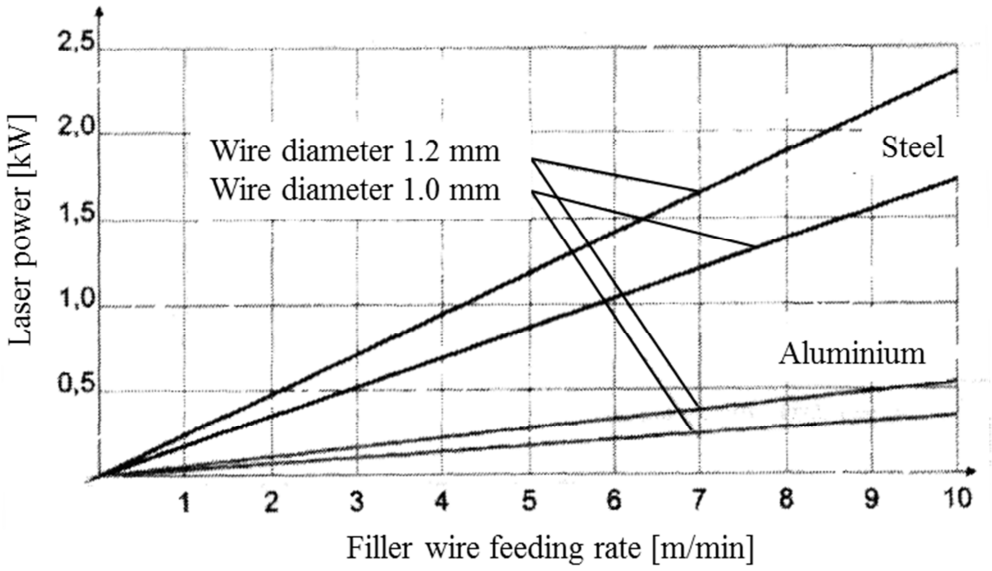


*Figure 8. The effect of laser power as a function of wire velocity. (Gebhardt, 2001)*

### 2.1.3 Laser welding of aluminum alloys

The main differences in laser welding of aluminium and steel are the absorption coefficients of aluminium and iron and the bigger heat conductivity and greater margin between melting and vaporization temperature of aluminium as shown in table 1. This means that in aluminium welding, there is more molten material and the HAZ is larger. With alloying elements, such as Mg and Zn, vaporization can be increased. (Trautmann, 2009)

*Table 1. Physical properties of aluminium (Al) and iron (Fe). (Trautmann, 2009)*

| Physical property | unit | Al | Fe |
|---|---|---|---|
| Specific heat capacity | $J\ K^{-1}\ cm^{-3}$ | 2.47 | 3.6 |
| Temperature of melting | °C | 660 | 1536 |
| Temperature of vaporization | °C | 2518 | 2859 |
| Conductivity of heat | $W\ J\ K^{-1}\ cm^{-3}$ | 2.7 | 0.4 |

Similarly to arc welding of aluminium, also in laser welding the generation of pores is a major problem. Different assumptions about the origin of these pores have been made. It has been shown in experiments that in keyhole welding, the process gas and the alloying

elements play a major role in generation of pores. Also the oxide layer on the surface of aluminium has an impact on this phenomenon. High heat conductivity of aluminium causes the keyhole to remain fairly narrow, and thus pressure of the vapour within high. This results into generation of pores, when the molten metal starts to solidify capturing some of the process gases within. As a solution to this problem, it has been suggested to widen the keyhole by augmenting the laser beam with some another process or dividing the already existing beam into two different beams, thus creating a longer keyhole. (Trautmann, 2009)

Different aluminium alloys have different properties when it comes to welding. Aluminium alloys are categorized by their main alloying element as shown in table 2. These alloying elements also determine the differences in weldability. Katayama showed in his research, that the alloying elements have specific properties in laser welding. The series of 5000 and 7000 contain magnesium and zinc. These elements increase the pressure of the vapour within the keyhole, which helps to keep the keyhole open and increase penetration. On the other hand series 1000 contains copper, whose high reflectivity and low pressure of vapour decrease penetration. High pressure of vapour is not only a good attribute. Katayama also showed the connection between vapour pressure and generation of pores. The alloys which contained zinc and magnesium had more pores than the other alloys, mainly because of their alloying elements. Shielding gas has also a significant impact on the generation of pores. Normally, welding of aluminium is done with argon as a shielding gas. Being an inert gas, argon has a great character in shielding the molten aluminium from oxidation. Katayama had great results by changing argon into nitrogen as a shielding gas. It is presumable that since nitrogen has a lower first excitation level it ionizes more easily than argon, thus mixing better with the vaporized and partly ionized aluminium. This way, the shielding gas is part of the vapour that keeps the keyhole open, and the whole system within the keyhole behaves as one. Therefore it is possible to gain almost poreless welds by using nitrogen as a shielding gas. (Katayama et al., 2009)

*Table 2. The classification of aluminium alloys. (Ion, 2005)*

| Alloy | Alloying element |
|---|---|
| 1xxx | "pure" aluminium (min 99 %) |
| 2xxx | Copper (Cu) |
| 3xxx | Manganese (Mn) |
| 4xxx | Silicon (Si) |
| 5xxx | Magnesium (Mg) |
| 6xxx | Magnesium and silicon |
| 7xxx | Zinc (Zn) |
| 8xxx | Others |

## 2.2 Process emissions during laser welding

The basic character of laser welding consists of high temperatures and melting and vaporizing of material. With these properties come also various emissions. The emissions can be categorized into two groups: reflection from primary radiation and secondary emissions. The first mentioned are mostly reflected radiation of the laser beam. Also refraction and scattering of a beam from a plasma plume or metal vapour can be detected by the observation sensor. For instance, steel has great reflectivity on $CO_2$-laser in room temperature, as shown in figure 9, but as the laser intensity is increased, absorption increases. The deep slope in reflectivity is a result from vaporization and plasma generation. (Dietrich, 2009) (Beyer, 1985)

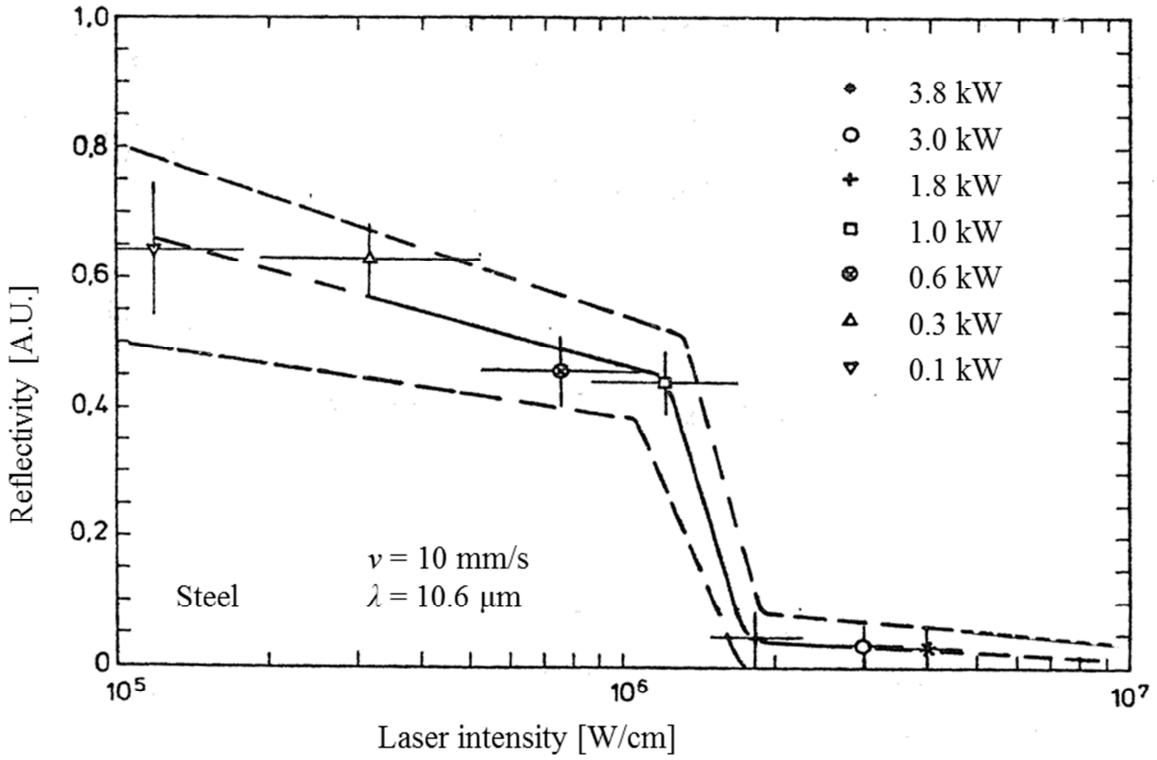


*Figure 9. Reflectivity of steel on $CO_2$-laser as a function of laser intensity. (Beyer, 1985)*

Secondary emissions can be divided further into two groups: heat radiation from the weld pool and emissions from the vaporized material. The laser beam heats the work piece above evaporating point. The absorbed laser beam increases heat in the work piece, which results into heat radiation. Heat input in laser welding is sufficient for the material to evaporate. Temperature is so high at this stage of the process that some atoms in the metal vapour becomes ionized and excited. This results in specific emissions at the fundamental wavelength of these excited atoms. This kind of metal vapour can be found inside the keyhole as well as above the keyhole. In this research the focus is in the emissions from the metal vapour. (Dietrich, 2009)

### 2.2.1 Metal vapour and its properties

In the case of properties of the vaporized metal, it is needed to create a division between $CO_2$ laser welding and laser welding with a solid state resonator lasers. It has been noticed in spectroscopic studies that the temperature of the plume generated above the keyhole is much lower when welding with solid state lasers (above 2000 K) than in the case of $CO_2$ laser welding (7000 - 11000 K). Also the degree of ionization is therefore considerably

lower with solid state lasers. This concludes to a statement that when welding with solid state lasers, no plasma is generated, only excited metal vapour. The recent research conducted by Glasschröder (Glasschröder, 2010) supports this statement. He discovered in his studies that in the emission spectrum no emissions from ionized atoms were found, only the emissions from excited neutral atoms. Although $CO_2$ welding is not of concern in this research, the properties of plasma are also presented and discussed in the following chapters. It is necessary to understand the nature of the metal vapour as well as the plasma to achieve better results in laser welding and monitoring the process. (Greses et al., 2001)

During keyhole welding some vaporization of the welded material occurs. And because of the absorption behaviour in high temperatures, some of the atoms in the metal vapour become ionized. This ionized metal vapour is called plasma. The vaporization begins already from the walls of the keyhole. Because of the low density of the vapour, it starts to rise upwards. The ionization begins already before the vapour reaches the surface of the work piece. When the plasma is inside the keyhole it has mainly positive effects on the welding process by absorbing more efficiently. Also the metal vapour has already quite high pressure and density which helps to keep the keyhole open. But once it rises above the surface, the negative properties become evident. Especially in $CO_2$-welding, the absorption of the plasma can reach 100 %. The density of plasma, being different than of air, can also cause problems. If not blown away by the process gas, the plasma plume can behave as a lens, refracting and refocusing the laser beam away from the intended focal spot. (Skupin, 2004) (Beyer, 1985)

Plasma is defined as a system, which consists of multiple particles, some of which have an electrical charge. It gets its energy from an external source of energy and its properties are strongly influenced by the interaction with the source of energy and its internal particles. The plasma in laser welding consists of the vaporized metal atoms, ionized atoms and free electrons. (Schittenhelm, 2000)

The emission spectrum of the metal vapour formed during laser welding is a result of changes in energy levels of the electrons. To analyse the spectrum, the excitations of the electrons need to be evaluated. Boltzmann equation (9) describes the relation of a number of electrons at two excitation levels in local thermodynamic equilibrium (LTE). The

equation presumes that the number of electrons on a certain energy level obeys the Boltzmann distribution. (Galmed & Harith, 2008)

$$\frac{n_1}{n_0} = \frac{g_1}{g_0} e^{\frac{-(E_1 - E_0)}{kT}}, \tag{9}$$

where

$n_1$ : population on the upper energy level

$n_0$ : population on the lower level

$g_1$ : degeneracy of the upper level

$g_0$ : degeneracy of the lower level

$E_1$ : excitation energy of the upper level

$E_0$ : excitation energy of the lower level

$k$ : the Botzmann constant

$T$ : temperature

Steen (Steen, 2003) presents a reformulation (equation (10)) from the Saha-equation first presented by Cobine (Cobine, 1941). The equation describes how plasma is absorbing radiation as a function of free electron density.

$$\ln\left(\frac{N_1}{N_0}\right)^2 = -5040\left[\frac{V_1}{T}\right] + 1.5\ln(T + 15.385), \tag{10}$$

where

$N_1$ : number of ionized atoms

$N_0$ : number of neutral atoms

$V_1$ : ionization potential of the species

The density of free electrons within metal vapour defines the absorption rate and the ionization level as a function of temperature. As shown in figure 10, the ionization level increases with temperature, thus increasing absorption by the plasma. (Steen, 2003)

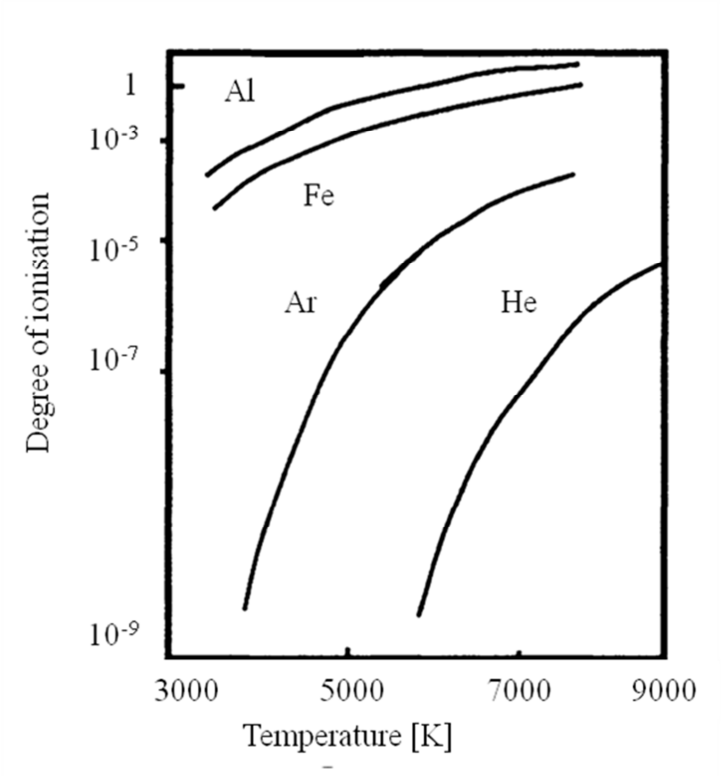


*Figure 10. The degree of ionization for different elements as a function of temperature. (Steen, 2003)*

In case of Nd:YAG laser ablation, the wavelength enables the absorption and photoionization to increase exponentially. This results in an increased production of plasma. According to Schittenhelm, this phenomenon occurs already at the beginning of the process (Schittenhelm, 2000). Although plasma plume has been proved to be almost transparent to the wavelength of an Nd:YAG laser, the intensity of the laser still decreases. This is because of the scattering effect of the plume. So if the beam of an Nd:YAG laser is not absorbed completely into the plasma plume, it still loses some of its intensity. (Trautmann, 2009)

Lambert-Beer law (equation (11)) defines the reduced intensity of radiation which propagates through plasma. The law presents that the intensity decreases exponentially as a function of different absorption coefficients of different phenomena. (Schittenhelm, 2000)

$$I(z) = I_{full} e^{-(\sum a_j)z}, \tag{11}$$

with

$$\sum a_j = a_{Mie} + a_{ib} + a_{pi} + \ldots, \tag{12}$$

with

$I(z)$ : intensity of the radiation in the depth of $z$ inside the vapour

$I_{full}$ : intensity of the radiation before the vapour

$a_{Mie}$ : absorption coefficient of Mie-scattering

$a_{ib}$ : absorption coefficient of inverse Bremsstrahlung

$a_{pi}$ : absorption coefficient of photoionization

As mentioned before, the inverse Bremsstrahlung is a vital phenomenon in deep penetration welding. Mie-scattering is a method for describing how electromagnetic radiation scatters from spherical particles which have diameters in the same scale as the wavelength of the incoming radiation. The main difference to Rayleigh-scattering is that in Rayleigh-scattering the particles are much smaller than the wavelength of the radiation. Also the scattering process is different. In this case a photon interacts with a particle only once and thus getting absorbed into the metal vapour. Photoionization happens when a photon comes to an atom with a certain speed and with its kinetic energy detaches an electron. The free electron now has the energy of the photon minus the binding energy. The photon does not have to excite the electron to an upper energy level, but it can anyway be absorbed. As a result of photoionization the metal vapour has more free electrons, which makes the vapour more absorptive to the laser beam. (Schittenhelm, 2000)

### 2.2.2 Diagnostic methods

Visual monitoring in laser welding can be divided in three categories according to which part of the welding process is monitored. Monitoring can be done before the actual welding process. This kind of pre-process monitoring is normally seam tracking. With the information from a seam tracking system, accurate positioning of the laser beam can be adjusted. If the monitoring is done after the laser beam, it is called post-process monitoring. In this case, the quality of the weld is evaluated and analysed. The irregularities on the surface of the weld are detected and the process parameters changed to improve the quality of the weld. The third method of monitoring is the so-called in-process

monitoring. This is also the method that is used in this research. Here the main concern is in the actual welding process and the phenomena that occur during laser welding, such as emissions from the metal vapour. (Precitec Group, 2011)

According to Dietrich (Dietrich, 2009), the sensors used in measuring process emissions can be categorized into three different types, depending on the distance from which the measurement is done. In his thesis Dietrich clarifies how the measurement equipment has to be chosen in respect to what kind of equipment and machinery is used. Especially for $CO_2$-lasers the best design would be a fibre-based measurement system. This kind of technique is also the best when measuring from short distances, as is the situation in this research. The detecting unit can be fixed to the welding head or as a separate apparatus. For medium measurement distances and for solid state lasers a sensor that is integrated to the optics is the most suitable choice. In this case it is essential that the laser focusing has a constant focal length, since this measuring equipment detects the reflecting emissions through the focusing optics. For longer measurement lengths, which can reach above one meter, the best choice would be to use on-axis sensors with long monitoring distances. This technique is especially developed for modern remote processing machinery as an adaptive on-axis measurement technology. (Dietrich, 2009)

There are multiple methods for monitoring optical emissions from a laser welding process. Some techniques monitor the intensity of the emissions from the plasma without separating the wavelengths. This way imaginary from a "good welding process" can be compared to the one at hand and thus change the process parameters to gain better quality for the welding. Some monitoring techniques concentrate on a certain area of wavelengths, such as infrared (IR), visible light (VIS) or ultra-violet radiation (UV). Infrared emissions can be analysed to evaluate the geometry of the weld pool. Visible light and ultra-violet radiations reveal more accurate information from the metal vapour. In this case spectroscopic study could be applied to gain information about intensities of some certain emission lines or presence of some particular element. This kind of analysis was adapted also for this research. (Sibillano et al., 2009)

### 2.2.3 Laser-induced breakdown spectroscopy

The analysing of laser induced metal vapour is a major research subject in this thesis. Methods used for this analysis are similar to LIBS (laser-induced breakdown spectroscopy). In LIBS technique a pulsed, high intensity laser beam is focused onto an examined work piece to produce a plasma plume. Plasma consists of the ionized vapour from the work piece and of the process gases. The basis of this experiment is to analyse the properties of the plasma by detecting the emissions of the excited atoms. Collecting of the data is done by visually recording the emissions. This data is then analysed. As a result of this experiment a spectrum of emitted radiation is formed. (Cremers & Radziemski, 2006)

The two main courses of analysing the results from LIBS are qualitative and quantitative spectral analysis. The idea of qualitative analysis is to detect certain lines in the spectrum to identify the elements in the examined test piece. In quantitative analysis the emission lines of the detected elements are more closely examined. The goal of this analysis is to find out the quantities of different elements in the test piece. If LIBS is adapted for laser welding the aim of this examination could be to find out the loss of elements or material during welding process, the amount of impurities or alloying elements, or investigate which elements take part in metal vapour phenomenon. (Cremers & Radziemski, 2006)

To gain information about the quantities of different elements, the intensity lines for these elements have to be precisely measured from the spectrum. In LIBS analysis a calibration curve for each studied element is formed. This is done by vaporizing and ionizing a sample piece that has a known amount of that element. Then from the spectra, the areas under the peaks of that element are calculated to get the quantities. These percentual quantities are then plotted as a function of intensity to create a calibration curve. Then the intensities of the test piece are set against the calibration curve to determine the amount in the examined work piece. (Cremers & Radziemski, 2006)

Problems can also occur when obtaining the intensities from the spectrum. One of the most important interferences is the so called chemical matrix effect. The examined work piece usually consists of several elements in varying compositions. All of these elements are theoretically detectable in the spectrum (depending on the resolution and sensitivity of the measurement equipment and also on the excitation energy for the element) and their

intensities can be so strong that they can make the calibration of the detecting software quite difficult. Since the calibration is done by adjusting the integration time of the collimator in respect to the strongest intensities in the spectrum, smallest intensities can be difficult to detect. (Ohnesorge, 2008)

The principal of defining relations between temperatures, energy levels and emitted intensities can be represented by Maxwell-Boltzmann equation (13). This method can be adapted to evaluate the properties of the vaporized metal in local thermodynamic equilibrium (LTE). (Skupin, 2004)

$$I_{nm} \propto const_{nm} e^{-E_n/(kT_M)}, \tag{13}$$

where

$I_{nm}$ : measured intensities of minimum two energy levels *n* and *m*

$E_n$ : energy of the level *n*

$T_M$ : temperature of the vaporized metal

From a well printed spectrum also the temperature of plasma can be calculated. Boltzmann distribution describes the population density and the states of electrons in local thermodynamic equilibrium (LTE). Applying the Boltzmann equation in a manner shown in equation (14), requires accurate measurement results of the intensities and wavelengths of the spectral lines. (Mohamed, 2007)

$$I = \frac{hc}{4\pi\lambda} N(T) \frac{A_{ki} g_1}{U(T)} \exp\left(-\frac{E_1}{kT}\right), \tag{14}$$

where

$A_{ki}$ : transition probability of energy level *i*

*U(T)* : partition function

*N(T)* : total density of neutral atom or ion

This equation can be reformulated as (15) for plotting a straight line to obtain the electron temperature: (Sibillano et al., 2009)

$$\ln \frac{I\lambda}{A_{ki} g_1} = -\frac{E_1}{kT_e} + \ln\left[\frac{Nhc}{U(T)}\right], \tag{15}$$

where

$T_e$: electron temperature

$N$ : total number of states.

$h$ : the Planck constant

$c$ : speed of light

To resolve the electron temperature from two emission lines with intensities $I_1$ and $I_2$, equation (16) can be applied. This is called the two line method. (Sibillano et al., 2009)

$$\frac{I_1}{I_2} = \frac{A_{k1} g_1 \lambda_2}{A_{k2} g_2 \lambda_1} \exp\left[-\frac{E_1 - E_2}{kT_e}\right] \tag{16}$$

and from equation (17) resolving $T_e$: (Sibillano et al., 2009)

$$T_e = \frac{E_1 - E_2}{\left[\frac{I_1 A_{k2} g_2 \lambda_1}{I_2 A_{k1} g_1 \lambda_2}\right]} \tag{17}$$

## 2.3 Lasers for welding

In the following chapters principles of Nd:YAG laser and diode laser are shown. These kind of lasers were used in this research. Also many other lasers are used in welding applications. Traditionally, the best welding lasers for steel were $CO_2$-lasers. However, within the last two decades, other lasers have also come to markets. Light pumped Nd:YAG lasers made the first breakthrough especially in welding of aluminium alloys, but also in laser welding of steel. Another variables of Nd:YAG lasers have launched to markets to increase the efficiency of a resonator. In these resonators the low efficiency pumping method has been replaced by diodes. The laser is called diode pumped slab-laser, where the laser beams from diodes are guided through a lasing rod via total reflection. As a

result, the rod emits coherent and parallel radiation, with a higher efficiency (about 10-15 %). (Steen, 2003)

Recently, new lasers that utilize fibre optics have come to markets. Fibre lasers and disk lasers are excited by diode lasers and they emit high quality laser beam. In fibre lasers the lasing medium is normally ytterbium and in disk lasers the medium is the same material as in Nd:YAG laser. Output power produced by a fibre laser can be up to 30 kW. In the case of disk lasers, the output power is currently about 12 kW. (Black & Copley, 2010)

### 2.3.1 Nd:YAG laser

When traditional laser welding is done with a $CO_2$-laser, the laser beam is formed in a resonator consisting of $CO_2$-gas. So in this case the laser medium is a gas. In Nd:YAG laser, the resonator is quite different: the laser medium is a solid rod. In a classic case, the rod, which consists of neodymium ($Nd_3^+$-ions) and yttrium-aluminium-pi-oxide ($Y_3Al_5(SiO_2)_6$), is positioned within the resonator as a common axis for two elliptical cylinders and as the individual axes are pumping lamps, as shown in figure 11. (Kujanpää et al., 2005)

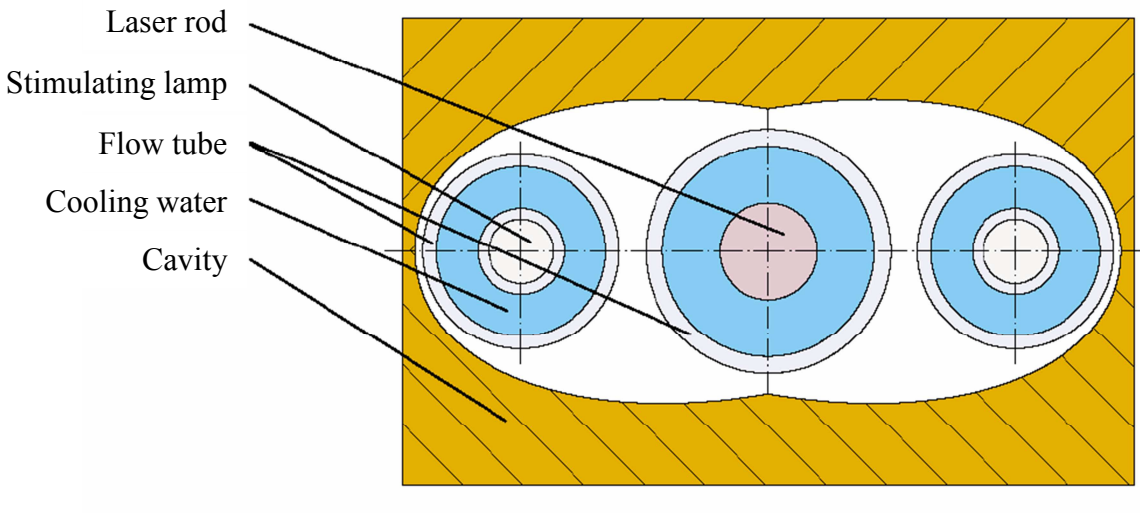


*Figure 11. Cross-section of a traditional Nd:YAG resonator. (Kujanpää et al., 2005)*

An Nd:YAG laser is a solid-state laser that emits radiation with a wavelength of 1064 nm. The laser medium in this kind of laser is neodymium, whose atoms are excited to upper

energy levels. When they return to ground level, they emit photons as coherent and parallel radiation. Most of the exciting energy transforms into heat, which makes cooling extremely important. Because of this energy waste, the coefficient efficiency is only 2-3 %. To raise the power of a laser, resonators can be coupled in series or in parallel. The major advantage of Nd:YAG laser is its wavelength. The radiation of this wavelength is not absorbed into glass, but goes straight through it. This makes it possible to guide the laser beam within an optical fibre almost lossless in comparison to the $CO_2$-lasers. (Kujanpää et al., 2005)

Figure 12 shows the basic principle of the lasing process in case of Nd:YAG laser. Pumping energy is needed to excite the electrons of neodymium atoms to higher energy levels. Electrons return then to a ground level via middle levels. The first shift happens spontaneously and without emissions, but the second shift of energy levels emits a photon with a wavelength of 1064 nm. This phenomenon is called lasing, since it is not a spontaneous emission, but a result of stimulation. (Kujanpää et al., 2005)

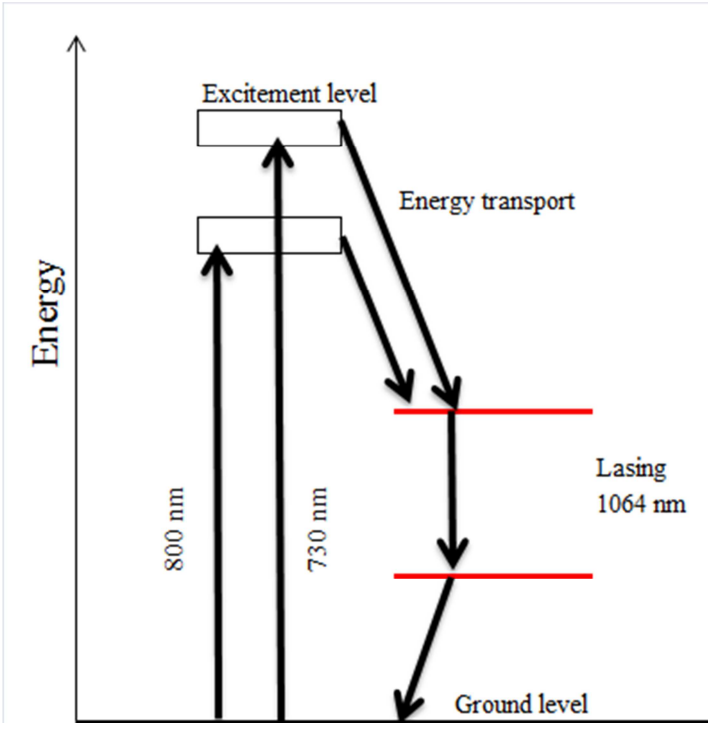


*Figure 12. The lasing of Nd:YAG laser. (Kujanpää et al., 2005)*

### 2.3.2 HPDL (High-Power Diode Laser)

A common problem for both $CO_2$- and Nd:YAG lasers are their size and inefficiency. For example, theoretical maximum efficiency of a $CO_2$-laser is about 21 %, but in practice

modern day $CO_2$-lasers reach an electrical efficiency of 10-15 % (Kujanpää et al., 2005). Traditional light pumped Nd:YAG lasers have an efficiency of about 2-3 % (Ion, 2005). On the other hand, modern day diode lasers can reach an electrical efficiency of about 40 % (Laserline, 2010). Also a need for frequent service (lifetime for Nd:YAG laser's pumping lamps is only a few hundred hours), brings unwanted costs. Development of semiconductor technology has raised diode lasers to a whole new power level. With these new high-power diode lasers power intensity ranges from $10^4$ to $10^6$ W/cm$^2$. This also enables welding of steels and aluminium alloys. (Ullmann & Eltze, 2001)

In diode lasers the laser beam is generated in a semiconductor by excitement of electric current. This semiconductor is inside a diode, which is very small, usually about 0.6 mm. These diodes are then bunched together to form a diode bar. Laser beam is emitted as a band that has two axes: the slow axis is in the direction of the bar's width and the fast axis is in the direction opposite to the width of the bar. This bar is soldered with a collective lens to a cooling plate. The lens is situated immediately after the diodes to collect the emitted laser beam. The bars are combined to create a stack, and from these stacks the final laser is built. (Kujanpää et al., 2005)

Usually the wavelength in diode lasers used in metal welding is between 770 - 1000 nm (Solarz, 2001). The focal spot has normally a rectangular geometry. Although fairly high power densities are achievable, relatively low beam quality is an obstacle for diode lasers to perform keyhole welding. Nevertheless, these low-power diode lasers are in their element in conduction mode welding and surface treatment of metals, as well as in the welding of plastics. The company Laserline GmbH has brought new diode lasers to the markets. These high-power diode lasers use four wavelengths (915 nm, 949 nm, 980 nm and 1030 nm) and their output power reach 10 kW (Laserline, 2010). With these lasers, regardless of the relatively poor quality of the laser beam, also keyhole welding of steels and aluminium alloys is possible. Diode lasers have a sparse service frequency, since the lifetime of diodes is several tens of thousands hours. Also their notable efficiency lowers energy costs. The actual hardware for a diode laser is relatively small and light compared to Nd:YAG or $CO_2$ laser. (Ullmann & Eltze, 2001)

### 2.3.3 Bifocal hybrid laser beam welding (BHLW)

All hybrid welding technologies combine two processes. In bifocal hybrid laser beam welding two laser processes are combined. This term doesn't determine the two individual processes, but usually the principle is to combine two different processes. This can be done by utilizing both keyhole welding and conduction-mode welding. In this research a high-power diode laser and an Nd:YAG laser are combined to gain the advantages of bifocal hybrid laser beam welding. (Zäh et al., 2008)

The major benefit of utilizing this technique is achieved when welding aluminium alloys. Aluminium alloys have a bad tendency of forming cracks and pores during welding. The aluminium used in this research is EN AW-6060 alloy, which is considered as a hardly weldable alloy. The recent researches conducted at the *iwb* have shown that this welding technique performs well when welding EN AW-6060 alloy. The wide focal spot of the HPDL has a great influence on surface quality. In addition, these two processes interact with each other in a beneficial manner so that the process results into a great quality weld overall, without pores or cracks. (Zäh et al., 2008)

## 2.4 Statistical methods for describing the process and the measurements system

Statistics was chosen as one of the point of views for analysing the results from the welding experiments. It was one goal of this research to determine the figures of merit, stability, sensitivity and repeatability, for the in-situ melt identification technique at the laboratory of *iwb.* The criteria for the statistical analysis were taken from "*Statistische Verfahren zur Maschinen- und Prozessqualifikation"* by Dietrich & Schultze (Dietrich & Schultze, 2002). In the book *stability of a gauge* is defined as the difference of the highest and the lowest value of data of one measurement. According to Dietrich & Schultz, stability stands for the ability of the gauge to produce even data from one measurement. Repeatability, however, is defined as a deviation of measurement results from a group of identical measurement. (Dietrich & Schultze, 2002)

To prove reliability of measurements certain statistical terms and methods have been established. "Gauge R&R studies" is in literature a frequently mentioned method to ensure the reliability of data gained in repeated measurements. The terminology behind gauge R&R represents repeatability and reproducibility of measurements. Repeatability means the variance of identical measurements done with same equipment in identical environment. Reproducibility represents the variation of measurements done by different appraiser, otherwise the same as repeatability. In this research the materials are the same, as are equipment and environment during all the experiments. So, the method used here is repeatability analysis. (Mason et al., 2003)

While the statistical measure for stability was the difference of the extreme values, the measure for repeatability is standard deviation of all the measurements (Dietrich & Schultze, 2002). These definitions were adapted for the experiments so that stability was examined from all of the emissions, whereas repeatability was examined from the average intensities of the emissions.

Standard deviation and variability index were also used to descript stability and repeatability of the measurements. These measures are basic terms in the field of statistics. The equation for standard deviation is presented in (18). Standard deviation describes the divergence of the values of the data, i.e. the bias from the average. Variability index describes the percentual divergence of the data from the average. It is calculated as a relation of average and standard deviation. The equation for variability index is given in (19). (Statistics Finland, 2007)

$$s = \sqrt{\frac{\sum_{i=1}^{n} (x_i - \bar{x})^2}{n-1}} \tag{18}$$

$$V_{\text{var}} = \frac{s}{\bar{x}} \cdot (100\,\%), \tag{19}$$

where

$s$: standard deviation

$V_{var}$: variability index

$\bar{x}$: average of the data.

# 3 METHODS AND MATERIALS

## 3.1 Processed materials

All the experiments in this research were done on aluminium alloy. The main concern was in the alloying elements, more specifically magnesium. Therefore all the materials used in these experiments had a significant amount of magnesium as one of alloying components. The experiments investigated different aspects of spectral and metallurgical analysis. In stability experiments it was needed to have a relatively great amount of magnesium in the alloy to get magnesium line show clearly in the spectrum.

On the other hand, in repeatability and sensitivity experiments the material itself had a much lower concentration of magnesium. In repeatability experiments the concern was the constancy of emission intensities in respect of aluminium and magnesium lines.

Sensitivity experiments were welded with filler wire to vary the amount of magnesium in the weld. Feeding filler wire allowed manipulation of the magnesium concentration in the weld in small amounts depending on welding speed and filler wire feeding rate.

The loss of mass experiments included also measurements from samples that were welded before (Glasschröder, 2010). These samples were especially casted material with rising magnesium content from zero to ten percents by mass. The chemical composition of these materials is shown in table 3. In this table the content of magnesium is presented as "x", which stands for varying Mg-amount. The material with 8 % of magnesium was used also for stability experiments. All the plates from these materials had a thickness of 3 mm.

*Table 3. Chemical composition of materials used in **loss of mass** and **stability** experiments. (Glasschröder, 2010)*

| Element | Si | Fe | Cu | Mn | Mg | Cr | Zn | Ti | P | Ni | Ag |
|---|---|---|---|---|---|---|---|---|---|---|---|
| [mass-%] | 4.0070 | 0.0685 | 0.0010 | 0.3130 | x | 0.0003 | 0.0046 | 0.0002 | 0.0004 | 0.0028 | 0.0001 |
| Element | B | Ce | Co | Ga | Pb | Sb | Sn | V | Zr | Al | Mo |
| [mass-%] | 0.0004 | 0.0006 | 0.0003 | 0.0142 | 0.0006 | 0.0009 | 0.0001 | 0.0115 | 0.0012 | Remainder | 0.0011 |

The other materials used in the studies were standard materials. This allowed comparison of results from this and other researches and experiments made with the same materials. The material in **repeatability** and **sensitivity** experiments was the same, aluminium alloy EN AW-6060 as designated in standard EN 573-3:2007 and chemical composition is AlMgSi0.5. The chemical composition of this material is shown in table 4. The thickness of the plates were 2 mm. (EN 573-3:2007)

*Table 4. Chemical composition of EN AW-6060. (EN 573-3:2007)*

| Element | Si | Fe | Cu | Mn | Mg |
|---|---|---|---|---|---|
| [mass-%] | 0.30 - 0.60 | 0.10 - 0.30 | 0.10 | 0.10 | 0.35 - 0.60 |
| Element | Cr | Zn | Ti | Al | Other |
| [mass-%] | 0.05 | 0.15 | 0.10 | Remainder | 0.15 |

The filler wire used in sensitivity experiments had higher magnesium content. It was used to change the magnesium contents in the weld seams. The filler wire was chosen to be AlMg5, which had approximately 5 % of magnesium. The standard designation for this wire is Al 5356 according to standard EN ISO 18273:2004 and chemical composition is AlMg5Cr(A). The chemical composition of the used filler wire is shown in table 5. (EN ISO 18273:2004)

*Table 5. Chemical composition of aluminium alloy AlMg5. (EN ISO 18273:2004)*

| Element | Si | Fe | Cu | Mn | Mg | |
|---|---|---|---|---|---|---|
| [mass-%] | 0.25 | 0.40 | 0.10 | 0.05 - 0.02 | 4.50 - 5.50 | |
| Element | Cr | Zn | Ti | Al | Be | Other |
| [mass-%] | 0.05 - 0.20 | 0.10 | 0.06 - 0.20 | Remainder | 0.0003 | 0.02 |

## 3.2 In-situ melt identification system

The experiments were done with a high-power diode laser (HPDL) with a maximum output power of 6000 W and with an Nd:YAG laser with a maximum output power of 3000 W. Although diode lasers are traditionally presumed as equipment for conduction mode welding or for welding of non-metallic materials, e.g. plastics, with new state-of-the-art HPDL-equipment also keyhole welding of metals, in this case aluminium alloy, is possible. The nominal power of the HPDL is 8000 W, but after combining all four

wavelengths into one fibre, the output power is decreased to 6000 W. With great beam characteristics this amount of power would be easily utilized for deep penetration welding, but because of the typical properties of diode lasers, i.e. combining the raw beam from many small beam sources, the quality of the beam cannot reach the quality of other industrial lasers, e.g. fibre laser. Beam parameter product for high power diode laser with maximum power of 8000 is 100 mm*mrad (Laserline, 2010). For comparison, a typical BPP for a fibre laser is around 5.2 mm*mrad (Wandera, 2010). The welding experiments for this research were made with a bifocal optics, where the raw beams of Nd:YAG and diode laser are refracted onto a same optical axis. In the following chapters different parts of the experimental setup are preseented.

### 3.2.1 Experimental setup

All the test welds were done so that the test piece would stay still and a robot would do the welding movement. The actual welding head was fixed to the robot. The robot, shown in figure 13, used for these experiments was manufactured by KUKA and the model was KR150. The welding head was designed by the *iwb* laboratory. The welding head allows bifocal hybrid laser welding. The fibres of Nd:YAG laser and diode-laser are integrated to the same optical axis. The integration is done so that the raw beam of the diode laser comes from behind of the Nd:YAG laser and is refracted by a mirror that is transparent to the wavelength of the Nd:YAG laser. This refraction demands, that all the wavelengths of the diode laser cannot be used, since the longest wavelengths are so close to the wavelength of the Nd:YAG laser, and one mirror cannot refract the other and let the other through. Therefore, the longest wavelengths of the diode laser were switched off reducing the output power of the diode laser to approximately 3000 W.. This way the shorter wavelengths of the diode-laser are refracted to the same optical axis as the Nd:YAG laser. Filler wire feeding system is also integrated to the welding head. The used filler wire feeding apparatus was DIX WD 300 from the company Dinse. The complete welding head is shown in figure 14.

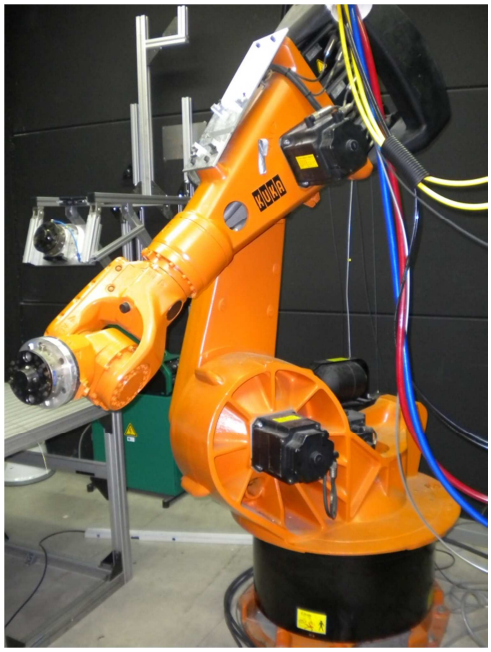

*Figure 13. KUKA KR150 was the robot used in the welding experiments.*

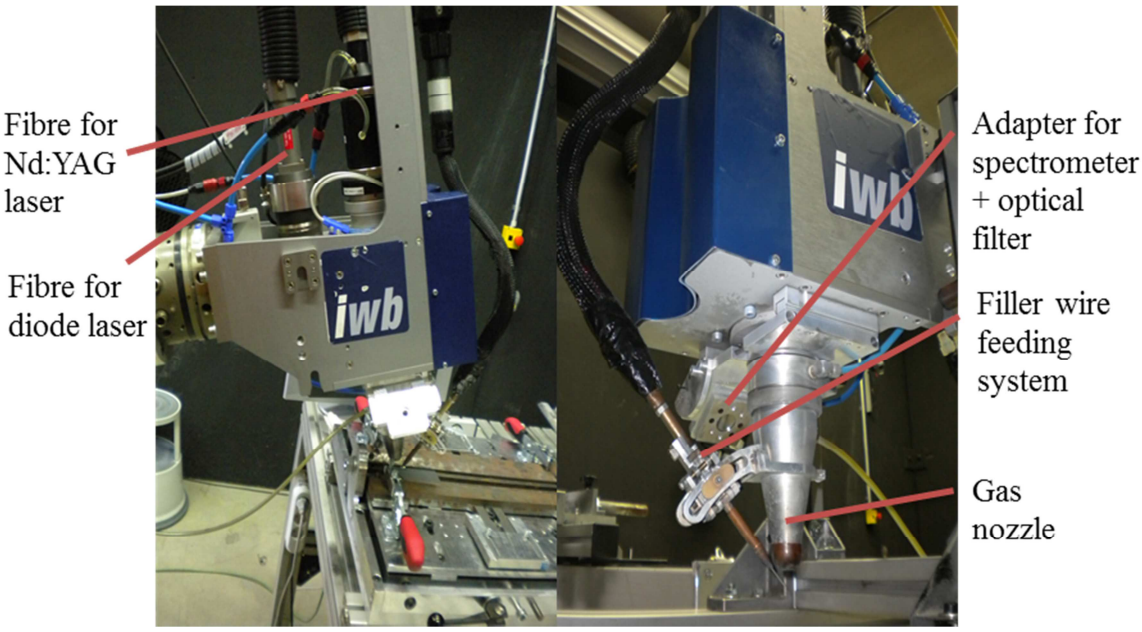


*Figure 14. Bifocal hybrid laser beam welding head with an adapter for the spectrometer AvaSpec-2048-USB2.0.*

#### 3.2.1.1 Measurement of the beam parameters

To produce the best possible result in the welding experiments, the focusing equipment needed to be calibrated. The calibration consisted of three stages. First the welding head was dismantled to separate all the optical parts for cleaning. Once all the mirrors and lenses

were cleaned, the welding head was reassembled. The second stage was to find the focus of the two laser beams and to calibrate them onto a same optical axis. This was done by detecting the intensity distribution of the focused laser beams. The measuring equipment was connected to a computer which analysed the data given by the measuring device. The computer had a software that produced 2D- and 3D-images of the laser beams. With this information the focal spot of the both lasers could be found and the diameter of the focal spots could be measured. Figure 15 illustrates the waists of the two beams and their focal spot diameters.

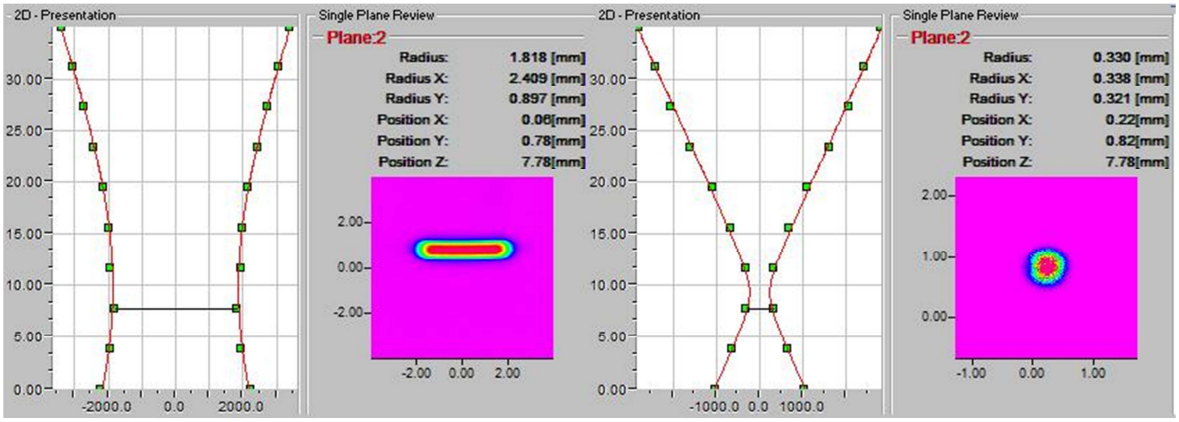


*Figure 15. 2D-images of intensity distributions of the diode laser (left) and Nd:YAG laser (right).*

When the two lasers were on a same optical axis, the beam of the Nd:YAG laser was positioned in the middle of the diode lasers rectangular distribution, as shown in figure 16. The intensity distribution was utilized so that welding direction was always parallel to the long side of the rectangular intensity distribution of the diode laser. Figure 16 illustrates quite well the differences in intensity distributions of the two lasers. The much higher peak of the Nd:YAG laser creates the keyhole and is the main factor in deep penetration welding.

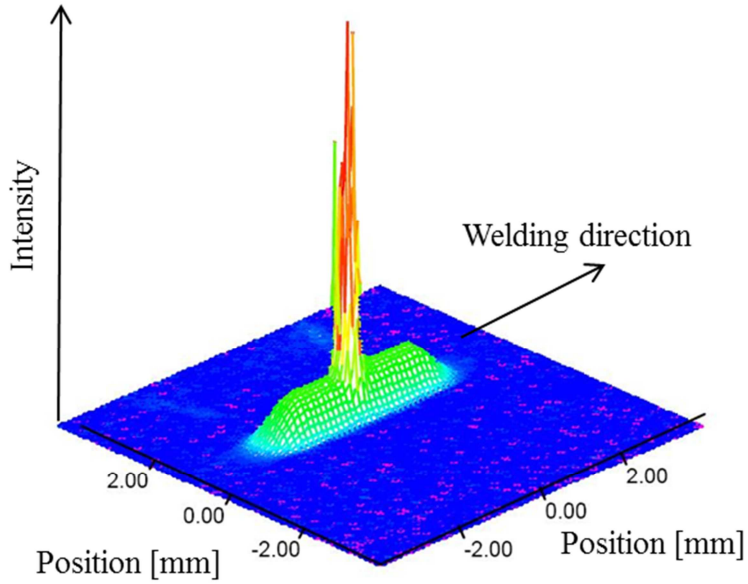


*Figure 16. Intensity distribution of the bifocal hybrid laser with Nd:YAG and diode laser.*

### 3.2.1.2 Positioning the focal spot

After the beams were on the same optical axis, the focus for processing needed to be found. The calibrating gave exact information of the position of the focus. Since the main function of the calibrating was to unify the two foci, the position of the focus on a surface of a work piece needed to be found yet more precisely. This was done with a *focfind*-program. This program creates a path for the robot, illustrated in figure 17, where the robot moves step by step upwards. On every step the Nd:YAG laser shoots a short pulse. The program is written so that the robot first moves to a presumed focus point that is given to the program. The program then makes this point the middle point. Then it moves the robot 25 mm forwards and 5 mm downwards and gives the first pulse. From there on it moves 5 mm backwards and 1 mm upwards and shoots a pulse, step by step, until all eleven pulses are made. When the program is complete, the test piece is examined in respect of which mark made by the laser pulse is the most accurate, i.e. the laser is in focus. For sensitivity experiments, the *focfind*-program was run with only 0.5 mm steps to find the focus even more accurately. This was done to avoid possible problems with the positioning of the filler wire.

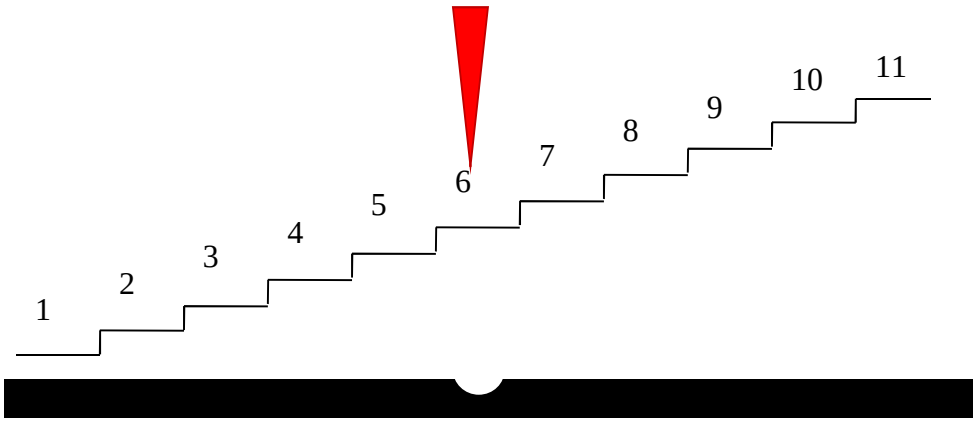


*Figure 17. Basic principal of the focfind-program.*

### 3.2.2 Spectrometer and optical filter

The used spectrometer was AvaSpec-2048-USB2.0 by the company Avantes. Avantes is a company specialised in spectroscopy instruments and they offer a wide range of spectrometers for various purposes (Avantes, 2010). This particular spectrometer had a detection range from about 350 nm to 881 nm, but the company also offers spectrometers with a wider range. The spectrometer had an accuracy of 0,1 – 0,2 nm in wavelengths and integration time from 1.1 milliseconds up to 10 minutes. Integration time stands for the time the spectrometer records the spectrum, i.e. the longer the integration time, the stronger the intensities. So the basic idea is the same as exposure time in photography. The spectrometer had a fast USB version 2.0 connection possibility to a computer, which made data transfer speeds up to 480 Mbps available. (Avantes, 2010)

It was noticed during test welding, that with reasonable integration times the intensities were so high that they were not noticeable anymore. Therefore, an optical filter was needed. The filter chosen for these experiments was a short-pass filter XIS0810 from the company Ahasi Spectra. This filter was chosen because of its great compatibility with the used spectrometer, having the filtering range from about 350 nm to 810 nm, as shown in figure 18. The filter had a substrate of fused silica and thickness of 1 mm. The positioning of the filter was right in front of the collimator. (Ahasi Spectra USA Inc., 2010)

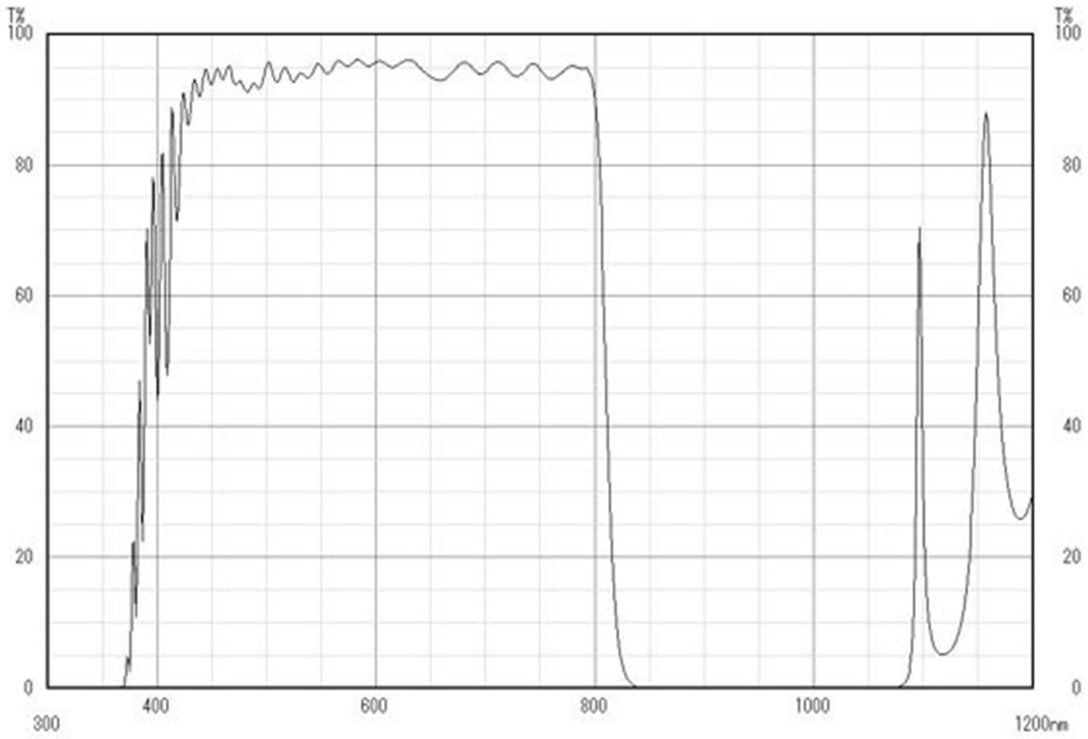


*Figure 18. Filtering capability of the optical short-pass filter XIS0810. (Ahasi Spectra USA Inc., 2010)*

When all of this monitoring equipment was build together, the emissions from the welding process would first go through the optical filter. The filter would reduce the intensity of the emissions to a more detectable range, penetrating intensity being about 3 %. Immediately after the filter, the collimator would gather the emissions to the optical fibre. In the fibre, which had a diameter of 8 μm, the gathered beam would travel almost lossless due to total reflection. The fibre was then connected to the actual spectrometer via a *SubMiniature version A* entrance connector (SMA-entrance connector). After that, the beam was collimated by a mirror and reflected to a grating. The grating has the most crucial meaning in the spectrometer. It functions like a prism, refracting different wavelengths with their particular angles. Once the beam was refracted, the beam was no longer collimated, but all the wavelengths were separated. Therefore, the beam was collimated before the detector with a focusing mirror. All these components that can be found inside the spectrometer device are presented in figure 19, which illustrates the basic assembly of a spectrometer. (Avantes, 2010)

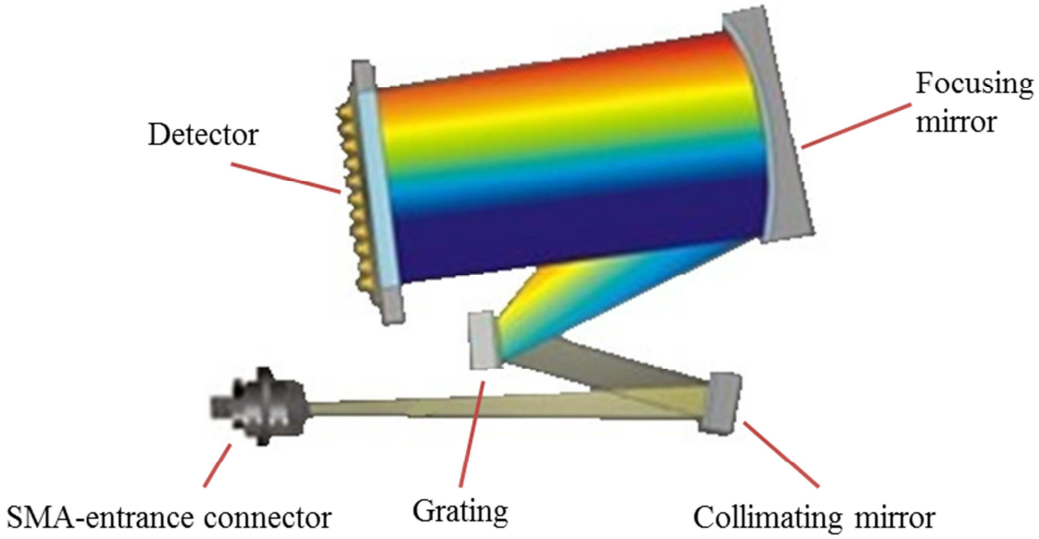


*Figure 19. Components inside a spectrometer. (Avantes, 2010)*

The detector is an electronic component which has the main function of receiving, detecting and counting the photons from an incoming radiation. In the detector component there is a Charged Detector Device (CDD). Integration time determines the time after which the CCD is read out. Each photon has kinetic energy and this energy is stored by the detector array. At the end of the integration time, the remaining energy is transmitted to an analog-to-digital converter (AD-converter) via a buffer. The integration time is not limited by the CCD array, but by the AD-converter and thermal effects. CCD arrays are very adaptive to dynamics of the incoming radiation. (Avantes, 2010)

#### 3.2.2.1 Positioning the spectrometer

During the welding experiments, process emissions were monitored by a spectrometer. The spectrometer was manufactured by Avantes and the model was AvaSpec-2048. The collimator of the spectrometer was fixed to the welding head with a custom made adjustable adapter. Figure 20 shows the measurement geometry for the spectrometer and adapter. The collimator was focused to the welding spot with a similar collimator that was fixed to another optical fibre. That was because the fibre of the spectrometer should not be detached. If detached, the spectrometer should be calibrated again. The focusing was done so, that light of a laser pointer was directed to the fibre and then the collimator and the adapter were adjusted to get as sharp as possible focal spot in the middle of the pilot laser spot from the Nd:YAG laser. Once focused, the spectrometer was fixed to the robot and a

USB-cable and a trigger cable were attached to the spectrometer. The USB cable was used for the data transfer from the spectrometer to the computer, from which the emissions were recorded. The other end of the trigger cable was attached to the control unit of the welding cell. The trigger wire relayed the trigger signal from the control unit to the spectrometer. The function of the trigger signal was to start the spectrometer to measure the emissions. It was set to start the spectrometer at the very same moment as the lasers were turned on and the welding begun. The spectrometer and its parts are shown in figure 21.

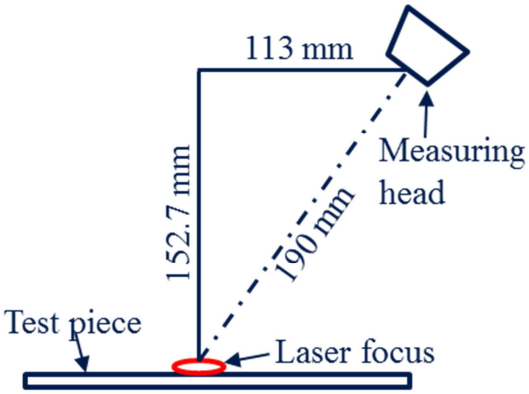


*Figure 20. Measurement geometry of the spectrometer AvaSpec-2048.*

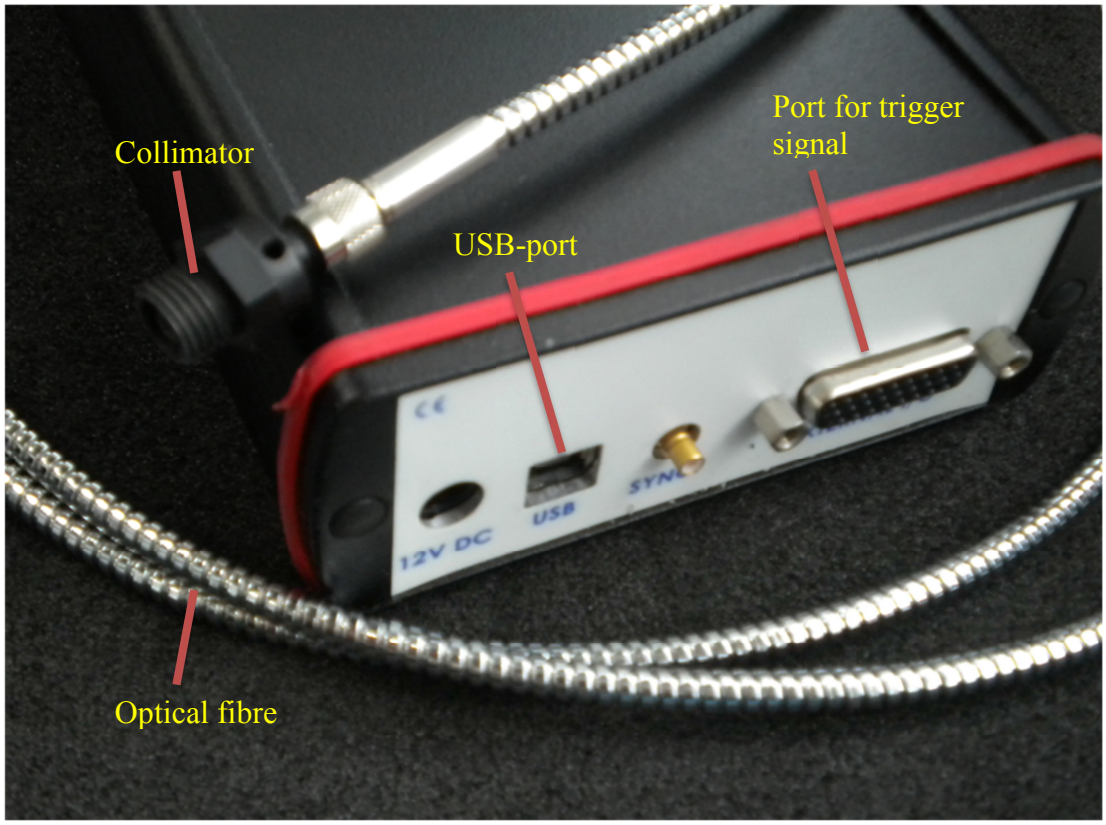


*Figure 21. AvaSpec-2048 and connections.*

### 3.2.3 Software for monitoring

Two programs were used to record the emissions from the welding process. SpecTUM and SpecTUMall were both created by Johannes Glasschröder during his Master's Thesis (Glasschröder, 2010). The difference of the programs was that SpecTUMall shows all the data from the emissions, whereas SpecTUM shows only the maximal and average values of the emissions. From both of the programs same parameters could be adjusted. The most important parameters were starting and ending pixels, integration time, dark reference, number of pictures to be recorded and acceptable noise level. The window of SpecTUM is shown in the figure 22. For all the experiments the integration time was the same 2 ms. The start pixel for all the experiments was 0 and the end pixel 1600. Also the number of pictures was held the same throughout the experiments. The used number of pictures was 250. The connection between the number of pictures and the integration time is that each of the 250 pictures has been produced during the integration time. SpecTUM calculates the average and maximum values of those 250 pictures for each wavelength and SpecTUMall just prints the data from all the pictures and wavelengths.

The pixels describe the resolution of the spectrometer and when the scale of the spectrometer is from 350 nm to 880 nm, the maximum number of pixels is 2048 (Avantes, 2010). Integration time describes the time after which the CCD array is read out. Dark reference is used to minimize the influence of the background emissions caused by the lighting in the welding cell and other emission sources. Number of scans describes the number of spectra to be recorded. The theoretical maximum is 255, since Excel cannot process functions that go over 255 columns. Excel was used for the analysis of the data. Before the welding experiments, the background emissions were recorded to find out the maximum background intensity. This intensity with safety factor was then saved as an acceptable noise level. This means that every spectrum that has a maximum intensity below the acceptable noise level is not usable for the data analysis. Both of the programs used show a file where all the taken pictures are listed. The file shows for each picture if it is useful or not. This means, that if some line of the spectrum of that particular picture exceeds 60 000 counts, which is the maximum amount for the spectrometer to detect, the picture gets disqualified. In the end of the file the number of useful spectra is presented. This sums up the exceeded spectra and also the spectra whose highest intensities stay under the acceptable noise level.

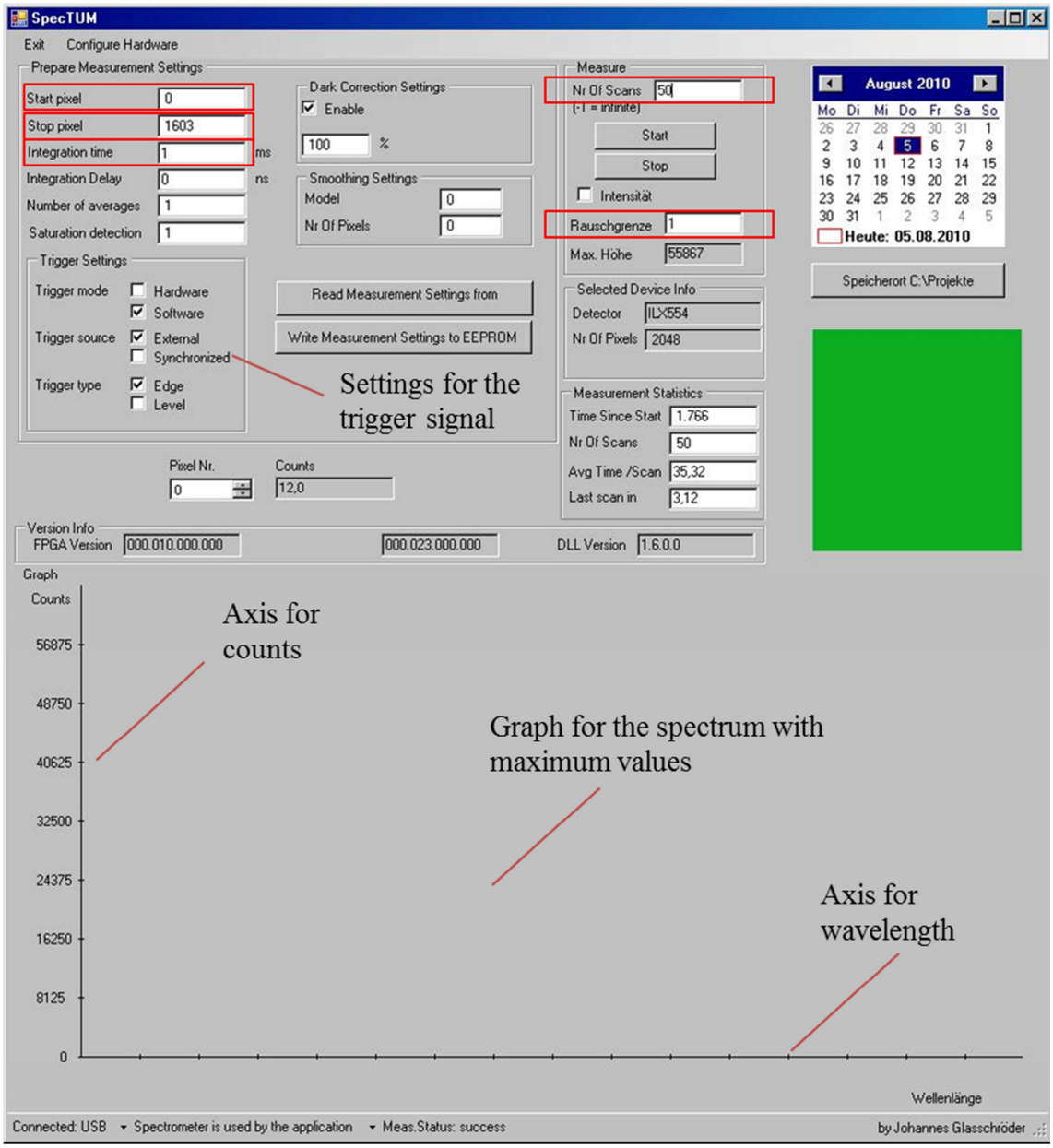


*Figure 22. Main window of the program SpecTUM/SpecTUMall. Start and stop pixel, integration time, number of pictures and the acceptable noise level are marked as red quadrangles.*

## 3.3 Figures of merit of measurement systems

The objective in repeatability inspection was to determine the variations in separate identical experiments through quantitative analysis of the emission spectrum. Here, only the average intensities of the recorded spectra would matter. The average intensities were calculated by the SpecTUM-software.

In stability part of the research the quantitative analysis concentrated in deviation of magnesium concentration within one weld. Sometimes during keyhole welding the keyhole can collapse, as explained before. When the keyhole collapses, welding is insufficient. That means that no vaporization or metal vapour plume occurs and therefore emissions also disappear. The stability studies were conducted to find out how stable the incident welding process was and how the measurement equipment correlated with the process. The actual study concentrated on the relation of clear and unclear spectra and the stability of the aluminium and magnesium emissions during the whole welding process. The spectra of the stability experiments were analysed to see how much deviation occurs in magnesium and aluminium emissions during laser welding. This analysis was conducted in two stages. Firstly, the emissions of aluminium and magnesium were analysed independently in absolute intensities. This way the whole stability of the process could be discussed. At the second stage the emissions of magnesium were normalized by an aluminium line at 394.3414 nm. Since aluminium has a fairly constant content in the alloy, it was presumable that the intensities of aluminium would stay constant. The emission line at 394.3414 nm was chosen to be the reference line since it was the one used also by Glasschröder (Glasschröder, 2010). If this kind of stable emission would have significant variance, it would represent the variance of the whole process. Therefore, by normalizing the emission intensities by aluminium intensities, the impact that the instable process would have on the emissions could be minimized and the stability of magnesium emissions could be clarified.

The sensitivity part of this research concentrated in analysing the changes in spectra from the objective of quantitative analysis. Since a previous research was conducted with aluminium alloys that were alloyed by magnesium from zero to maximum of ten percent, in this research the objective was to take this previous research further and to clarify how sensitively smaller changes in magnesium concentrations are detected from the spectrum while feeding various amounts of filler wire to the welding process. Also here, only the average intensities of the emissions were the ones that mattered.

## 3.4 Detecting of silicon and magnesium emission lines

In previous researches (Glasschröder, 2010) it was noticed that all of the alloying elements of the used aluminium alloy were not detected in the spectroscopic analysis of the laser welding process. The neutral silicon has main emission lines in the UV-area of EM-radiation. These lines should be detectable by the spectrometer that was used in the previous research (Glasschröder, 2010). Other strong lines of silicon are at over 600 nm, but these lines are the emissions of the singly ionized silicon atom. And as Mohammed (2007) suggested, it is most likely that the ionization potential energy of silicon is too high for the output power of a welding laser. And since the detection level of silicon is not significantly lower than of the other easily detected elements, it is presumable, that the problem is not within the detection technology, but it has to do with the excitation energy. Silicon is nevertheless detected with a normal LIBS-experiment, but the energy density of the laser beam is then much higher than in laser welding. To get silicon to show up in the spectrum, the power of the welding laser should be increased, but then the quality of the weld would most probably suffer. (Mohamed (2), 2007) (Popov et al., 2009) (NIST, 2010)

To clarify the problem in the detection of the emissions of silicon, excitation of magnesium was also studied. Two of the main lines of magnesium were chosen to be examined. These lines at 383.23 nm and 517.268 nm are detectable with the used spectrometer. To compare the excitation of these two elements the Boltzmann equation was applied (equation (9)). All the data required for the calculations of the Boltzmann equation were taken from the NIST database (NIST, 2010). As a result a plot was formed to illustrate the degree of excitation as a function of temperature. The plots are presented in the figures 23 and 24. The emission lines of silicon that were used for this plot were 251.4130 nm and 288.1579 nm, since these are the main lines for neutral silicon. It is clearly visible from this plot that the density of excited silicon atoms is much lower compared to magnesium at the same temperatures.

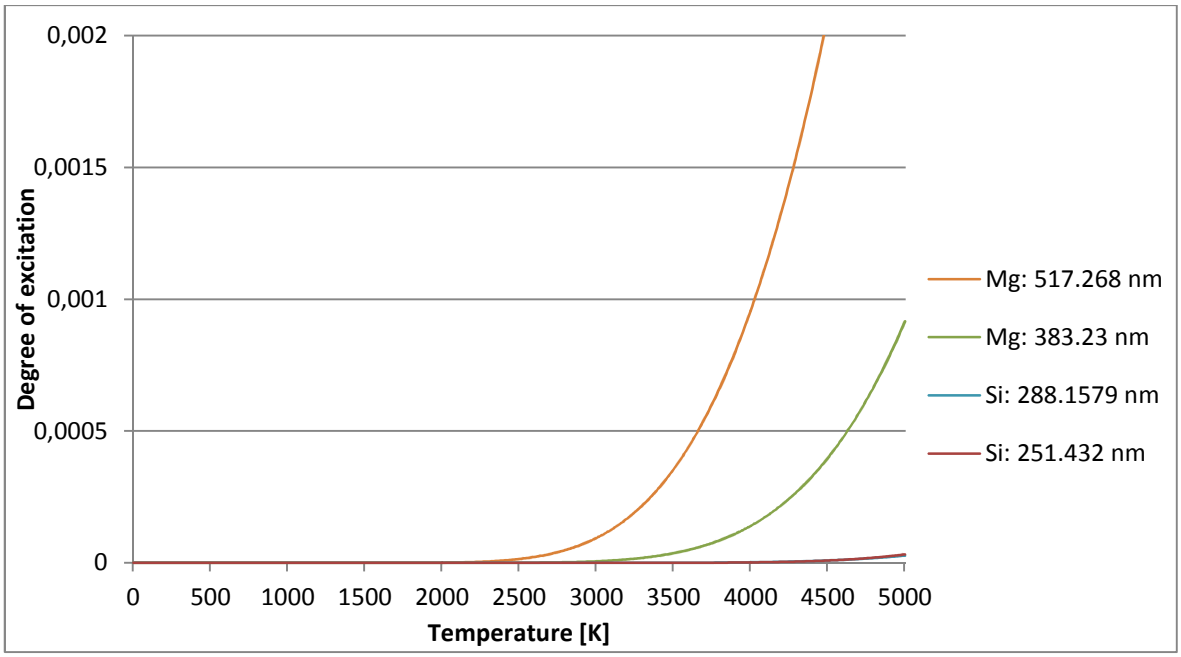


*Figure 23. Comparison between the degrees of excitation of the two main emission lines of silicon and magnesium.*

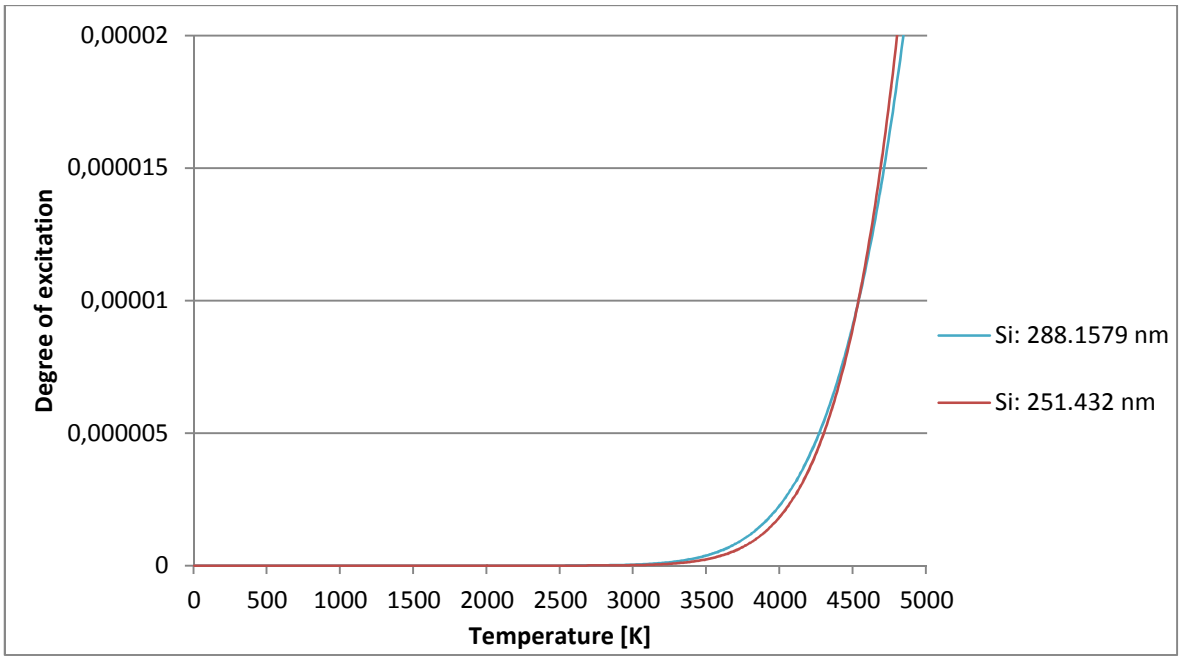


*Figure 24. Degree of excitation of two main emission lines of silicon.*

## 3.5 Procedures for different courses of the research

The objective of this research was to find statistical support for stability, sensitivity and repeatability of the process radiation and the emission measurement system. To gain

results to study, in each part of the research certain experimental welds were produced. Figure 25 shows the courses of the figures of merit research. In stability part of this research the main objective was to observe unsteadiness and relation between magnesium and aluminium lines during welding. In the case of sensitivity experiments, the main objective was to investigate how sensitive the measurement equipment was to detect alloying elements when they are in varied amounts. During these experiments, several welds were made, each with different amount of magnesium, which was adjusted by changing the concentration and feeding rate of the filler wire. The element studied here was magnesium (Mg), since it is the only element, which was possible to feed as a filler wire and was still detectable in the spectrum. The other possibility for the filler wire would have been silicon (Si), but since it cannot be detected as proved before, it was put aside. During repeatability experiments, several unique tests were carried out. This was realized by welding 10 test pieces with a same welding program and parameters with welding length of 70 mm. The objective was to perceive how separate but still identical tests differ. In figure 26 the welding setup is illustrated.

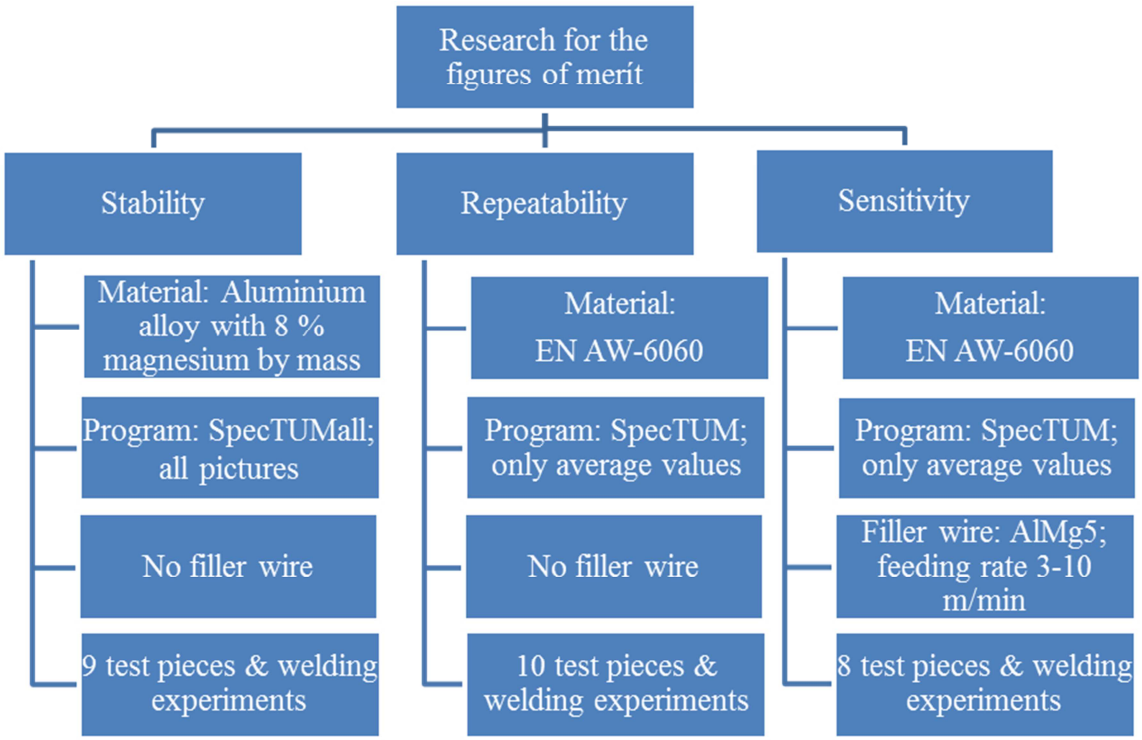


*Figure 25. Courses of the research for the figures of merit.*

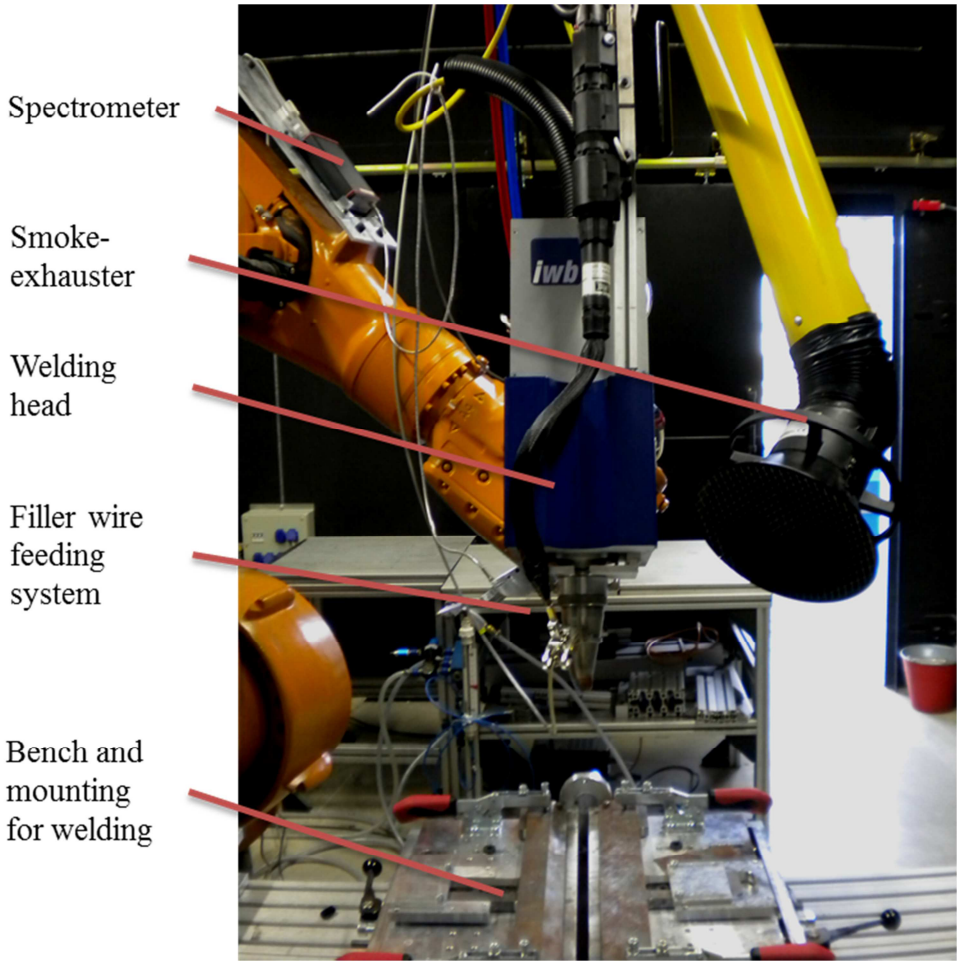


*Figure 26. Welding cell and equipment for the welding experiments.*

### 3.5.1 Loss of mass

In laser deep penetration welding partly vaporization of the molten material is a basic phenomenon. This means that if laser welding is done without a filler material, some material will be lost. Two sets of samples were used to analyse the lost material during laser welding. The first set consisted of 33 test pieces that were welded on a material that had magnesium content from zero to ten percent by mass. The second set of samples was from the test pieces of sensitivity experiments. Here the magnesium content was varied by feeding filler wire. In the next two chapters the procedures of the measurements from these two sets of samples are introduced. The courses of the research for the loss of magnesium are shown in figure 27.

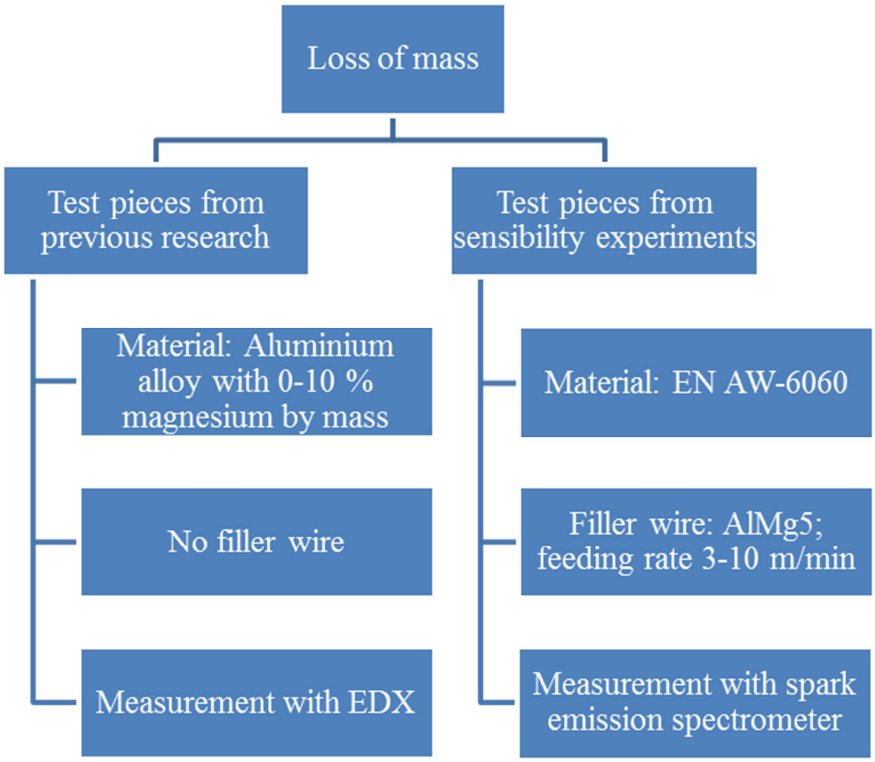


*Figure 27. The courses of the research for loss of magnesium.*

#### 3.5.1.1 Samples with magnesium in various amounts

The study was conducted in two stages. At the first stage, which took place in previous research (Glasschröder, 2010), the test pieces were laser welded. At the second stage these welded test pieces were cut along the weld and polished to be examined with an electron microscope with EDX-method (*Energy-dispersive X-ray spectroscopy*). The electron microscope gave the current magnesium content. Figure 28 illustrates the EDX-measurement method. The numbered points determine the measure points. Then the original and final magnesium concentrations were compared to find out the loss of material.

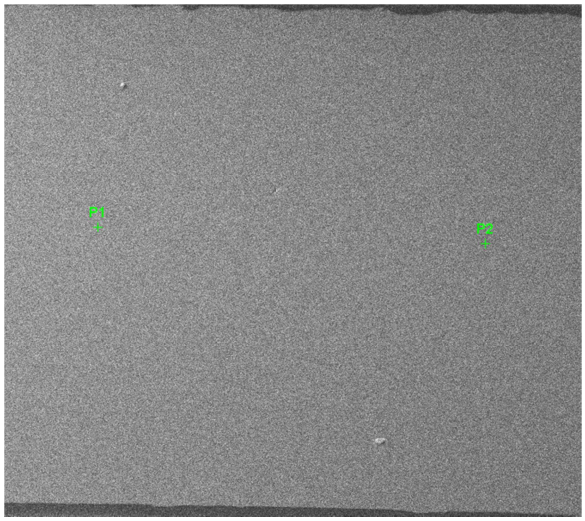

*Figure 28. Basic principal of the EDX-measurements. The green dots are the measurement points.*

The test pieces were welded by a diode laser with parameters shown in table 6. The parameters were the same for each test piece. The only parameter that changed was the magnesium content in the test pieces. The test pieces were 3 mm thick. In total 34 test pieces were welded, from 0 % to 10 % nominal magnesium content by mass.

*Table 6. Welding parameters for the samples from a previous research. (Glasschröder, 2010)*

| Welding parameters | | | | | | | | Spectrometer parameters | |
|---|---|---|---|---|---|---|---|---|---|
| Consecutive numbering | Welding speed | Power HPDL | Power YAG | Welding angle | Gas flow | Shielding gas | Mg - content | Integration time | Number of pictures |
| | m/min | W | W | deg | l/min | | | ms | |
| 1-4 | 2.0 | 6000 | 0 | 18 | 20 | Ar | 0 | 2 | 250 |
| 5-7 | 2.0 | 6000 | 0 | 18 | 20 | Ar | 1 | 2 | 250 |
| 8-10 | 2.0 | 6000 | 0 | 18 | 20 | Ar | 2 | 2 | 250 |
| 11-13 | 2.0 | 6000 | 0 | 18 | 20 | Ar | 3 | 2 | 250 |
| 14-16 | 2.0 | 6000 | 0 | 18 | 20 | Ar | 4 | 2 | 250 |
| 17-19 | 2.0 | 6000 | 0 | 18 | 20 | Ar | 5 | 2 | 250 |
| 20-22 | 2.0 | 6000 | 0 | 18 | 20 | Ar | 6 | 2 | 250 |
| 23-25 | 2.0 | 6000 | 0 | 18 | 20 | Ar | 7 | 2 | 250 |
| 26-28 | 2.0 | 6000 | 0 | 18 | 20 | Ar | 8 | 2 | 250 |
| 29-31 | 2.0 | 6000 | 0 | 18 | 20 | Ar | 9 | 2 | 250 |
| 32-34 | 2.0 | 6000 | 0 | 18 | 20 | Ar | 10 | 2 | 250 |

The previous measurements for these test pieces were made with EDX-method from the end part of the weld. Each work piece was measured in 4-5 different points. All these measurements were from the weld. However, these results were not comparable with the results from the base material carried out with a spark-emission spectrometer, since the measurement equipment would have been different. The previous results of the electron microscopic measurements had also considerable deviation and inconsistence. Therefore, new measurements from the base material were made with slight changes to the measurement procedure. These measurements were done also with electron microscope using EDX-method. First, one test piece from each nominal magnesium content was chosen for the measurements. Then small samples were cut off from each of the chosen test pieces. The samples for these measurements were cut from the base material and from the beginning part of the weld. The samples from the welds were cut parallel to the weld, as shown in figure 29. The samples had geometry of 15 x 20 mm and they were polished before EDX-analysis. The middle line of the weld was on one side, so that it would be easy to measure.

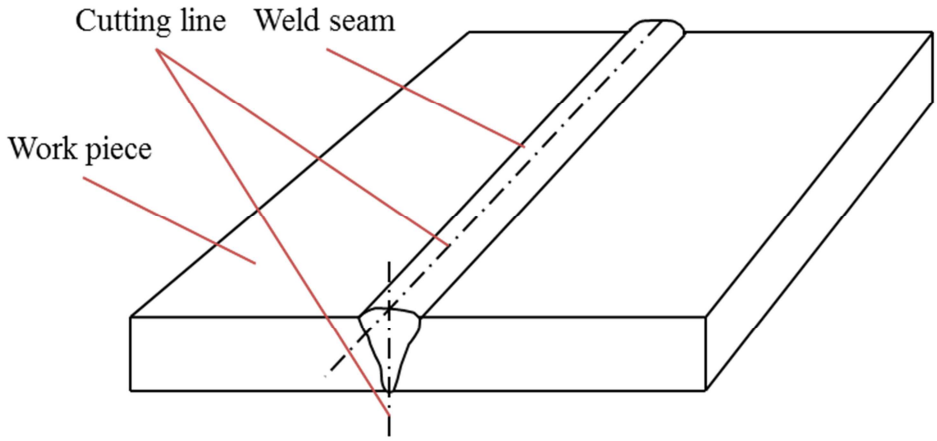


*Figure 29. The principal for cutting of the test pieces.*

### 3.5.1.2 Samples from welding with filler wire

The test pieces of sensitivity experiments were cut to produce samples for measuring the elemental content of the weld. Since the EDX-method for detecting magnesium in the weld was realized to be unsuitable since it cannot measure under 1 % concentrations, another method was needed. Spark-emission spectrometer proved to be an efficient tool in

detecting small concentration in material, so it was decided to try this method here as well. The only problem was that the measure area was quite large, diameter about 10 mm, and the test piece were only 2 mm thick. This problem was solved by cutting the test piece perpendicularly to the weld. Then the sample was pressed to produce a thin, even and wide surface. This surface was then large enough to cover the measure area of the spark-emission spectrometer. After preparing the samples, the measurements were made with the spark-emission spectrometer.

### 3.5.2 Sensitivity experiments

As mentioned before, the same equipment was used in all welding experiments, only the parameters and materials changed. In sensitivity experiments, the used material was aluminium alloy EN AW-6060. Once again, the welding process was monitored with a spectrometer and the emissions were recorded with the program SpecTUM. The geometry for these welds was a bit different than before; therefore the welding program needed to be changed (also because, the long weld demanded a different kind of mounting). The test pieces were 2 mm thick and the length of the weld was 29 mm. The varied parameters were welding speed and filler wire feeding rate. The used filler wire was AlMg5, which had magnesium content of 5 % by mass. The goal of this particular experiment was to determine the loss of magnesium during a laser welding process while feeding filler wire to the process. To get various amounts of magnesium into the weld, the welding speeds and filler wire feeding rates were set to maximize the effect of the magnesium in the filler wire. The amount of magnesium in a joint welded with a filler wire cannot be known; therefore it needs to be calculated. For this calculation the area of the weld needs to be known, and because this area is extremely difficult to evaluate before welding, only directional estimates could be made. Based on these estimates, the welding parameters shown in table 7 were chosen.

*Table 7. Welding and spectrometer parameters for sensitivity experiments.*

| Welding parameters | | | | | | | | | Spectrometer parameters | | | | | |
|---|---|---|---|---|---|---|---|---|---|---|---|---|---|---|
| Consecutive numbering | Welding speed | Power HPDL | Power YAG | Welding angle | Gas flow | Shielding gas | Filler Wire | Filler wire feeding rate | Start pixel | End pixel | Integration time | Number of pictures | Acceptable noise level | Useful pictures |
| | m/min | W | W | deg | l/min | | | m/min | | | ms | | counts | |
| 1 | 5.0 | 1.3x3000 | 3000 | 18 | 20 | Ar | AlMg5 | 3 | 0 | 1600 | 6 | 250 | 400 | 243 |
| 2 | 4.5 | 1.3x3000 | 3000 | 18 | 20 | Ar | AlMg5 | 4 | 0 | 1600 | 6 | 250 | 400 | 242 |
| 3 | 4.0 | 1.3x3000 | 3000 | 18 | 20 | Ar | AlMg5 | 5 | 0 | 1600 | 6 | 250 | 400 | 246 |
| 4 | 3.5 | 1.3x3000 | 3000 | 18 | 20 | Ar | AlMg5 | 6 | 0 | 1600 | 6 | 250 | 400 | 243 |
| 5 | 3.0 | 1.3x3000 | 3000 | 18 | 20 | Ar | AlMg5 | 7 | 0 | 1600 | 6 | 250 | 400 | 246 |
| 6 | 2.5 | 1.3x3000 | 3000 | 18 | 20 | Ar | AlMg5 | 8 | 0 | 1600 | 6 | 250 | 400 | 246 |
| 7 | 2.5 | 1.3x3000 | 3000 | 18 | 20 | Ar | AlMg5 | 9 | 0 | 1600 | 6 | 250 | 400 | 245 |
| 8 | 2.5 | 1.3x3000 | 3000 | 18 | 20 | Ar | AlMg5 | 10 | 0 | 1600 | 6 | 250 | 400 | 245 |

The welds for sensitivity and loss of mass experiments were longer than in other experiments. The length of the weld in previous weldings was 80 mm, but here the length was 295 mm. Therefore the same mounting used in previous weldings could not be used. Figure 30 shows the mounting used in the sensitivity and loss of mass experiments. The test piece was clamped to the mounting more firmly and along its whole length. Figure 31 shows a flow chart of the procedure in sensitivity analysis.

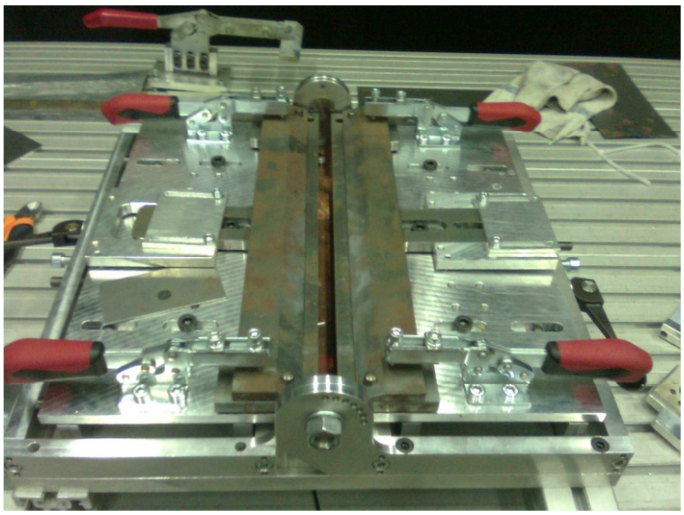

*Figure 30. Mounting for the sensitivity experiments.*

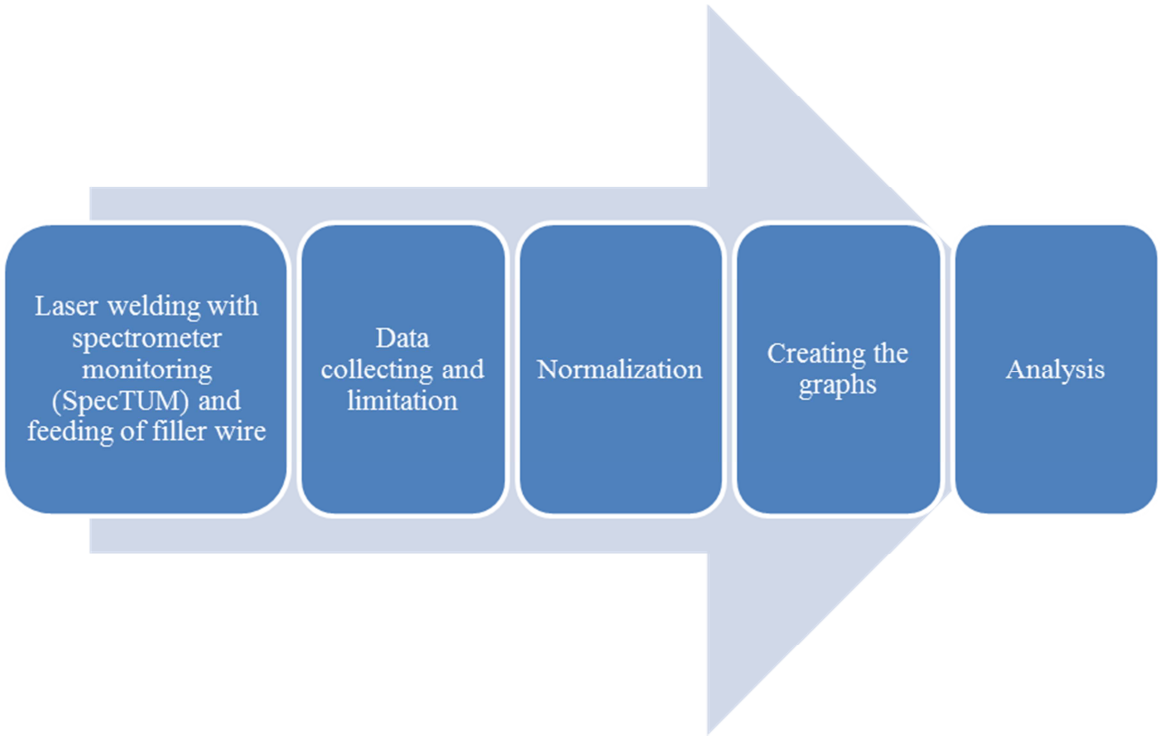


*Figure 31. Procedure of the analysis in sensitivity experiments.*

### 3.5.2.1 Calculations for the volume percentages

The contents of certain elements in any material are normally given in mass percentages in material standards. Usually the information mass percent gives is enough, but when calculations of material flow or volume are needed, the volume percentage of different elements in the material have to be known. Therefore the concentration of magnesium content in volume percentage needed to be calculated. The concentration in the base material could be measured with a spark-emission spectrometer, but the concentration in the filler wire needed to be calculated. Before calculating the actual magnesium content by volume, the linear density of the filler wire needed to be calculated. For that, density and mass percentage of each alloying component of the filler wire needed to be known. This information was taken from material standards. The linear density was calculated from the equation given in (20) and the data for the calculation and the result are presented in table 8.

$$\rho_{lin} = \sum_i a_i \cdot \rho_i \cdot V_i \,, \tag{20}$$

where

$\rho_{lin}$ : Linear density of the filler wire

$a_i$ : Mass percentage of *i*:th element

$\rho_i$ : Density of *i*:th element

$V_i$ : Volume of *i*:th element in one meter of the filler wire

*Table 8. Data and result for the linear density of the filler wire AlMg5.*

| | Si | Mn | Cr | Cu | Ti | Zn | Fe | Mg | Al | Sum |
|---|---|---|---|---|---|---|---|---|---|---|
| mass % | 0.0020 | 0.0015 | 0.0013 | 0.0008 | 0.0013 | 0.0008 | 0.0002 | 0.0500 | 0.9421 | 1.00 |
| Density | 2330 | 7210 | 7150 | 8960 | 4506 | 7140 | 7860 | 1738 | 2700 | **Total mass/meter** |
| Filler wire volume | 7.85E-07 | 7.85E-07 | 7.85E-07 | 7.85E-07 | 7.85E-07 | 7.85E-07 | 7.85E-07 | 7.85E-07 | 7.85E-07 | **[kg/m$^3$]** |
| Elemental mass | 3.66E-06 | 8.49E-06 | 7.30E-06 | 5.63E-06 | 4.60E-06 | 4.49E-06 | 1.23E-06 | 6.83E-05 | 2.00E-03 | **0.00210** |

The volume percentage of magnesium in the filler wire was calculated from the equation given in (21). The data and the result of the calculation are presented in table 9.

$$b_{Mg} = \frac{\rho_{lin} \cdot b_{Mg}}{A_f \cdot \rho_{Mg}}, \tag{21}$$

where

$b_{Mg}$ : Volume percentage of magnesium in the filler wire

$A_f$ : Area of the filler wire cross-section

*Table 9. Data and result for the magnesium content in the filler wire AlMg5.*

| Name | Unit | Value |
|---|---|---|
| Density of magnesium | kg/m$^3$ | 1738 |
| Linear density of filler wire | kg/m | 2.1 x 10$^{-3}$ |
| Mass percentage of magnesium | mass -% | 5.0 |
| Filler wire area | m$^2$ | 7.9 x 10$^{-7}$ |
| **Volume percentage of magnesium** | **vol-%** | **7.69** |

Calculating the magnesium contents of the components in the weld with the given value from the standards could lead into severe miscalculations. The low density of magnesium causes the volume percentage to be significantly higher than the mass percentage as can be seen from table 9.

### 3.5.2.2 Calculations of elemental contents in weld

There is always vaporization of material during keyhole welding. One part of this research was to find out how much magnesium vaporizes during welding. To evaluate the loss of magnesium it was necessary to calculate how much magnesium there would be in the weld if no vaporization took place. To calculate a nominal content of magnesium in the weld seam certain parameters need to be known. These include welding speed, filler wire feeding rate, the elemental content in the base material as well as in the filler wire, the area of the filler wire and the weld cross-section and length of the weld. In principal, an elemental content within a weld cannot be calculated before the actual welding, since the area of the weld has to be known. And taking in concern the instable character of welding process, this cannot be accurately evaluated. The experiments for sensitivity were conducted with a filler wire to get different compositions of magnesium within the weld. The used filler wire was AlMg5, whose chemical composition was shown before. The diameter of the filler wire was 1 mm. The feeding of filler wire makes it even more difficult to evaluate the area of the weld cross-section and during these experiments the filler wire was fed in various rates to change the composition in the weld. Therefore, the area of the weld cross-section needed to be measured from each test piece.

The calculation of the Mg-content in the weld seam begins with an assumption that the actual weld consists of the volumes of the base material and the filler wire. First, it is important to define the volume of the weld before Mg-contents can be calculated. Equation (22) presents the basic hypothesis of the resulting volume of the weld.

$$V_w = V_m + V_f , \tag{22}$$

where

$V_w$ : Volume of the weld

$V_m$ : Volume of the base material

$V_f$ : Volume of the filler wire.

The volumes can be calculated from the equations given in (23), (24) and (25).

$$V_w = A_w l_w \tag{23}$$

$$V_f = A_f v_f V_w \tag{23}$$

$$V_m = V_w - V_f , \tag{24}$$

where

$A_w$ : Area of the weld cross-section

$l_w$ : Length of the weld

$t_w$ : Welding time

The welding time can be calculated from the equation (26) and substituted into equation (23) thus reformulating into equation (27). The acceleration and deceleration of the robot were ignored in the calulations.

$$t_w = \frac{l_w}{v_w} \tag{26}$$

$$V_f = \frac{A_f v_f}{v_w} l_w , \tag{27}$$

Now the base material volume can be reformulated and calculated from the equation (28) i.e. if the area of the weld cross section is known.

$$V_m = l_w \left[ A_w - \frac{A_f v_f}{v_w} \right] \tag{28}$$

When the volumes of the components are known, the elemental concentrations can be taken into calculation. Equation (29) allows the calculation of elemental concentration in the weld seam. It presumes that the contents are in volume percentages. That way the volume concentration of a specific element can be summed.

$$x_{Mg} \cdot V_w = b_{Mg} \cdot V_f + a_{Mg} \cdot V_m , \tag{29}$$

where

$x_{Mg}$ : Mg-content in the weld

$b_{Mg}$ : Mg-content in the filler wire

$a_{Mg}$ : Mg-content in the base material

Now, when the equation is solved in terms of the Mg-content in the weld and all the known variables are substituted, the Mg-content in the weld can be calculated from the final equation given in (30).

$$x_{Mg} = \frac{b_{Mg}\frac{A_f v_f}{v_w} + a_{Mg}\left[A_w - \frac{A_f v_f}{v_w}\right]}{A_w}, \tag{30}$$

### 3.5.3 Repeatability experiments

The material in the repeatability experiments was the same as in the sensitivity experiments, EN AW-6060. During the 80 mm long weld, the emissions were monitored and recorded by the spectrometer and its programs. The used program was SpecTUM, since only the average intensities were of interest. The parameters for the welding equipment and the spectrometer are shown in table 10. In total ten welds were made and 250 pictures per weld were taken. All the test pieces were marked after welding with consecutive numbering and welding direction for further examination. Figure 32 shows a flow chart of the procedure in repeatability analysis.

*Table 10. Welding and spectrometer parameters for the repeatability experiments.*

| Welding parameters | | | | | | | Spectrometer parameters | | | | | |
|---|---|---|---|---|---|---|---|---|---|---|---|---|
| Consecutive numbering | Welding speed | Power HPDL | Power YAG | Welding angle | Gas flow | Shielding gas | Start pixel | End pixel | Integration time | Number of pictures | Acceptable noise level | Useful pictures |
| | m/min | W | W | deg | l/min | | | | ms | | counts | |
| 1 | 2.0 | 1.3x3000 | 3000 | 18 | 20 | Ar | 0 | 1600 | 6 | 250 | 400 | 246 |
| 2 | 2.0 | 1.3x3000 | 3000 | 18 | 20 | Ar | 0 | 1600 | 6 | 250 | 400 | 246 |
| 3 | 2.0 | 1.3x3000 | 3000 | 18 | 20 | Ar | 0 | 1600 | 6 | 250 | 400 | 245 |
| 4 | 2.0 | 1.3x3000 | 3000 | 18 | 20 | Ar | 0 | 1600 | 6 | 250 | 400 | 245 |
| 5 | 2.0 | 1.3x3000 | 3000 | 18 | 20 | Ar | 0 | 1600 | 6 | 250 | 400 | 245 |
| 6 | 2.0 | 1.3x3000 | 3000 | 18 | 20 | Ar | 0 | 1600 | 6 | 250 | 400 | 245 |
| 7 | 2.0 | 1.3x3000 | 3000 | 18 | 20 | Ar | 0 | 1600 | 6 | 250 | 400 | 245 |
| 8 | 2.0 | 1.3x3000 | 3000 | 18 | 20 | Ar | 0 | 1600 | 6 | 250 | 400 | 245 |
| 9 | 2.0 | 1.3x3000 | 3000 | 18 | 20 | Ar | 0 | 1600 | 6 | 250 | 400 | 245 |
| 10 | 2.0 | 1.3x3000 | 3000 | 18 | 20 | Ar | 0 | 1600 | 6 | 250 | 400 | 245 |

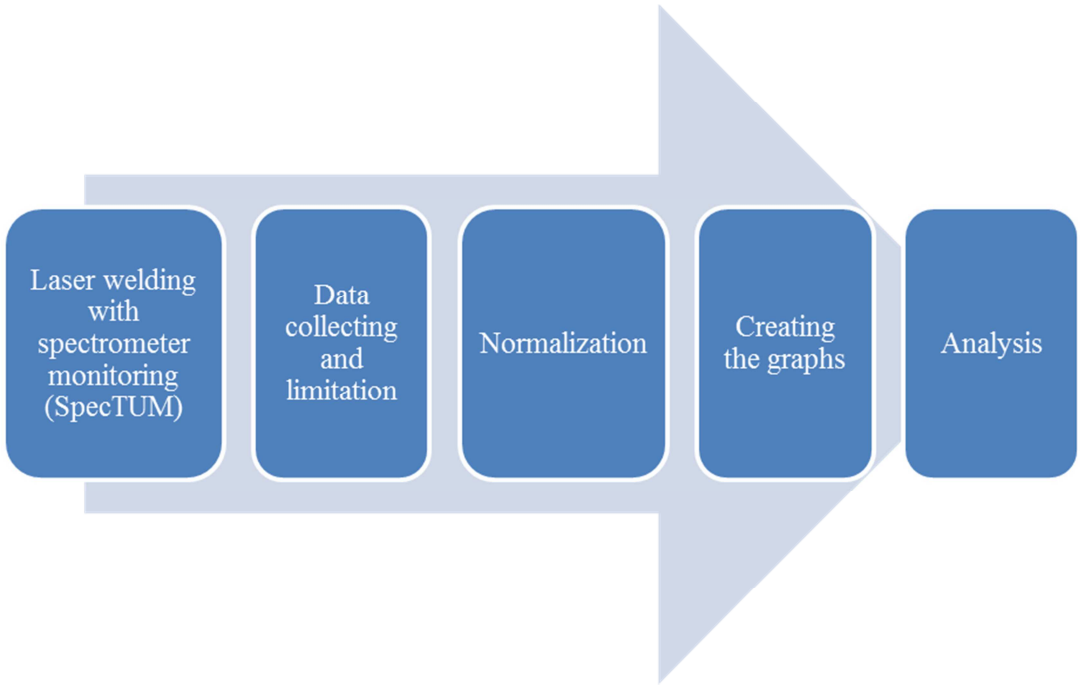


*Figure 32. Procedure of the analysis in repeatability experiments.*

### 3.5.4 Stability experiments

The material for the stability experiments can be seen from table 3. The actual volume content was measured with a spark emission spectrometer before the welding. Table 11 shows the average magnesium contents in the test pieces and their deviations. In total eight measurements per test pieces were made. It can be seen from table 11 that the measured contents varied relatively much. Also the average contents from test piece to test piece vary considerably.

*Table 11. Average magnesium contents in the test pieces for stability experiments.*

| Test piece | Average | Standard deviation | Variability index |
|---|---|---|---|
| | vol-% | vol-% | % |
| Ex1 | 9,23 | 0,24 | 2,63 |
| Ex2 | 9,08 | 0,21 | 2,27 |
| Ex3 | 8,78 | 0,53 | 6,00 |
| Ex4 | 9,39 | 0,14 | 1,49 |
| Ex5 | 8,21 | 0,64 | 7,83 |
| Ex6 | 9,22 | 0,15 | 1,65 |
| Ex7 | 8,96 | 0,15 | 1,70 |
| Ex8 | 8,63 | 0,36 | 4,15 |
| Ex9 | 8,86 | 0,27 | 3,05 |

Both stability and repeatability experiments were welded with the same parameters, including welding length. Figure 33 illustrates the mounting of the two experiments. Here the clamps were shorter than the ones in sensitivity experimental setup. The welding program was designed so that the test piece could be set against the metal plate at the top of the mounting. Figure 34 shows a flow chart of the procedure in stability analysis.

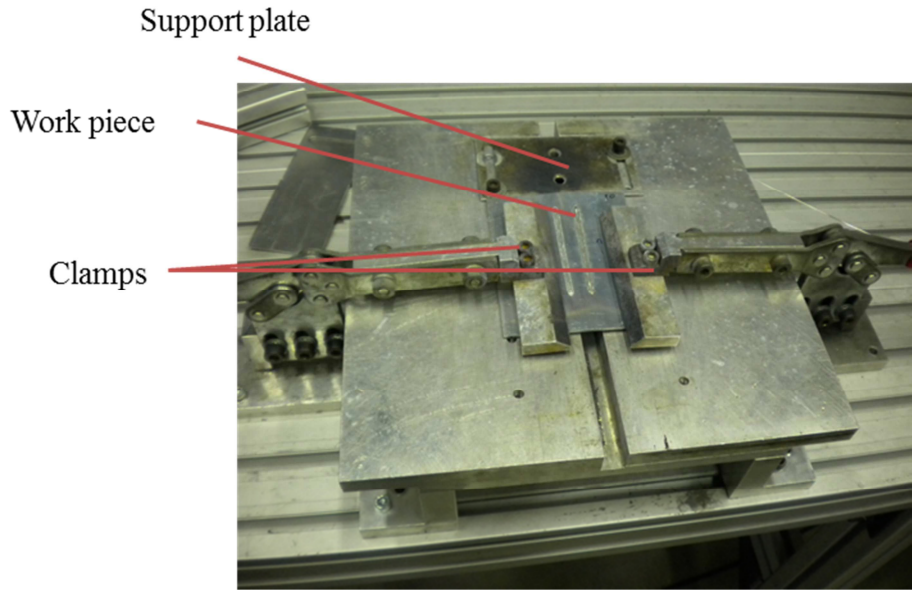


*Figure 33. Mounting for stability and repeatability experiments.*

The same preparations were made to the test pieces for stability experiments as for the ones for repeatability experiments. The material thickness for the stability experiments was 3 mm, which meant that the welding program was changed so that the welding head was raised 1 mm upwards. Other parameters were the same as before, as shown in table 12.

*Table 12. Welding and spectrometer parameters for stability experiments.*

| Welding parameters | | | | | | | Spectrometer parameters | | | | | |
|---|---|---|---|---|---|---|---|---|---|---|---|---|
| Consecutive numbering | Welding speed | Power HPDL | Power YAG | Welding angle | Gas flow | Shielding gas | Start pixel | End pixel | Integration time | Number of pictures | Acceptable noise level | Useful pictures |
| | m/min | W | W | deg | l/min | | | | ms | | counts | |
| 1 | 2.0 | 1.3x3000 | 3000 | 18 | 20 | Ar | 0 | 1600 | 6 | 250 | 400 | 247 |
| 2 | 2.0 | 1.3x3000 | 3000 | 18 | 20 | Ar | 0 | 1600 | 6 | 250 | 400 | 244 |
| 3 | 2.0 | 1.3x3000 | 3000 | 18 | 20 | Ar | 0 | 1600 | 6 | 250 | 400 | 246 |
| 4 | 2.0 | 1.3x3000 | 3000 | 18 | 20 | Ar | 0 | 1600 | 6 | 250 | 400 | 247 |
| 5 | 2.0 | 1.3x3000 | 3000 | 18 | 20 | Ar | 0 | 1600 | 6 | 250 | 400 | 248 |
| 6 | 2.0 | 1.3x3000 | 3000 | 18 | 20 | Ar | 0 | 1600 | 6 | 250 | 400 | 247 |
| 7 | 2.0 | 1.3x3000 | 3000 | 18 | 20 | Ar | 0 | 1600 | 6 | 250 | 400 | 245 |
| 8 | 2.0 | 1.3x3000 | 3000 | 18 | 20 | Ar | 0 | 1600 | 6 | 250 | 400 | 247 |
| 9 | 2.0 | 1.3x3000 | 3000 | 18 | 20 | Ar | 0 | 1600 | 6 | 250 | 400 | 247 |

The monitoring and recording of the emissions during the stability experiments was done with SpecTUMall, which shows the emissions of every picture taken in separate text files. It also calculates the maximum and middle intensities in separate text files. There were two columns in the text files. The first column had the wavelengths and the other one had the corresponding value of emission intensity. All these files were imported to Excel with a macro that imported only the values of the text files to columns and copied the name of the text file to the cell of the first row. Last thing it copied the wavelengths from the text file of maximum values to the first column. After the macro had finished, the Excel sheet had all the names of the text files on the first row and under the names were the values of that particular text file. After importing all the text files to one Excel sheet, another macro was used. This macro collected all the important aluminium and magnesium intensities to the bottom of the sheet, so that they could be easier to analyse. Then another macro plotted the curves for these important intensities as a function of time. The last macro plotted all the aluminium curves to their own plot and the magnesium curves to theirs.

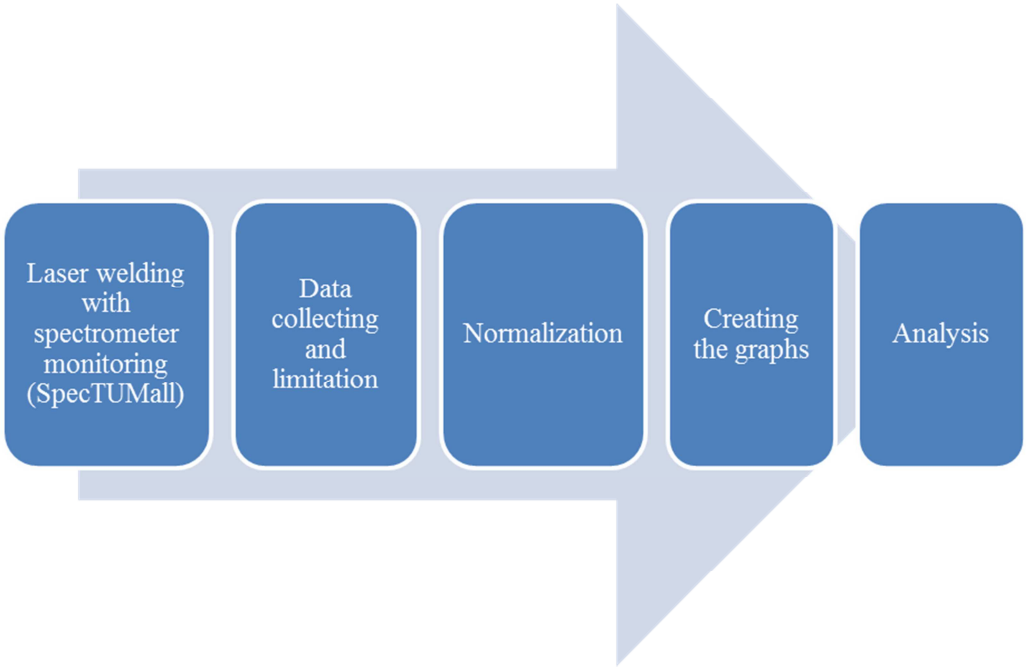


*Figure 34. Procedure of the analysis in stability experiments.*

# 4 RESULTS AND ANALYSIS

For the examination of the results a qualitative analysis needs to be made. The focus of this research was the analysis of the behaviour of magnesium and aluminium emission lines during laser welding. Therefore, in qualitative analysis the emission lines of these two elements have to be found in the characteristic spectrum. Qualitative analysis for this experimental setup was already investigated by Glasschröder (Glasschröder, 2010). Since this research was meant to be a continuation of the work done by Glasschröder, the same methods from the qualitative analysis were used here. Figure 35 shows a spectrum of maximum values of the emissions during laser welding of aluminium. The data for the figure is taken from the sensitivity experiment number two. The parameters for that experiment are shown in table 7. Here, the character of dominating alumina lines is clearly visible. Also the second magnesium line at 518.21 nm and its direct location right next to the alumina lines is observable. The two aluminium peaks at 394.34 nm and 396.06 nm are always present when welding aluminium. The line at 396.06 nm is normally a bit stronger than the line at 394.34 nm. The magnesium line at 383.47 nm is here quite strong. On low magnesium contents this line stays weaker and is sometimes rather difficult to observe. This spectrum, taken from the maximum emission values of that welding process, has fairly strong intensities. From here on, average intensities will be examined and thus the intensities will also be much weaker. The only exception is stability research, where every recorded emission matters.

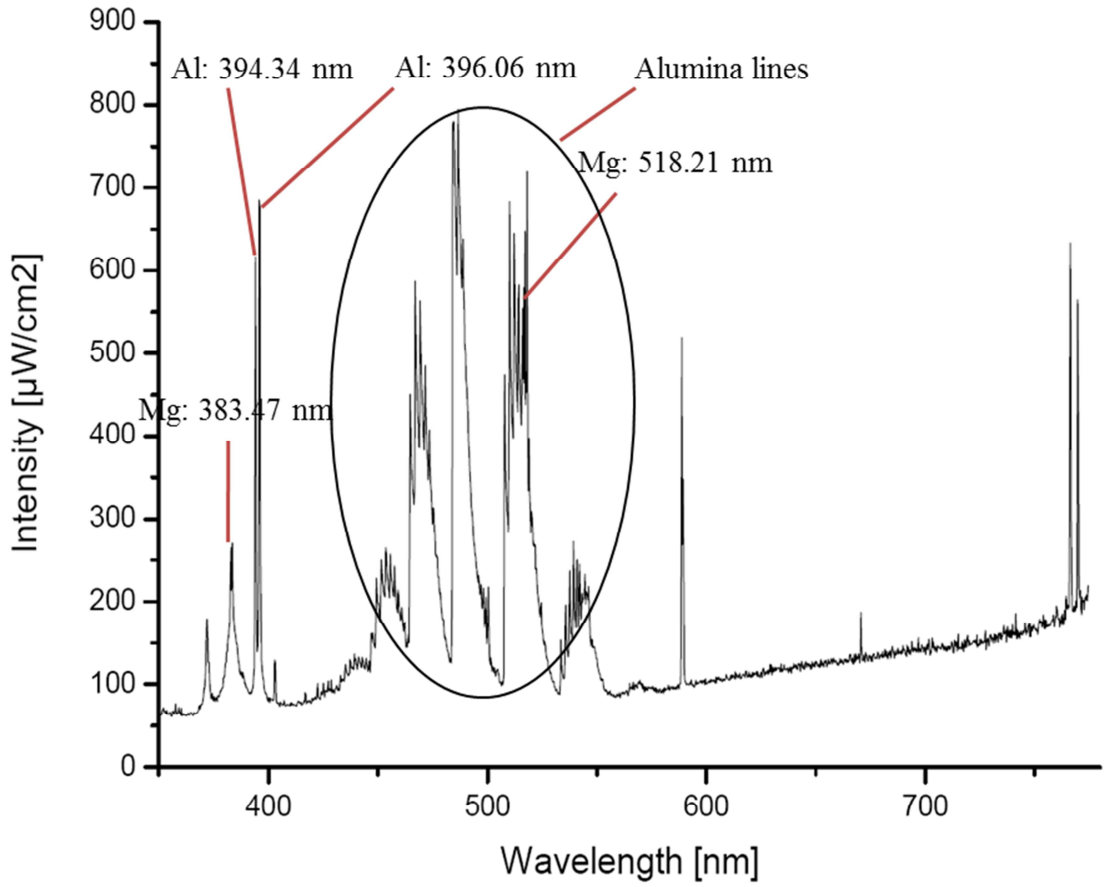


*Figure 35. Typical spectrum of maximum emissions detected during laser welding of aluminium alloy.*

## 4.1 Repeatability experiments

The weldings were conducted with the parameters shown earlier in table 10. After welding, the text files printed by SpecTUM were imported to Excel for the analysing. After all the ten files were imported, averages and deviations for the wavelengths were calculated and curves of the spectra plotted. In early stages of analysing the results, it was noticed that normalizing of the intensities would be necessary. The emissions in laser welding are always somewhat instable and emissions of different welds can differ quite a lot. So to compare emissions of different welding processes, the emissions should be normalized. A different approach to this matter would be to analyse the repeatability roughly only by comparing the emissions quantitatively. This kind of analysing would include also the natural behaviour of the laser welding emissions to the repeatability examination. Both types of analysing were used in this research.

The normalizing should always be done by some very constant value. Since the material used in these experiments was aluminium alloy EN AW-6060, the aluminium content in the test pieces should stay quite constant and the percentual changes in the content should be small. So, the normalizing was done by aluminium and as the actual wavelength was chosen 394.3414 nm, since this wavelength was also used in previous research (Glasschröder, 2010). The emissions of this aluminium line seemed to be a bit more stable than of the other one at 396.0554 nm. From here on all the normalized results are presented so that ratio=1.0 represents the intensity of aluminium line at 394.3414 nm of that particular spectrum and ratio=1.2 represents intensity that is 20 % stronger. Average spectra of ten welds from the repeatability experiments that are not normalized are shown in figure 36, and in figure 37 spectra of the same welds with normalizing are shown. It is quite clearly visible that the normalizing makes the spectra more uniform, which means that the emissions are in fact very similar regardless of the number of experiment. On the other hand, the non-normalized spectra are also quiteuniform, but the character of unstableness of laser beam welding is still visible, especially in the two aluminium peaks at 394.3414 and 396.0554 nm and the aluminium oxide lines.

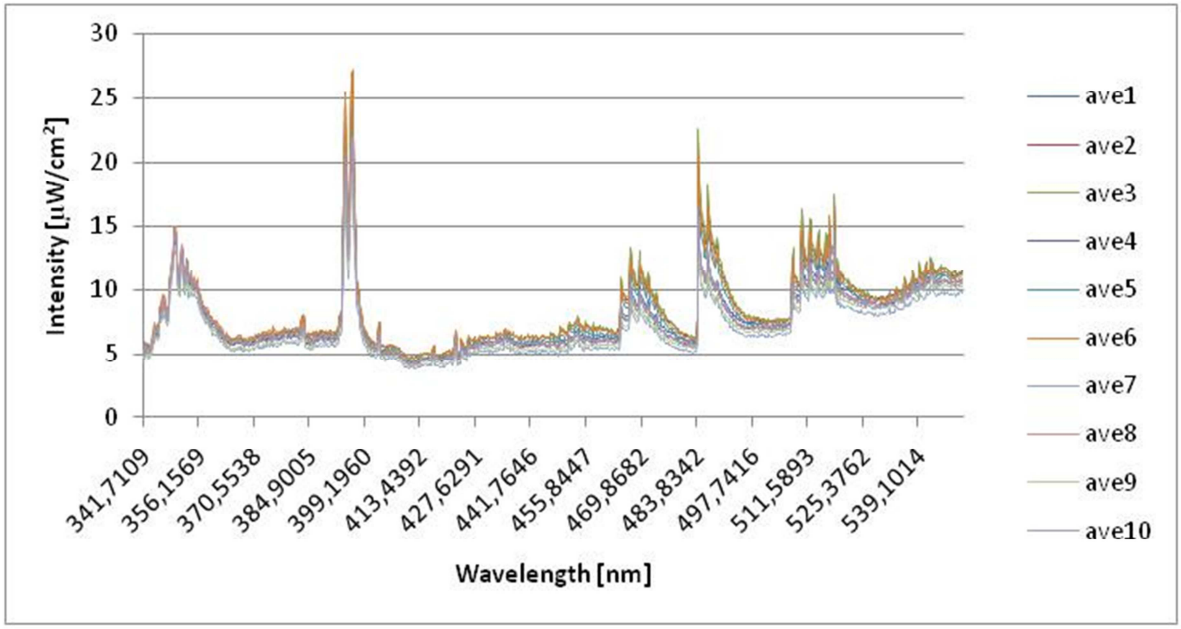


*Figure 36. Average spectra of the repeatability experiments without normalizing.*

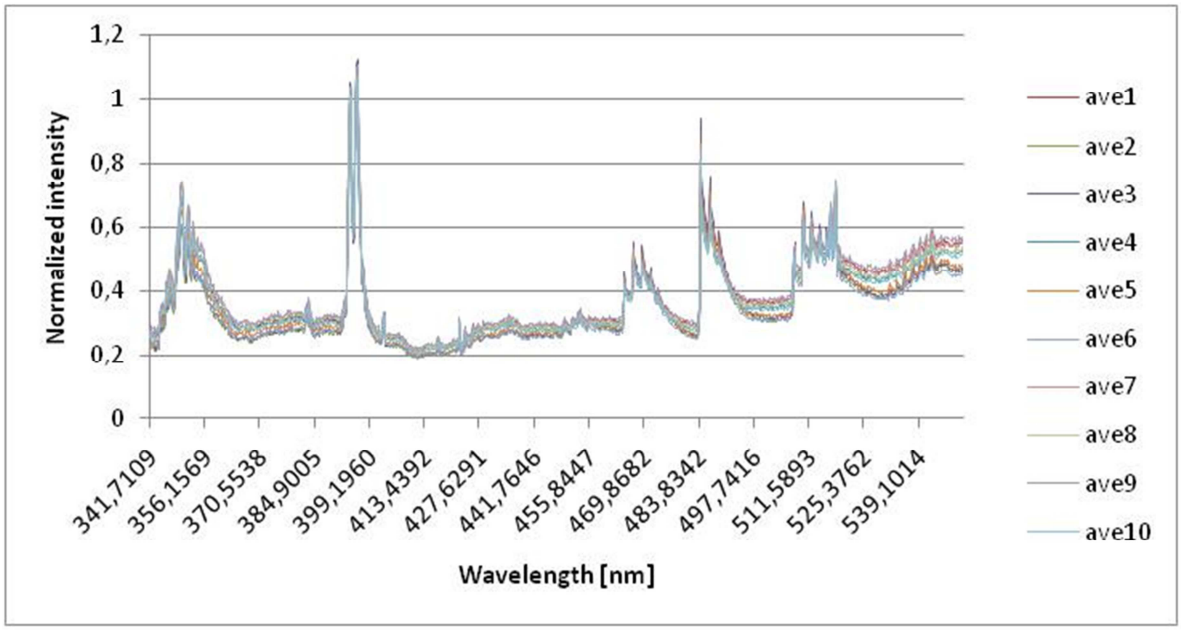


*Figure 37. Normalized average spectra of the repeatability experiments.*

Table 13 shows the average and standard deviation of the two main magnesium lines and the two main aluminium lines used for repeatability analysis. From the table it can be clearly seen that the deviations of magnesium and aluminium intensities are quite mild. Variability index is a statistical term that describes the percentual deviation of a test sample. Sometimes standard deviation of different values is not directly comparable, because when values are greater, also deviation is greater. Only percentual deviations are directly comparable. In table 13 also variability index is given for each wavelength. The table shows that the percentual deviation of the absolute values is quite mild, especially for magnesium lines. This can, however, be disturbing, since the bigger deviation of aluminium lines suggests that between different tests there has been some variety in emission intensities. Therefore, if one wants to examine the intensities without the unstable character of emissions during a welding process one should concentrate on the normalized values and their deviation. The percentual deviation of all the examined wavelengths showed in table 13 is very small. Especially, it seems that the emissions of the magnesium line at 518.2147 nm behave really stable and the repeatability of measuring this wavelength with identical experimental setup is relatively good, variability index being only 2.74 %. The repeatability as a statistical measure is the standard deviation in table 13.

*Table 13. Absolute and normalized values of the results from the repeatability experiments.*

| Absolute values | | | | | | | | | | | | | | |
|---|---|---|---|---|---|---|---|---|---|---|---|---|---|---|
| | Wavelength | 1 | 2 | 3 | 4 | 5 | 6 | 7 | 8 | 9 | 10 | Average | Standard deviation | Variability index |
| | [nm] | [μW/cm$^2$] | | | | | | | | | | | | % |
| Aluminium lines | 394,3413 | 20,33 | 24,43 | 24,08 | 20,34 | 22,42 | 24,56 | 17,78 | 20,23 | 18,16 | 20,36 | **21,27** | **2,48** | **11,68** |
| | 396,0554 | 21,05 | 26,91 | 27,11 | 21,71 | 24,59 | 27,21 | 19,35 | 21,62 | 19,14 | 21,92 | **23,06** | **3,15** | **13,65** |
| Magnesium lines | 383,4681 | 7,18 | 8,01 | 7,96 | 7,03 | 7,65 | 8,03 | 6,56 | 7,4 | 6,83 | 7,2 | **7,39** | **0,52** | **6,99** |
| | 518,2147 | 14,97 | 17,28 | 17,49 | 14,71 | 16,31 | 16,61 | 13,08 | 14,58 | 13,61 | 14,81 | **15,35** | **1,51** | **9,82** |
| **Normalized values** | | | | | | | | | | | | | | |
| | Wavelength | 1 | 2 | 3 | 4 | 5 | 6 | 7 | 8 | 9 | 10 | Average | Standard deviation | Variability index |
| | [nm] | | | | | | | | | | | | | % |
| Aluminium lines | 394,3413 | 1 | 1 | 1 | 1 | 1 | 1 | 1 | 1 | 1 | 1 | **1,00** | **0,00** | **0,00** |
| | 396,0554 | 1,035 | 1,102 | 1,126 | 1,067 | 1,097 | 1,108 | 1,088 | 1,069 | 1,054 | 1,077 | **1,08** | **0,03** | **2,50** |
| Magnesium lines | 383,4681 | 0,353 | 0,328 | 0,331 | 0,346 | 0,341 | 0,327 | 0,369 | 0,366 | 0,376 | 0,354 | **0,35** | **0,02** | **5,05** |
| | 518,2147 | 0,736 | 0,707 | 0,726 | 0,723 | 0,727 | 0,676 | 0,736 | 0,721 | 0,749 | 0,727 | **0,72** | **0,02** | **2,74** |

Based on the results of the repeatability experiments it can be said that the standard deviation of aluminium lines describe the repeatability of the whole spectrum of emissions. In other words, the deviation of aluminium lines represents the deviation of all the spectra between different welds. It describes the unstableness of the process. But when the interest is only in some particular emission line and how it behaves, the emissions should be examined after normalization. The result of the repeatability experiments is that the repeatability of the recorded spectrum has a percentual deviation of about 12 % and the normalized emissions of magnesium lines at 383.4681 nm have a percentual deviation of about 5 % and at 518.2147 the percentual deviation is fewer than 3 %. In absolute values the percentual deviation of magnesium emissions is a bit under 10 %. These results are competent only for this particular experimental setup and material EN AW-6060. More illustrative results are shown in figures 38 and 39. The data for these figures are the same as for the figures 36 and 37 and table 13. In these curves the absolute and normalized values of aluminium and magnesium emissions are shown. The latter curves with normalized intensities seem to behave quite steadily. The two lines are almost even, which suggests that the process is well repeatable. Stronger alteration in the emission values between tests would have a negative effect on the repeatability of the process.

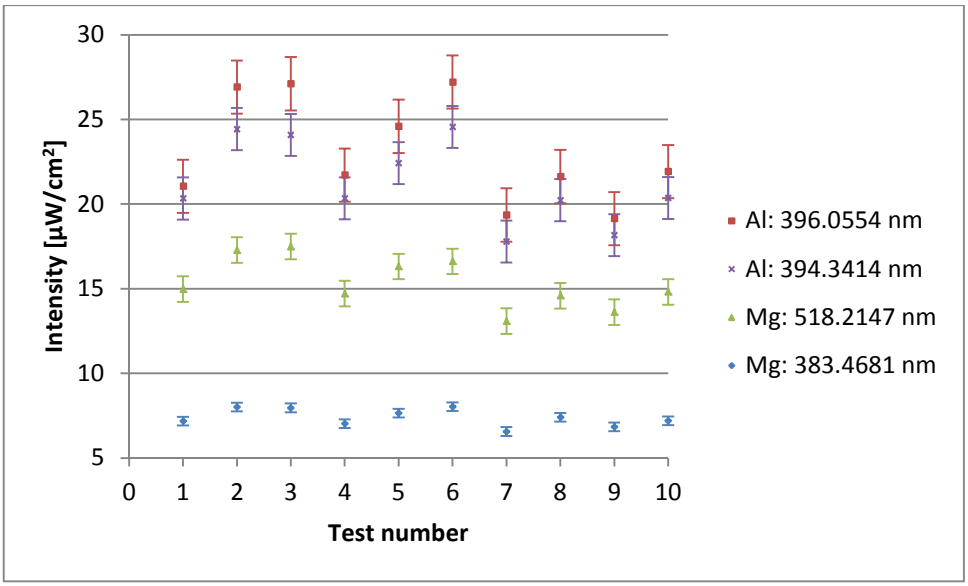


*Figure 38. Absolute intensities of the analysed emission lines.*

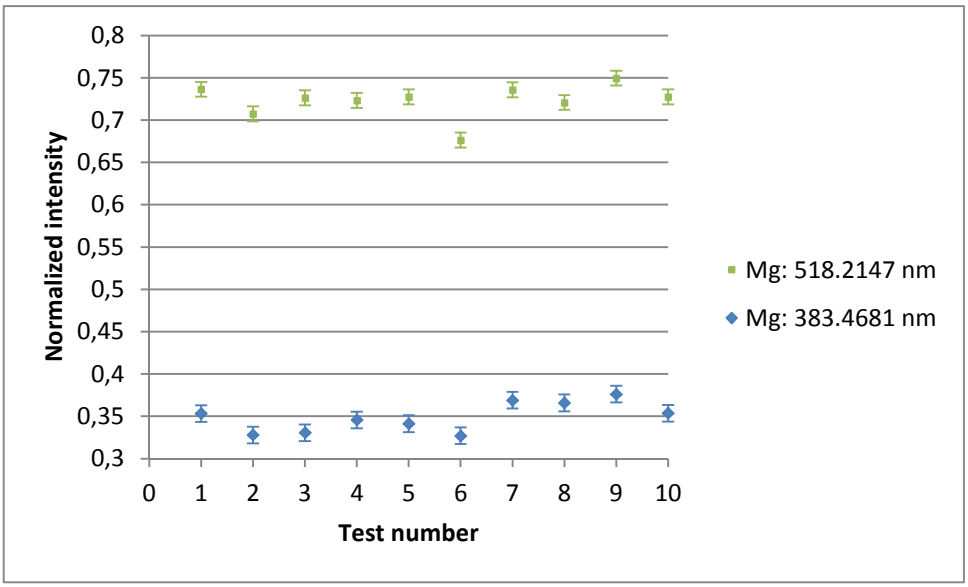


*Figure 39. Normalized intensities of the magnesium emission lines.*

The first figure with all four wavelengths has similar behaviour on different levels. This means that the changes in each curve have been global change. It is also observable that the higher the intensities of one emission line are the stronger is the deviation. The second figure, with the two magnesium lines, shows the great repeatability of the process. Also here the changes seem to be global. Because of the normalization the deviations caused by the changes in the whole process emissions have been minimized. Therefore the changes visible in figure 39 have remained relatively small and insignificant. In conclusion, the repeatability of measuring magnesium and aluminium emissions is the following:

- absolute intensities:
    - Al - 394.3414 nm: 88 %
    - Al - 396.0554 nm: 86 %
    - Mg - 383.4681 nm: 93 %
    - Mg - 518.2147 nm: 90 %
- normalized intensities:
    - Mg - 383.4681 nm: 95 %
    - Mg - 518.2147 nm: 97 %

## 4.2 Stability experiments

There were nine test pieces for stability experiments from the material presented in table 3. In total nine Excel sheets were combined into one Excel workbook. Average values and standard deviations were then calculated from the important wavelengths of all the test results. From these averages, deviations and plots, the final analysis was done. There were two main courses of analysis. Firstly, it was to be examined how stable the process was by calculating the ratio of useful and useless spectra. Secondly, the stability of magnesium and aluminium lines as a function of time was to be examined. This was then divided into analysing the intensities as absolute values to clarify the stability of the whole spectra and into analysing the intensities as normalized values to clarify the stability of these particular wavelengths.

Table 14 shows the great stability of the welding and monitoring process when comparing the ratio of useful pictures and all the pictures taken during welding. The result states that when monitoring an identical welding process with an identical spectrometer setup 98.6 % of the spectra are useful for analysing. Still there may be variation within these useful spectra. But only 1.4 % of the total pictures taken and their maximum intensities remain under the acceptable noise level or out of scale for some reason. This can be caused by a collapse of a keyhole, smoke blocking the detection of the spectrometer or for some other reason.

*Table 14. The ratio of useful and useless spectra.*

| Test piece | Pictures taken | Pictures taken | Ratio % |
|---|---|---|---|
| **Ex1** | 250 | 247 | 98,80 |
| **Ex2** | 250 | 244 | 97,60 |
| **Ex3** | 250 | 246 | 98,40 |
| **Ex4** | 250 | 247 | 98,80 |
| **Ex5** | 250 | 248 | 99,20 |
| **Ex6** | 250 | 247 | 98,80 |
| **Ex7** | 250 | 245 | 98,00 |
| **Ex8** | 250 | 247 | 98,80 |
| **Ex9** | 250 | 247 | 98,80 |
| **Average** | **250** | **246** | **98,58** |

The test pieces had roughly 9 % magnesium by volume. This is a quite large amount for an alloying element such as magnesium in an aluminium alloy. For instance, aluminium alloys from the 6000-series have magnesium as one of their main alloying elements. For instance, EN AW-6060 has about 0.5 % magnesium by mass. It was noticed during welding, that this amount of magnesium caused quite a lot of sparkles and smoke during welding due to the burning of magnesium. This would most certainly have a considerable influence on the stability of the emissions detected by the spectrometer. During the early stages of analysing the results of the stability experiments was noticed, that the instability of the process emissions during welding was significant. The average intensity of each studied wavelength seemed to stay at a certain level after the low intensities of the beginning of the welding process. Also the instability stayed quite similar throughout the welding process. The figures 40 – 43 show quite figuratively the nature of the process. The pictures illustrate the intensities of the main lines of aluminium and magnesium as a function of picture number, which can be transformed into time and welding length since the integration time and the number of picture is known. Taking 250 pictures with an integration time of 6 ms takes about 1.5 seconds.

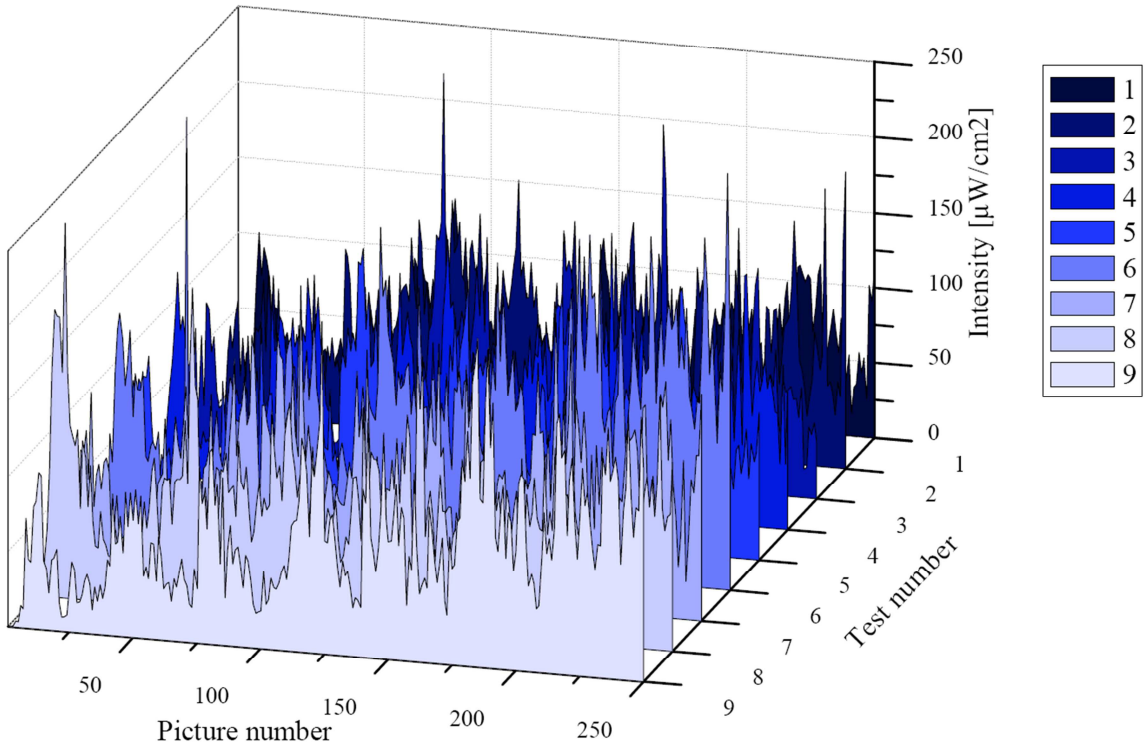


*Figure 40. Intensities of the aluminium line at 394.3414 nm as a function of picture number.*

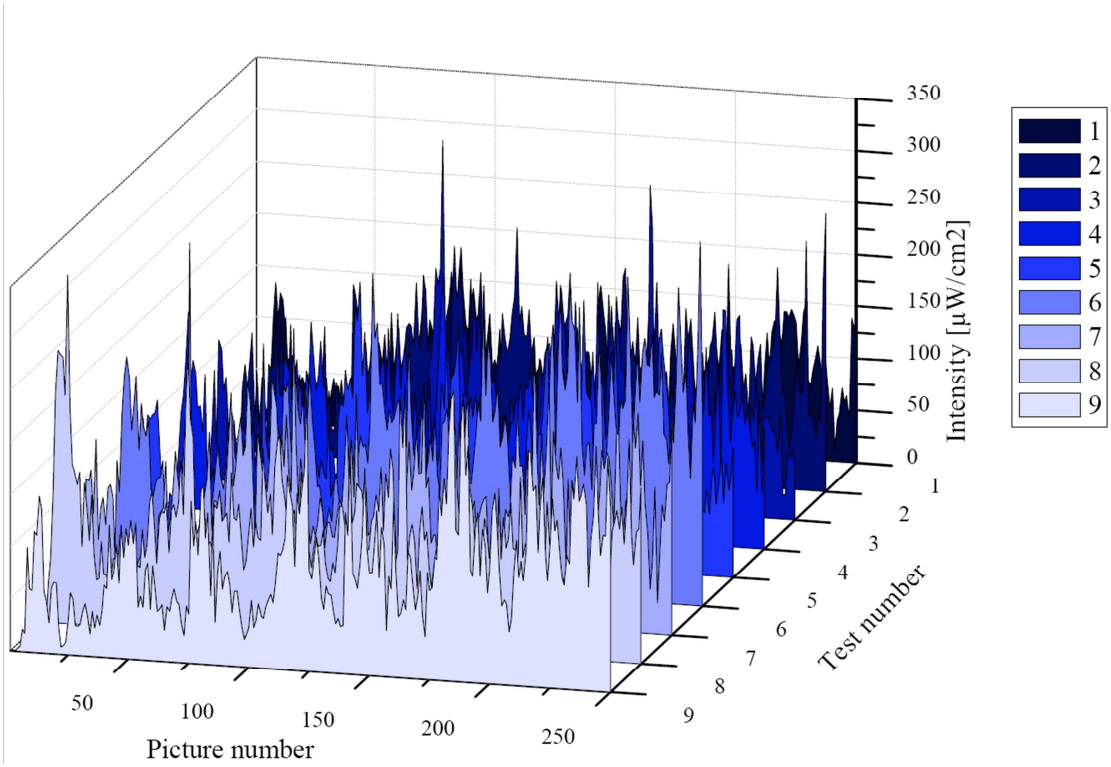


*Figure 41. Intensities of the aluminium line at 396.0554 nm as a function of picture number.*

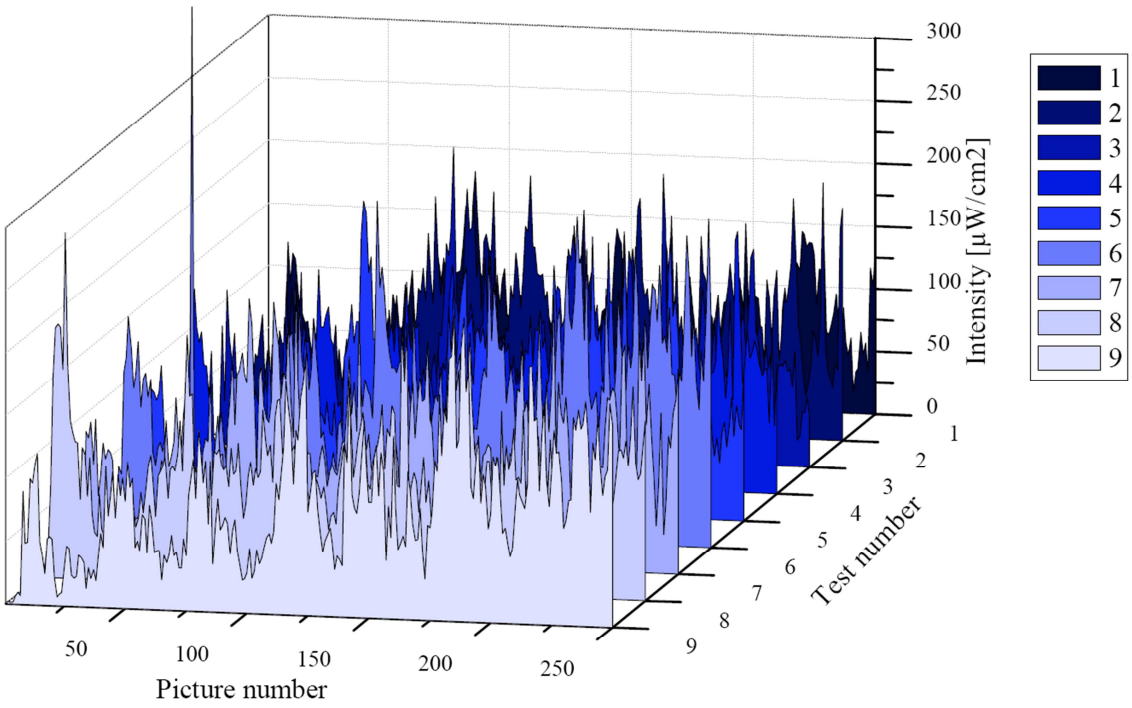


*Figure 42. Intensities of the magnesium line at 383.4681 nm as a function of picture number.*

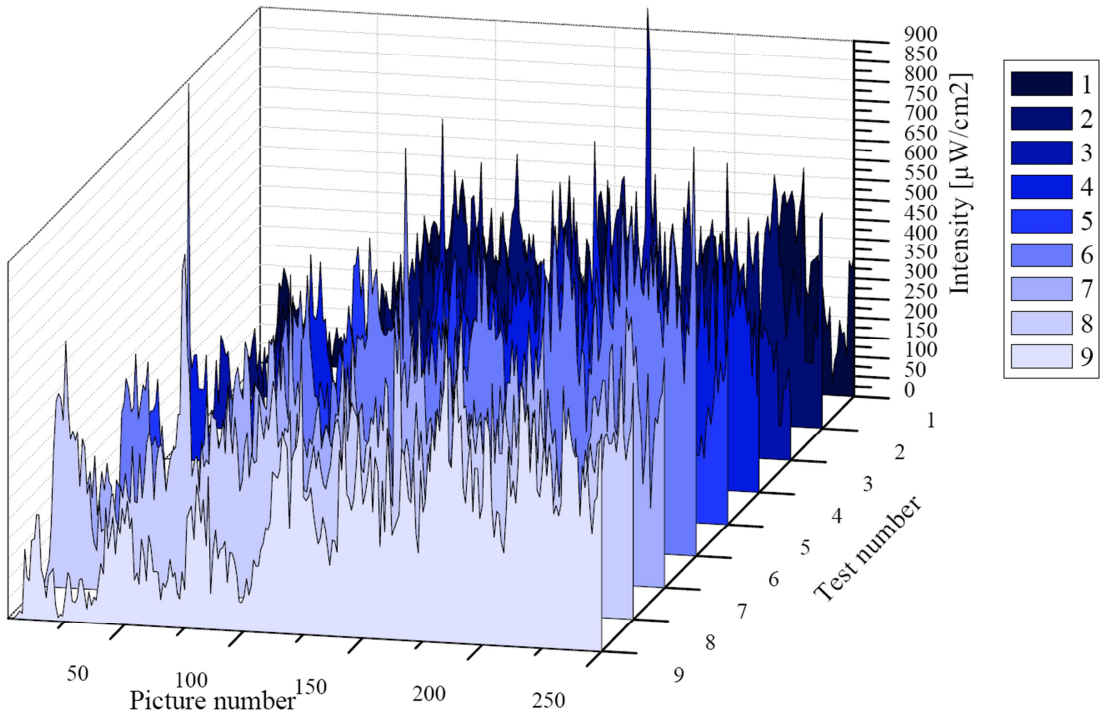


*Figure 43. Intensities of the magnesium line at 518.2147 nm as a function of picture number.*

Table 15 shows the standard deviation and percentual deviation for each of the important wavelengths. In the table the deviation is shown for each work piece and in total. The total average and deviation was calculated from the whole data pool, not from the already calculated average and deviation. The high deviation let assume of a very instable process. The deviation of the total intensities is a bit higher than the deviation of the individual test pieces. The higher value can be explained by the variance of intensity levels from test weld to test weld. From the table can also be seen that the average intensities of the same wavelength vary quite a lot. This shows that there were significant intensity level differences between different test welds. Therefore, the total deviation includes also the variance of the average intensity level when comparing different test welds, but it also describes quite well the stability of the emissions during welding. From table 15 it can also be seen, that all the wavelengths have quite similar deviation. All the wavelengths seem to have percentual deviation of roughly 55 %. From the figures 40 – 43 this kind of similarity could already be predicted. These results show that none of these examined wavelengths behave significantly more stable than the others.

The values presented in table 15 are absolute values for the intensities of the emissions from the welding processes. As mentioned before, there is always some natural variance in the average emission intensity level between different welds. Therefore, it is crucial to normalize the values in respect to some fairly stabile emission line. Normalizing the intensities allows analysing of the results without the influence of the natural variance of intensity levels and comparing the results of different welds with each other. Reliable analysing of magnesium emissions demand normalized intensities. Same as before, the normalizing was done by aluminium line at 394.3414 nm. This way the magnesium emissions from different test pieces could be analysed and compared.

*Table 15. Averages and deviations of the aluminium and magnesium lines.*

| Test piece number | Al: 394.3414 nm | | | Al: 396.0554 nm | | |
|---|---|---|---|---|---|---|
| | Average | Standard deviation | Variability index | Average | Standard deviation | Variability index |
| | µW/cm² | | % | µW/cm² | | % |
| 1 | 57,87 | 26,54 | 45,87 | 75,51 | 35,47 | 46,97 |
| 2 | 78,62 | 35,82 | 45,57 | 103,84 | 47,61 | 45,85 |
| 3 | 58,25 | 45,07 | 77,38 | 77,51 | 61,48 | 79,32 |
| 4 | 80,99 | 34,03 | 42,01 | 108,68 | 46,35 | 42,65 |
| 5 | 75,00 | 43,05 | 57,40 | 99,41 | 57,65 | 57,99 |
| 6 | 103,78 | 54,88 | 52,88 | 137,58 | 72,04 | 52,36 |
| 7 | 83,89 | 38,63 | 46,05 | 111,48 | 52,17 | 46,80 |
| 8 | 84,23 | 36,60 | 43,45 | 112,49 | 49,30 | 43,82 |
| 9 | 79,91 | 44,39 | 55,54 | 105,20 | 58,73 | 55,83 |
| **Total** | **78,06** | **42,57** | **54,54** | **103,52** | **56,98** | **55,04** |
| **Test piece number** | **Mg: 383.4681 nm** | | | **Mg: 518.2147 nm** | | |
| | **Average** | **Standard deviation** | **Variability index** | **Average** | **Standard deviation** | **Variability index** |
| | **µW/cm²** | | **%** | **µW/cm²** | | **%** |
| 1 | 69,96 | 33,52 | 47,91 | 254,82 | 125,81 | 49,37 |
| 2 | 91,49 | 43,77 | 47,85 | 328,72 | 166,41 | 50,62 |
| 3 | 65,39 | 49,88 | 76,28 | 236,75 | 198,83 | 83,98 |
| 4 | 90,11 | 38,05 | 42,22 | 333,10 | 152,90 | 45,90 |
| 5 | 86,15 | 52,94 | 61,45 | 279,04 | 183,65 | 65,82 |
| 6 | 113,01 | 61,79 | 54,68 | 436,98 | 227,69 | 52,10 |
| 7 | 97,33 | 45,81 | 47,06 | 354,82 | 162,63 | 45,84 |
| 8 | 93,65 | 39,66 | 42,35 | 392,80 | 127,47 | 32,45 |
| 9 | 92,04 | 50,67 | 55,06 | 308,73 | 173,30 | 56,13 |
| **Total** | **88,79** | **48,69** | **54,83** | **325,08** | **181,38** | **55,80** |

The normalization showed desired results, as can be seen especially from figure 44. Without normalization the emissions had a very instable behaviour, but particularly the emissions of magnesium at 383.4681 nm were really stable after the emergence of the keyhole. It becomes clear from all the graphs of the emission intensities that the normalized emissions at the beginning of the welding process behave very instable and the absolute values are a bit lower than during subsequent welding. However, the obvious stability in figure 44 is a bit misleading, since the strong lines at the beginning skew the scale of the plot. Therefore, to illustrate the stability better, in figure 45, the first twenty pictures have been left out. From that figure it can be seen, that the stability is still on a much higher level than with the absolute values.

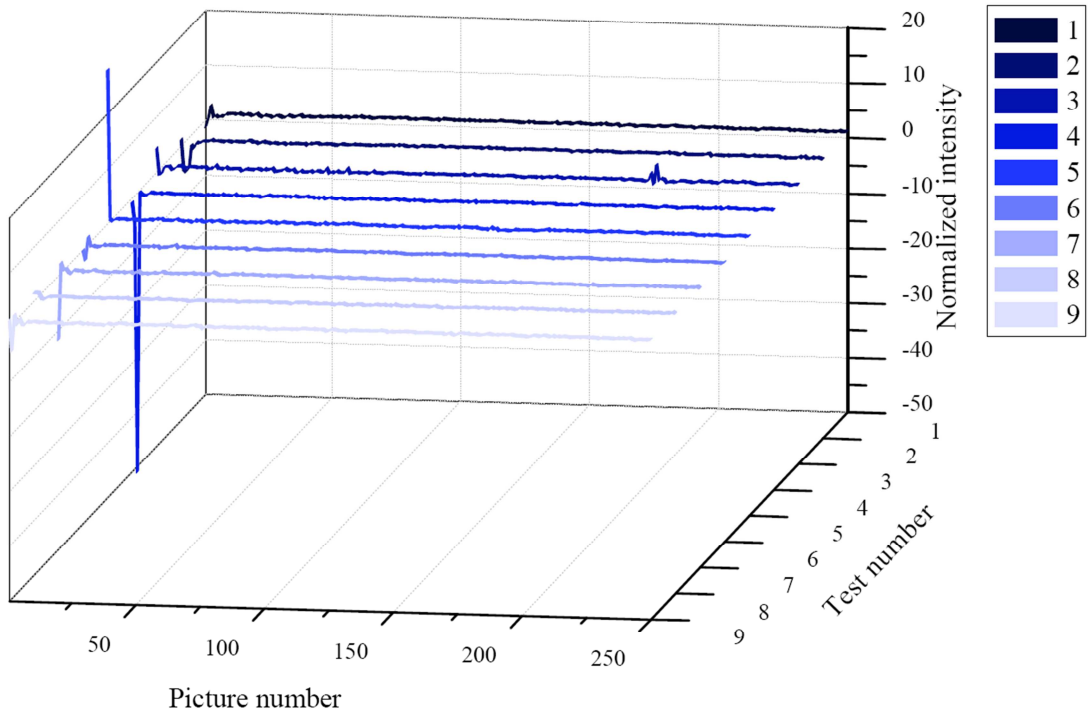


*Figure 44. Normalized emissions of the magnesium line at 383.4681nm.*

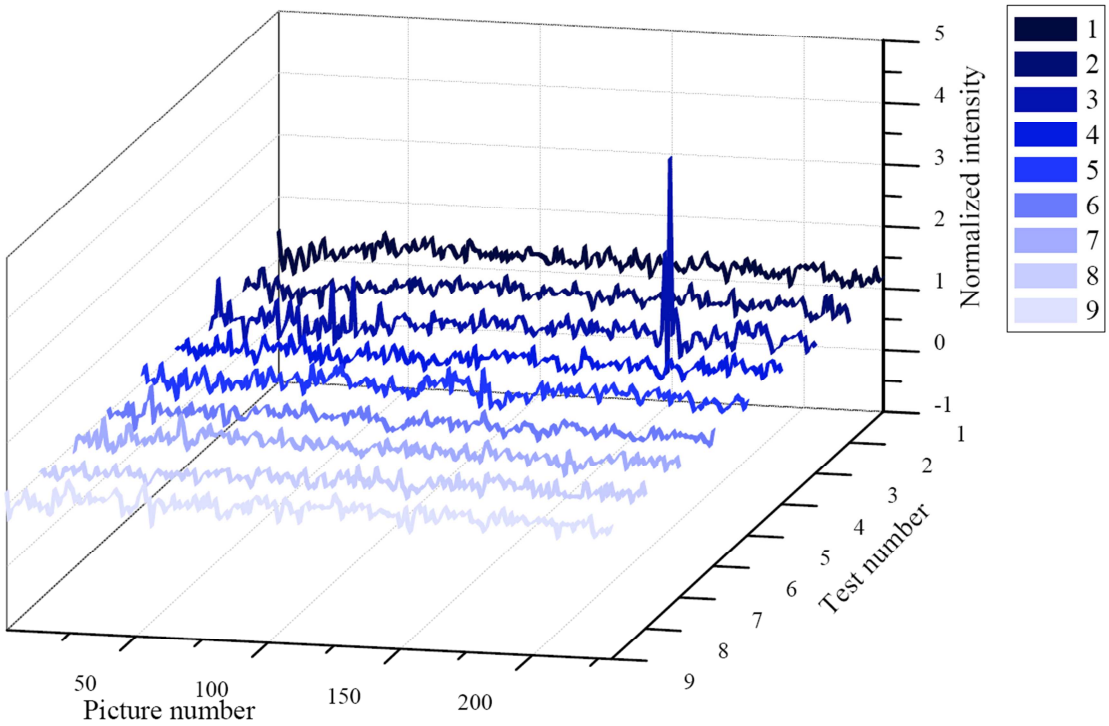


*Figure 45. Normalized emissions of the magnesium line at 383.4681 nm without the first 20 pictures.*

What is noteworthy in figures 44 and 45 is the fact that the intensities seem to stay quite still on same level. The same cannot be said from the figure 46, which represents the normalized intensities of the magnesium line at 518.2147 nm. The intensities are on a much higher level, which also makes it possible to hold more notable deviation. The line is very close to the lines of aluminium oxide which can have an effect on the intensities of magnesium. It can be that the changes in the amount of alumina emissions can create variance also in the magnesium emission line. The instable emissions of the beginning are also observable from figure 46. But their influence on the scale of the plot and on the detection of the stability of the subsequent emissions is not as significant as for the other wavelength.

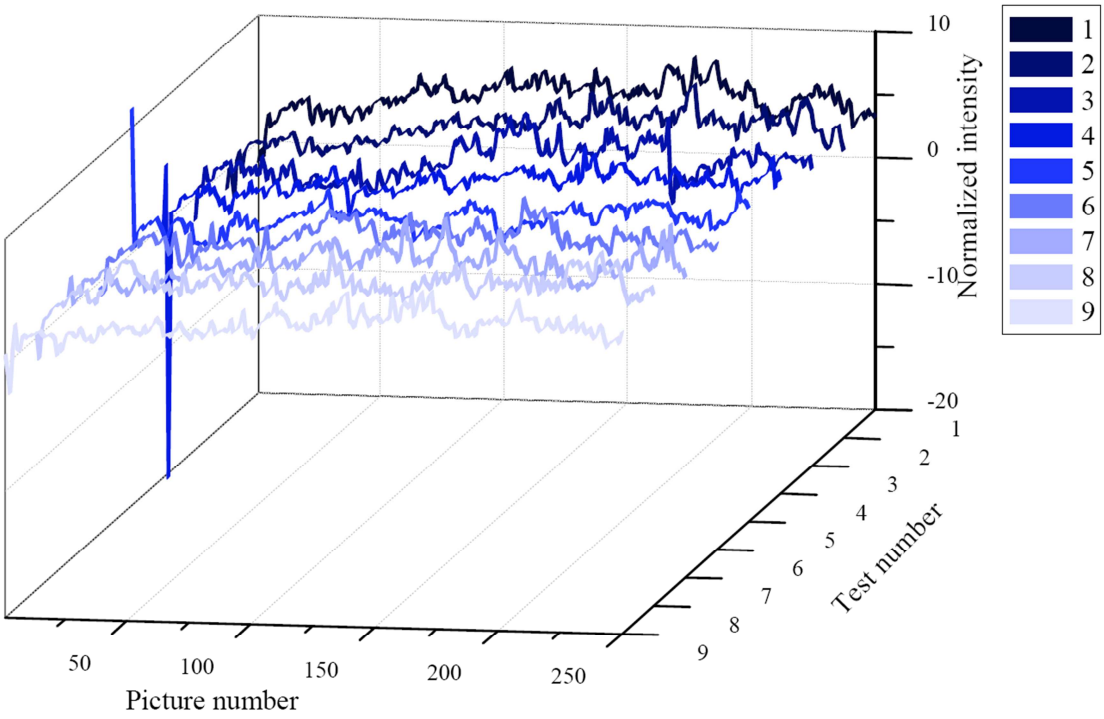


*Figure 46. Normalized emissions of the magnesium line at 518.2147 nm.*

Table 16 presents the normalized average intensities and their deviations of all the test pieces and in total. On the lower part of the table the first 20 pictures have been cut off to minimize the influence of the instable beginning of the welding process. The emissions in the beginning of the welding process are most likely strongly influenced by the emergence of the keyhole. Therefore, when the interest is in analysing the stability of the actual welding process and not the beginning, it would be wise to rule the early emissions out of the examination. As can be seen from the table, the deviation in total is fairly small. Also

the deviation seems to be quite the same from test piece to test piece, excluding the magnesium line at 383.4681 nm with all pictures. When comparing the figures 45 and 46, the more stable magnesium line is after all the one near the aluminium oxide emission lines at 518.2147 nm with only 3 % variability index during actual welding. But emissions of individual welds are still more stable at 383.4681 nm after eliminating the beginning. The strong deviations in some experiments, such as number 3 and 4, are caused by the instable emissions at the beginning of the process.

*Table 16. Averages and deviations of the normalized aluminium and magnesium lines.*

| Test piece number | Normalized Mg: 383.4681 nm | | | Normalized Mg: 518.2147 nm | | |
|---|---|---|---|---|---|---|
| | Average | Standard deviation | Variability index % | Average | Standard deviation | Variability index % |
| 1 | 1,19 | 0,23 | 19,74 | 4,24 | 1,36 | 32,18 |
| 2 | 1,08 | 0,60 | 55,88 | 3,98 | 1,54 | 38,56 |
| 3 | 1,13 | 0,35 | 31,31 | 3,47 | 1,61 | 46,29 |
| 4 | 0,87 | 3,40 | 391,98 | 3,90 | 2,03 | 52,03 |
| 5 | 1,23 | 1,71 | 138,82 | 3,40 | 1,21 | 35,52 |
| 6 | 1,07 | 0,23 | 21,43 | 4,10 | 1,21 | 29,56 |
| 7 | 1,11 | 0,82 | 74,16 | 4,19 | 1,35 | 32,27 |
| 8 | 1,12 | 0,12 | 10,90 | 4,86 | 1,22 | 25,09 |
| 9 | 1,13 | 0,37 | 33,09 | 3,75 | 1,20 | 31,93 |
| **Total** | **1,10** | **1,33** | **120,55** | **3,99** | **1,49** | **37,44** |
| **Test piece number** | **Without first 20 pictures** | | | **Without first 20 pictures** | | |
| | **Average** | **Standard deviation** | **Variability index %** | **Average** | **Standard deviation** | **Variability index %** |
| 1 | 1,21 | 0,12 | 10,00 | 4,43 | 1,15 | 26,04 |
| 2 | 1,16 | 0,11 | 9,88 | 4,22 | 1,31 | 31,09 |
| 3 | 1,13 | 0,27 | 23,58 | 3,61 | 1,57 | 43,54 |
| 4 | 1,11 | 0,11 | 9,43 | 4,15 | 1,02 | 24,69 |
| 5 | 1,13 | 0,12 | 10,93 | 3,48 | 1,06 | 30,56 |
| 6 | 1,09 | 0,09 | 8,26 | 4,27 | 1,03 | 24,09 |
| 7 | 1,16 | 0,10 | 8,73 | 4,37 | 1,24 | 28,39 |
| 8 | 1,13 | 0,10 | 8,56 | 5,07 | 0,93 | 18,34 |
| 9 | 1,16 | 0,11 | 9,84 | 3,92 | 1,04 | 26,54 |
| **Total** | **1,14** | **0,14** | **12,17** | **4,17** | **0,14** | **3,33** |

Some of the changes in the average emission levels can be explained by concentration changes in the base material. Table 11 shows the results of the measurements from the base material of the test pieces. It is clearly visible that the material was not at all homogenous.

In figure 47, the magnesium contents of the test pieces and the normalized intensities of the two magnesium lines are presented. In the figure also the standard deviations are shown. As it turns out, it seems that slight changes in the magnesium content in the base material have a significant impact on the emission levels. In the figure the instability of the welding process has been ruled out by normalization. That is why the changes in intensities should have been caused by some another factor. Heterogeneity of the material seems to be that factor. Especially the curve of the magnesium line at 518.2147 nm seems to follow the curve of the magnesium content quite accurately, excluding the last two test pieces. Those two experiments seem to be exceptions from the general trend. The high deviations on the intensity curves express the instable beginning of the welding process. As mentioned before, the magnesium concentration in the base material was measured with a spark-emission spectrometer.

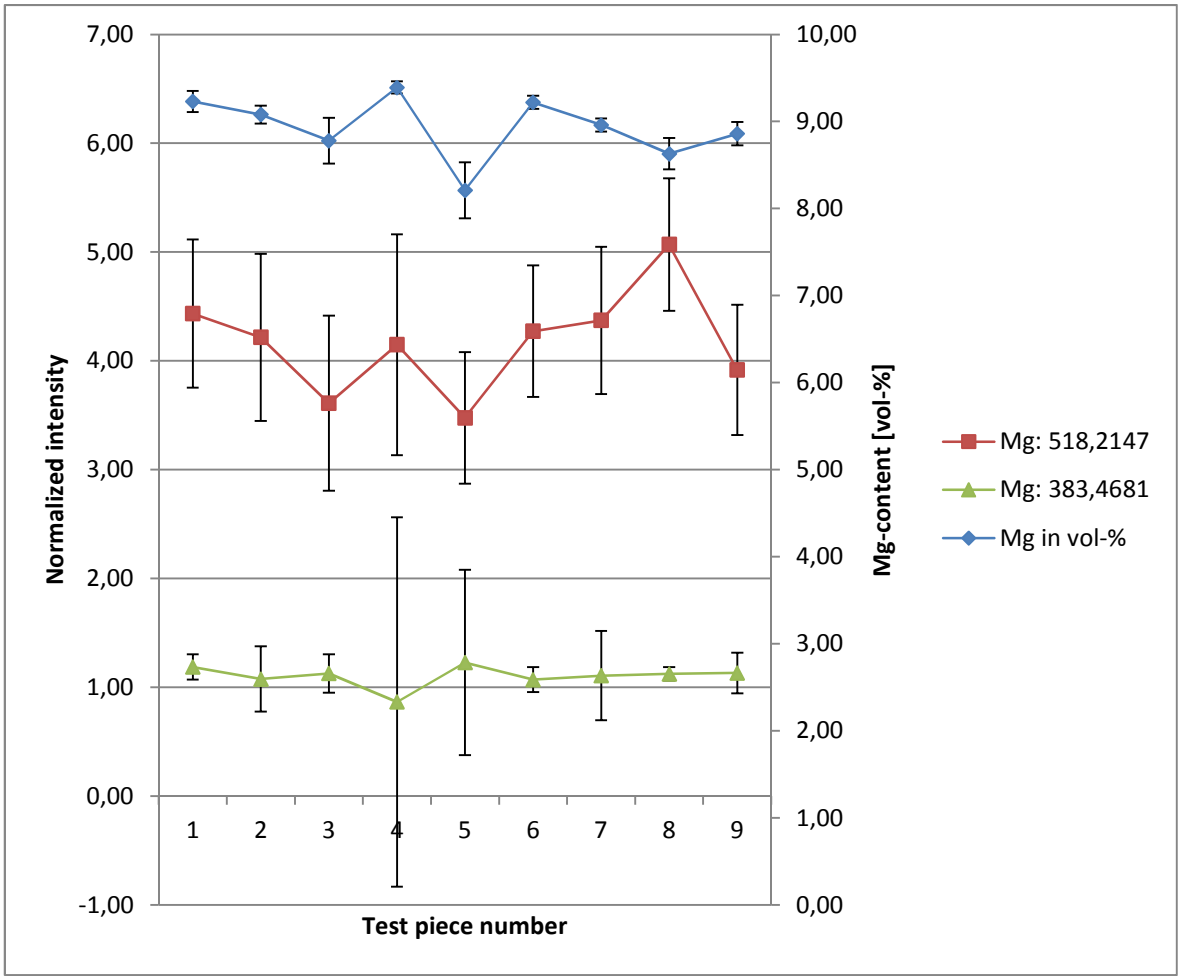


*Figure 47. Average normalized intensities of the two magnesium lines and the measured magnesium contents of each test piece.*

The emissions during one welding are presented in figure 48. The data for the figure are taken from the stability experiment number one. The parameters for that experiment can be seen from table 12. The figure shows the stability more illustratively. It is quite clearly visible, that there is much unsteadiness in the emissions. Also, there is no single specific point or frequency where the emissions would be significantly higher or lower than the average level, as determined before in context of analysing the emission lines of aluminium and magnesium.

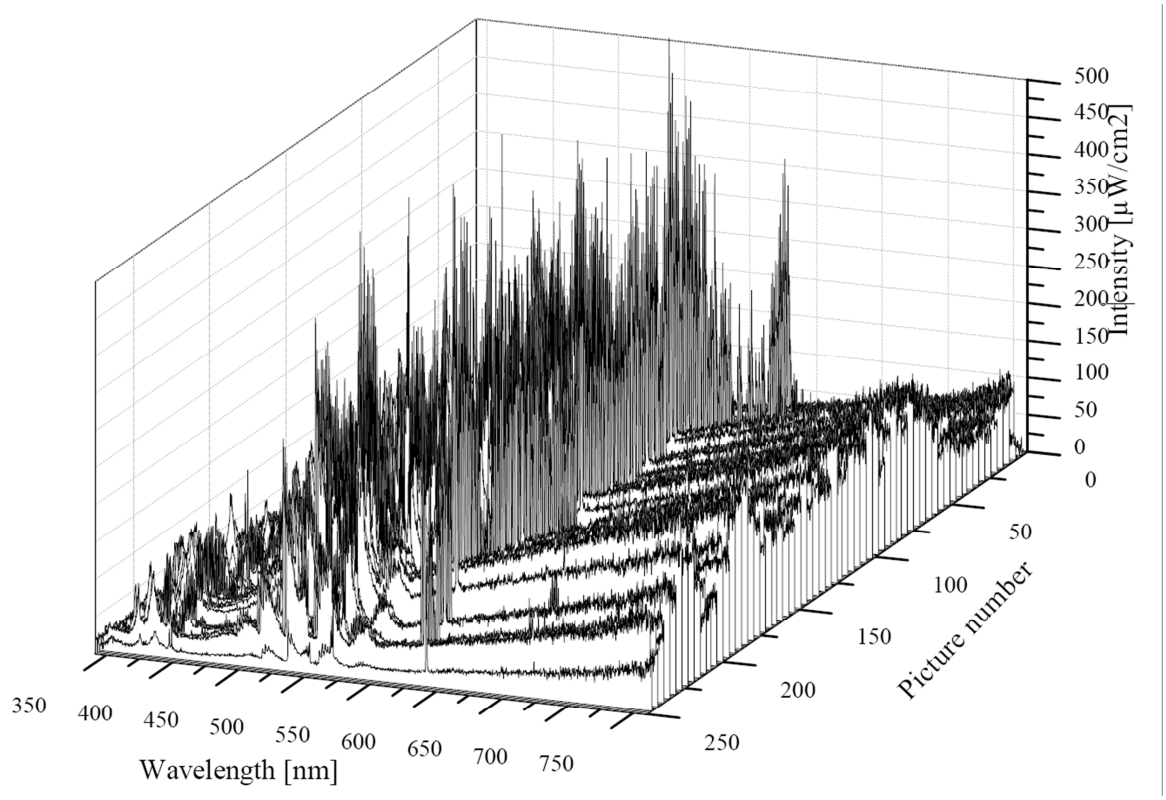


*Figure 48. Emissions of one welding process.*

Stability as a statistical measure is determined by Dietrich as the difference between the smallest and greatest value of the measured data (Dietrich & Schultze, 2002). Table 17 shows in conclusion that difference for all the tests individually and in total for the analysed wavelengths. The table shows the same information that was already observable in the deviations. The significantly higher difference in the magnesium line at 518.2147 nm is most probably caused by the aluminium oxide emission lines.

*Table 17. Stability of the analysed emissions.*

| Test number | Al: 394,3414 nm | Al: 396,0554 nm | Mg: 383,4681 nm | Mg: 518,2147 nm | Mg: 383,4681 nm (normalized) | Mg: 518,2147 nm (normalized) | Mg: 383,4681 nm (normalized) without beginning | Mg: 518,2147 nm (normalized) without beginning |
|---|---|---|---|---|---|---|---|---|
| | [µW/cm²] | | | | | | | |
| 1 | 134,64 | 182,67 | 182,00 | 573,63 | 3,92 | 9,13 | 0,73 | 6,11 |
| 2 | 197,86 | 268,10 | 205,64 | 651,62 | 5,99 | 9,74 | 0,69 | 6,48 |
| 3 | 262,26 | 343,23 | 245,24 | 1123,12 | 4,69 | 9,18 | 3,48 | 6,83 |
| 4 | 187,32 | 246,73 | 187,32 | 866,91 | 53,64 | 29,47 | 0,55 | 5,92 |
| 5 | 200,71 | 260,36 | 200,71 | 711,09 | 27,37 | 11,08 | 0,74 | 5,37 |
| 6 | 284,22 | 350,45 | 284,22 | 1123,01 | 4,15 | 8,54 | 0,73 | 6,16 |
| 7 | 201,04 | 269,45 | 224,70 | 741,40 | 14,07 | 7,58 | 0,68 | 6,71 |
| 8 | 251,37 | 335,87 | 277,90 | 863,51 | 1,09 | 9,65 | 0,51 | 5,20 |
| 9 | 222,34 | 280,27 | 246,45 | 822,39 | 6,62 | 9,02 | 0,68 | 5,88 |
| **all** | **284,88** | **352,20** | **417,83** | **1124,79** | **80,25** | **34,00** | **3,48** | **7,42** |

### 4.2.1 Repeatability of the stability tests

The tests for stability experiments were welded with identical parameters with the repeatability experiments. Only the material was different. Therefore, it was possible and useful to run repeatability analysis also for the emissions of the stability welding experiments. Unlike in stability analysis, in repeatability analysis only the average intensities of each experiment mattered. So, the standard deviation of the values presented in table 18 is calculated from the average intensities, not from all the intensities. As before, also here the analysis was done for both absolute and normalized intensities. All the percentage deviations of the absolute intensities presented in table 18 seem to remain between 15 % and 20 %. The deviation is significantly higher compared to the welding of standard material EN AW-6060. The high magnesium content and the fact that this material was custom made for research purposes may have had an influence on the instable emissions. The deviations of the normalized intensities are still quite low, which also suggests that there have been relatively big changes in base material compositions. The high deviation of the magnesium line at 518.2147 nm is probably due to the influence of the nearby aluminium oxide emission lines. The excluding of the first 20 pictures does not seem to have very positive effect on the repeatability of the magnesium emissions at 518.2147 nm. However, the excluding of the instable beginning of the welding experiment lowers the deviation of the magnesium emissions at 383.4681 nm significantly. Without the excluding, the percentual deviation of these magnesium emissions was a bit above nine percent, but with excluding the same emissions have a percentual deviation of only three percents. As mentioned before, the large amount of sparkles and smoke during welding may have had an influence on stability and also on the repeatability of these experiments done with this particular material with about 9 % magnesium by volume.

The statistical measure for repeatability is, according to Dietrich, standard deviation of the measured data (Dietrich & Schultze, 2002). So, the repeatability of stability experiments is shown in table 18.

*Table 18. Repeatability of the stability experiments.*

| Absolute values | | | | | | | | | | | | | |
|---|---|---|---|---|---|---|---|---|---|---|---|---|---|
| | Wave length | 1 | 2 | 3 | 4 | 5 | 6 | 7 | 8 | 9 | Average | Standard deviation | Variability index |
| | [nm] | [µW/cm²] | | | | | | | | | | | % |
| Aluminium lines | **394.3414** | 57.87 | 78.62 | 58.25 | 80.99 | 75.00 | 103.78 | 83.89 | 84.23 | 79.91 | **78.06** | **13.94** | **17.86** |
| | **396.0554** | 75.51 | 103.84 | 77.51 | 108.68 | 99.41 | 137.58 | 111.48 | 112.49 | 105.20 | **103.52** | **18.75** | **18.11** |
| Magnesium lines | **383.4681** | 69.96 | 91.49 | 65.39 | 90.11 | 86.15 | 113.01 | 97.33 | 93.65 | 92.04 | **88.79** | **14.19** | **15.99** |
| | **518.2147** | 254.82 | 328.72 | 236.75 | 333.10 | 279.04 | 436.98 | 354.82 | 392.80 | 308.73 | **325.08** | **64.42** | **19.82** |
| **Normalized values** | | | | | | | | | | | | | |
| | Wave length | 1 | 2 | 3 | 4 | 5 | 6 | 7 | 8 | 9 | Average | Standard deviation | Variability index |
| | [nm] | | | | | | | | | | | | % |
| Normalized magnesium lines | **383.4681** | 1.19 | 1.08 | 1.13 | 0.87 | 1.23 | 1.07 | 1.11 | 1.12 | 1.13 | **1.10** | **0.10** | **9.21** |
| | **518.2147** | 4.24 | 3.98 | 3.47 | 3.90 | 3.40 | 4.10 | 4.19 | 4.86 | 3.75 | **3.99** | **0.44** | **10.99** |
| Normalized without first 20 pictures | **383.4681** | 1.21 | 1.16 | 1.13 | 1.11 | 1.13 | 1.09 | 1.16 | 1.13 | 1.16 | **1.14** | **0.03** | **2.95** |
| | **518.2147** | 4.43 | 4.22 | 3.61 | 4.15 | 3.48 | 4.27 | 4.37 | 5.07 | 3.92 | **4.17** | **0.47** | **11.35** |

## 4.3 Loss of mass

It was noticed during analysing the results from the EDX-measurements that EDX is perhaps not suitable to measure small contents of a light element within material. The deviation of magnesium content was still quite strong, but after comparing the results from the weld to the results from the base material, the loss of magnesium was actually observable. The results of this comparison between the EDX measurements from the base material and from the weld are shown in table 19 and in figure 49.

The table 19 shows the average percentages of magnesium and their deviations in each test piece. The last column on the right represents the loss of magnesium, i.e. the amount of magnesium that vaporized during welding. The loss has no consistence and the number seems to vary from one tenth of a percentage unit to a whole percent. Of course, the test pieces with more magnesium had the capacity to lose more magnesium than the test piece of nominal magnesium content of 0 %, for instance. Nevertheless, loss of alloying

component, in this case magnesium, seems to happen during laser welding, and this loss may have unwanted consequences to the mechanical properties of the joint.

*Table 19. EDX-measurements from the test pieces welded in previous research.*

| | | Base material | | Weld | | Loss of magnesium | |
|---|---|---|---|---|---|---|---|
| Nominal magnesium content | Test piece number | Average | Deviation | Average | Deviation | Loss of magnesium | Percentual loss of magnesium |
| mass-% | | vol-% | vol-% | vol-% | vol-% | vol-% | |
| 0 | 1 | 0,62 | 0,17 | 0,46 | 0,01 | **0,16** | 26 % |
| 1 | 6 | 1,73 | 0,56 | 1,33 | 0,11 | **0,41** | 24 % |
| 2 | 8 | 2,36 | 0,80 | 1,61 | 0,24 | **0,76** | 32 % |
| 3 | 11 | 2,61 | 0,91 | 2,20 | 0,44 | **0,41** | 16 % |
| 4 | 16 | 3,18 | 1,22 | 2,75 | 0,30 | **0,43** | 13 % |
| 5 | 18 | 4,69 | 2,09 | 4,56 | 1,43 | **0,13** | 3 % |
| 6 | 20 | 6,74 | 2,29 | 5,75 | 1,61 | **1,00** | 15 % |
| 7 | 24 | 8,24 | 1,35 | 7,10 | 0,51 | **1,14** | 14 % |
| 8 | 27 | 9,01 | 0,72 | 8,74 | 0,17 | **0,28** | 3 % |
| 9 | 31 | 10,21 | 0,70 | 9,86 | 0,20 | **0,35** | 3 % |
| 10 | 34 | 11,41 | 2,35 | 10,60 | 0,71 | **0,81** | 7 % |

The data from the table 19 did not seem to have any consistence or any constant amount of lost magnesium. However, the same data plotted in figure 49 seems to behave rationally. The green triangles and error bars illustrate the data of the magnesium content in the base material. The purple crosses and error bars stand for the data from the weld. The distance between the two lines seems to grow when magnesium content gets higher. This makes sense: from large amount of some element the loss can also be larger than from smaller amount of that same element. The percentual loss of magnesium is however smaller in strong concentrations than in small concentrations as can be seen from table 19.

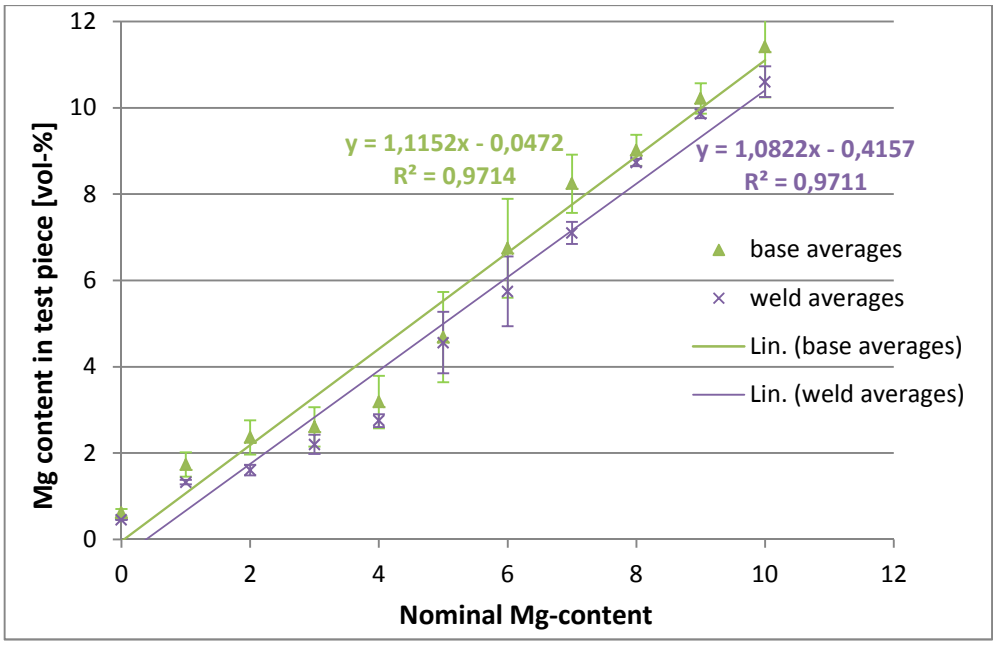


*Figure 49. The loss of mass from the test pieces welded earlier.*

## 4.4 Sensitivity experiments

The aim of the sensitivity experiments was to determine how sensitive the melt identification system is. The magnesium concentration in the weld seam was changed between the experiments by varying the filler wire feeding rate and welding speed as shown in table 7. The spectrometer monitored the welding experiments. It was presumed that some kind of change in the intensities of magnesium emissions should be observable. Only the magnitude and direction of the changes was uncertain. It was assumed that the intensities should follow the magnesium content in the weld. However, the content was difficult to estimate in beforehand, since the cross-sectional area of the weld was changing as a function of welding speed and filler wire feeding rate. The influence of these parameters was to be determined experimentally.

Figure 50 shows the normalized intensities of all the analysed magnesium and aluminium lines. The aluminium line at 394.3414 nm was the reference line in the normalization. This is the reason why this line has a normalized intensity of 1 throughout the experiments. The second aluminium line has a slight slop downwards which could be caused by numerous reasons. The slope of that curve is nonetheless relatively insignificant. That cannot be said of the two magnesium lines. Both emission lines seem to have significant changes. During

the planning phase of these experiments, the parameters were chosen to presumably increase the magnesium content in the weld. So, the assumption was that this increase would also be visible in the emissions. However, the increase is not that easily detected, especially the last two experiments seem to have descending trend in magnesium emissions. Nevertheless, the main trend of the magnesium emissions seems to be ascending.

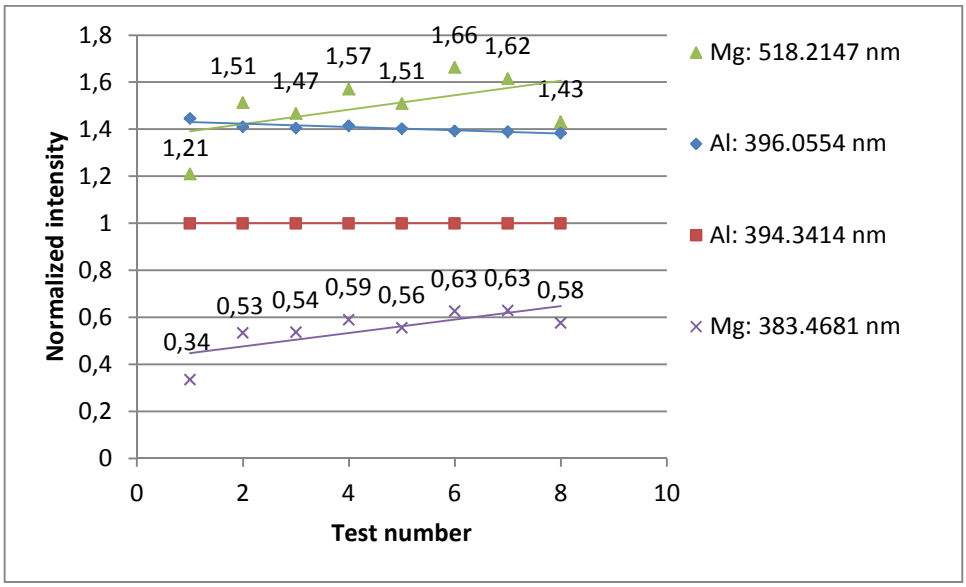


*Figure 50. The normalized intensities of the analysed emission lines.*

The nonlinearity in the magnesium emissions is most certainly caused by wrongly chosen parameters. The parameters were not changed evenly, but the welding speed was the same in three last experiments. The even increase in filler wire feeding rate still suggests that the magnesium content in the weld should have been increased. The energy input in laser welding comes mainly from the laser beam. The energy input can be changed by changing welding speed, but if welding speed stays the same, so does the energy input. If filler wire feeding rate is simultaneously increased, more energy is needed to melt and vaporize the extra material to produce excited metal vapour plume. So the descending slope of the last two experiments may have been caused by excessive material flow into the weld. While having to consume more energy for melting the material, the laser beam has less energy for the vaporization and excitation.

The two magnesium lines seem to have similar behaviour when reacting to the changes in welding parameters. The changes are stronger in magnesium line at 518.2147 nm, since the values are correspondingly higher. It can be said that magnesium line at 518.2147 nm shows more clearly the changes in magnesium content in the weld. However, this is true only to a certain point where the laser beam still has enough energy to vaporize material and thus produce excited metal vapour plume.

Another aspect of analysing the sensitivity experiments was to measure and calculate the magnesium contents in the welds of the experiments. Figure 52 shows the results of these measurements and calculations. The measurements of magnesium concentrations were done with a spark-emission spectrometer. The calculations were done with the equation given in (30). The areas of the weld cross sections were measured with a microscope and special measuring software. From the eight test pieces three samples were prepared for the area measurements. An average was then calculated for each experiment to be used in the calculations. Figure 51 shows the basic principle of the weld cross-sectional area measurements.

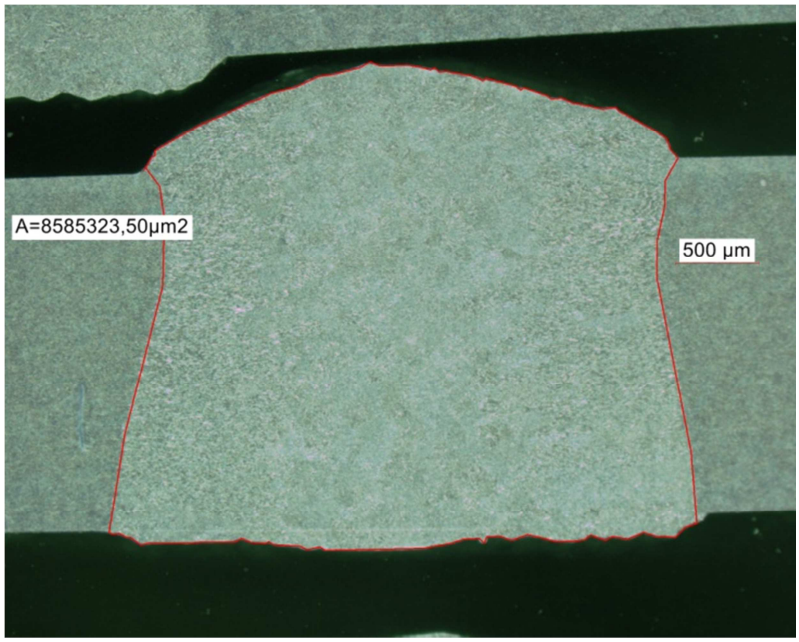


*Figure 51. Weld cross-sectional area measurement from the second sample of the fourth experiment*

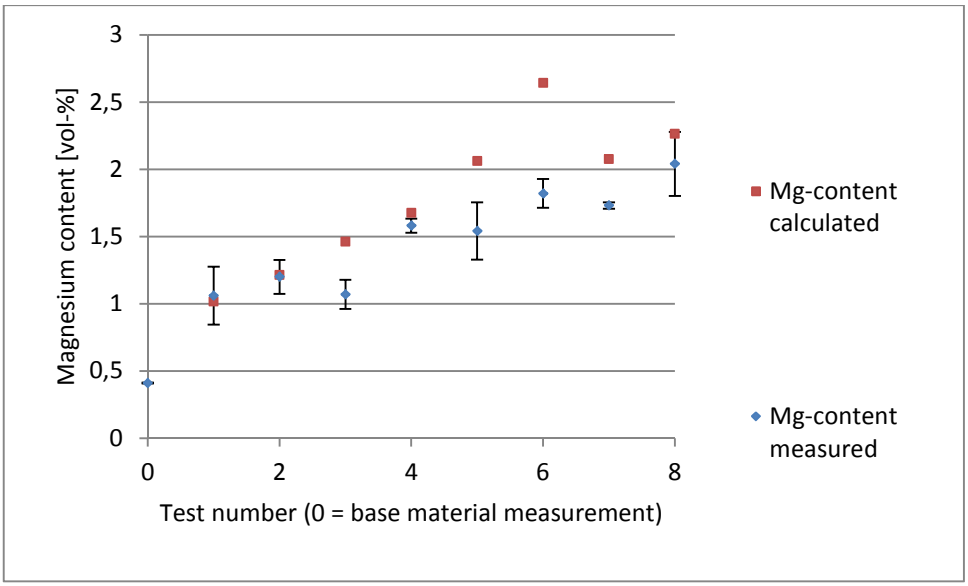


*Figure 52. Results from the measurements and calculations of the sensitivity test pieces.*

The most important thing to notice from figure 52 is that the loss of magnesium has been significant. The chosen parameters have had an exponential influence on the magnesium content in the weld, at least the first six experiments where the parameters were changed linearly. As noticed in analysing the emissions, also here both calculated and measured contents of the last two test pieces have lower magnesium contents than the sixth test piece. The reason for this surprising effect is probably that the volume of the weld grew bigger than predicted and the increase in weld area has a stronger influence in the magnesium content than the increase in filler wire feeding rate. Also the measurements from the weld cross-sectional areas may have been inaccurate, since the cross-section of a weld is rarely uniform throughout the lengths of a weld. Nevertheless, the influence of the weld cross sectional area cannot be underestimated. Figure 53 shows the results of the area measurements. As it turns out, the weld cross-sectional area has a significant change after the sixth test piece. Here the welding speed was no longer changed, but the filler wire feeding rate was increased. This has caused the cross-sectional area of the weld to increase.

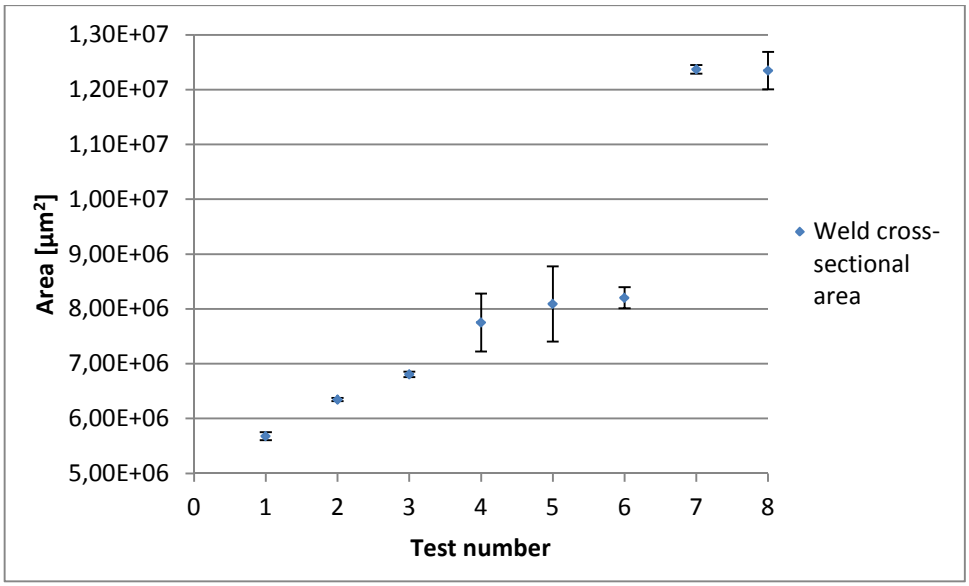


*Figure 53. Weld cross-sectional areas from sensitivity experiments.*

Combining these two results brings much more information about the sensitivity experiments. Figure 54 illustrates both magnesium contents and emissions and their relation. The numbers in the graph are the values of the measured magnesium content in the weld. The most interesting phenomenon is visible in the similarity of the magnesium emission at 518.2147 nm and the measured Mg-content. Also the emission intensities at 383.4681 nm seem to behave alike, but with smaller intervals. The steps in the measured Mg-contents may have also been influenced by measurement inaccuracy. One cannot rule out the possibility of an error in weld cross-sectional area measurements, either. The possibility of an error in these measurements was considerable, since the samples represented only the area in that particular point of the joint. And considering the instable behaviour of the welding process, the area of the weld may vary significantly. Nonetheless, it is quite clear that there is a strong relation between the magnesium emissions and the measured Mg-content in the weld. The measured and calculated Mg-content in the weld has a significantly higher value in the last experiment than in the second last experiment. Therefore, the decreasing of the emissions in the last experiment can be explained by excessive feeding of filler wire and thus insufficient vaporization, as explained before. Also the fairly mild vaporization of magnesium can be seen in the smaller loss of magnesium in the relation of calculated and measured contents. On the other hand, while the Mg-content rises to a certain point, so does the loss of magnesium due to vaporization.

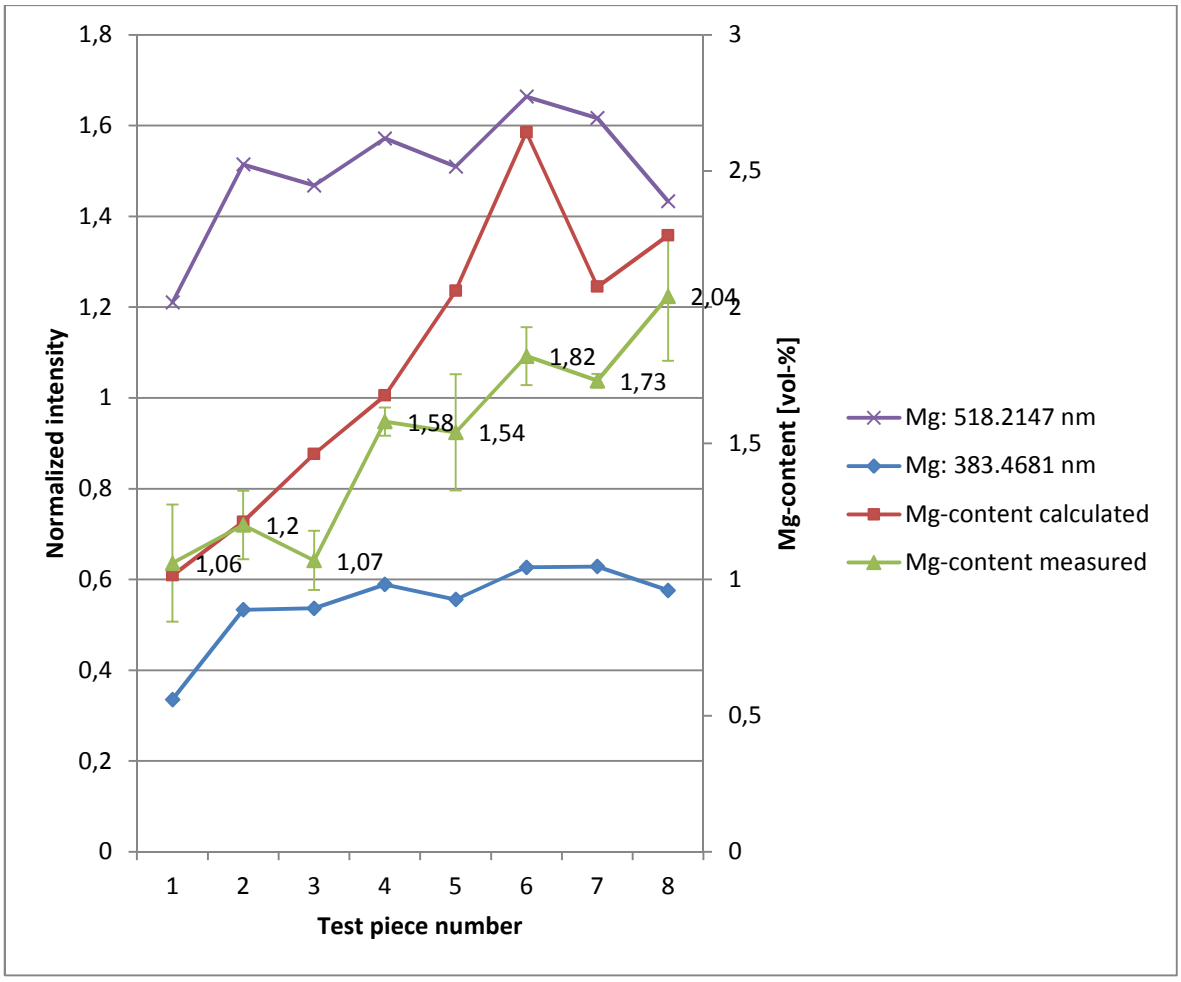


*Figure 54. Normalized intensities of the magnesium emission lines and measured and calculated Mg-contents of the sensitivity experiments.*

As a conclusion it can be said that the sensitivity of the melt identification system is very good. Figure 54 showed that the emissions of magnesium follow quite accurately the changes in magnesium concentrations of the base material. The intensities do not clearly inform the amount of magnesium or the amount of a change in concentration. The emission intensities tell however in which direction the change in concentration has happened. Figure 54 lets assume that when the filler wire feeding rate is not excessive, the melt identification system is sensitive enough to detect a change from 1.2 % to 0.7 % by volume. This represents the sensitivity to detect changes of 0.5 % by volume.

# 5 DISCUSSION

One of the goals set at the beginning of this thesis was to clarify the reason why detection of silicon has not been successful in previous researches. It was found that the required energies for the excitation of the main emission lines of silicon are so high, that the energy input in laser welding is not enough. This study was conducted only in theory, but practical experiments should also be done. This could be carried out with a spectrometer with greater sensitivity or with lasers of higher output power.

It was noticed during the analysis of the results from the experiments that there is much potential in spectroscopic monitoring of welding process. The only metallurgical aspect of analysis in this thesis was the study about loss of mass. Although direct relation between the process emissions and the loss of alloying components were not found, the data gained in monitoring the process had significance in other fields. Especially the statistical analysis of the emissions proved to be practical. There were three points of view in statistical analysis: stability, repeatability and sensitivity. The stability of the measuring system and process emissions was to be determined from absolute intensities and from normalized intensities. The stability analysis concentrated in examining the deviations of the intensities during the welding process. It was a bit surprising how instable the emissions are during one process and how the intensities can vary considerably from test to test. Perhaps the most important finding in statistical analysis was the significance of normalization. Once the normalizing was done by a constant aluminium line, the stability of magnesium rose to a much higher level. Also the normalization revealed the instable emissions at the beginning of a welding process. It was deduced that the instability was due to the emergence of a keyhole and plasma. The only useful information found in analysing the emissions in absolute intensities of one process was that there is no stability or continuance or even any periodic inconsistencies in the emissions.

While the absolute intensities seemed to have insignificant stability, the normalized intensities of magnesium were quite even throughout the measuring process. It was even noticed that this kind of monitoring method is surprisingly good in detecting composition changes in base material. As shown in figure 47, the emissions of magnesium followed well the changes in magnesium content in base material. Both magnesium lines are useful

for this purpose, but more noticeable is the line at 518.2147 nm. The material used in the stability experiments had magnesium about 9 % by volume, which is relatively much. Therefore, significant changes were observable also in the emission line at 383.4681 nm. Both magnesium lines have their complications. The line at 518.2147 nm is positioned right next to the aluminium oxide emission lines. This close positioning can easily distort the emissions of magnesium. The problem with the other emission line is that to react to the changes in the process or in the base material, there has to be enough magnesium. The low intensity of this line causes the observing of the changes to be rather difficult. When the intensities of these two emission lines are put on to a same scale, the lower wavelength can seem to be quite flat and even, but the higher wavelength has some significant changes. Therefore, to obtain some significant results from magnesium line at 383.4681 nm, the base material needs to have enough magnesium to start with.

The repeatability experiments were made with standard material EN AW-6060, but also with the results from stability experiments, repeatability analysis was conducted. During the analysis of these experiments it was noticed that repeatability of emission measurements is on a relatively high level. Repeatability analysis was also conducted for both absolute and normalized intensities. The analysis showed that with absolute values, the magnesium emissions represent the unstableness of the whole process; they do not give sufficient information specifically about magnesium. However, aluminium lines are a better way to analyse the changes in the measurement process between experiments. In fact, the changes in magnesium emissions proved out to be entirely different. After normalization, the true nature of magnesium emissions became apparent. So, if the goal is in observing especially magnesium emissions, normalizing is vital, but in monitoring the whole process, absolute magnesium emissions describe the process quite well, but aluminium emissions even better.

Perhaps the most useful and developable results were achieved by the sensitivity experiments. The experiments were conducted with changing parameters. Decreasing welding speed and increasing filler wire feeding rate gave expected and hoped results. By changing the magnesium content in the weld, the magnesium emissions could be altered. Although the alterations were not always congruent with the changes in parameters, the general trend of the magnesium emissions was as expected. Another positive finding was the relation of measured magnesium contents and emission intensities. It was shown in

figure 54 that especially magnesium line at 518.2147 nm follows quite well the measured magnesium content. Also the measured and calculated magnesium contents in the weld explained the phenomenon that was visible in lowered magnesium emissions of the last two experiments. The high filler wire feeding rate caused the energy of the laser beam to be consumed in melting, so less energy was left for the vaporization and plasma formation. The big differences and inconsistencies between measured and calculated Mg-contents could have been caused by measurement errors in spark-emission spectroscopic measurements or in microscopic measurements. The microscopic measurements were done to determine the area of the weld cross-section. However, dimensions of a weld are rarely constant, especially when feeding filler wire, so the possibility of measurement error here is rather high.

Loss of mass experiments were done in two stages. At the first stage, the test pieces welded earlier were measured with EDX-method from weld and base material. At the second stage, the test pieces from sensitivity experiments were measured with a spark-emission spectrometer. In both cases the magnesium content was the main interest. From the results of the both measurements same kind of conclusions were made: loss of magnesium was clear. Especially interesting was the almost constant amount of lost magnesium that was observed in EDX measurements. The feeding of filler wire had positive effects in increasing magnesium content in the weld. However, the control of the added magnesium was rather difficult due to complicated control of parameters like volume of the weld. But the information gained from the sensitivity experiments gives promising results. It seems that feeding filler wire, magnesium content in the weld can be increased, but the parameters should be tested and set in beforehand. Figure 55 shows the correlation of the two measurements of lost magnesium. The horizontal axis represents the magnesium content without vaporization. Although the approximated linear trend lines are not parallel, the set of points of the sensitivity experiments is positioned right where it should be.

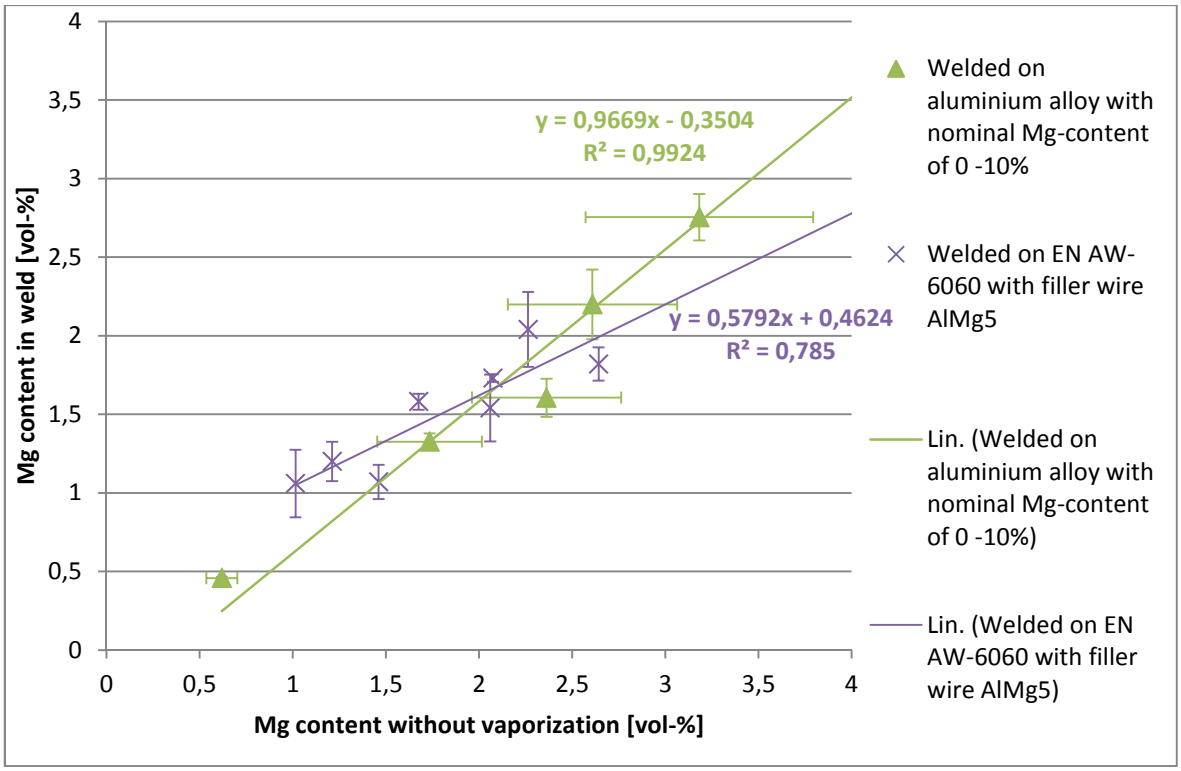


*Figure 55. Correlation of measurements from aluminium alloyed with magnesium and aluminium that was welded with filler wire.*

# 6 CONCLUSION AND PROSPECTS

Aluminium alloys are categorized by alloying elements. In this research only one alloy was used, EN AW-6060, which had magnesium and silicon as the main alloying components. This paper concentrated on analysing laser deep penetration welding from the aspect of magnesium. One of the goals of this research was to find out why silicon has not been detected in the emission spectrum of the welding process. The results showed that the energy input of the used laser welding equipment is not enough to excite silicon atoms enough to show in the spectrum.

The statistical analysis brought many new results from monitoring laser deep penetration welding process with a spectrometer. The current software was not able to save more than 250 spectra. In the future, to get more information of the emissions, the software should be modified so that the number of saved spectra would not be limited. Also monitoring emissions of other alloying components would be useful, naturally with a different

spectrometer. During the experiments done in this research, the emissions behaved extremely unstably. Stability analysis could be extended to attempt to find welding parameters that may have an effect on the stability of the emissions. It would be most useful also to determine, what kind of an effect stability of emissions would have on metallurgical quality of the weld. According to the results gained in this research, absolute intensities should only be used to analyse the total stability of the process, not only one particular elemental emission line. The use of normalized intensities is mostly in analysing stability and repeatability of a certain alloying component. Recording of emissions should also be optimized so that the beginning of the welding process would not skew the spectra, if the beginning is not the specific interest.

The conclusion from stability and repeatability experiments was that the repeatability of the measuring process is relatively good, but stability does not reach the same level. Although normalizing of magnesium emissions brought better results, the utilization of that data is not directly possible. Some research must still be made before adapting stability analysis into practice. For instance, more precise and suitable measuring device for measuring the whole elemental content of a test piece would bring valuable information of the correlation between emissions during welding and content of that corresponding element in the material. Analysis for sensitivity requires even more research in the future. The data and results gained here are vital, but more information for spectral analysis is still needed. For example, the repeatability of welding with filler wire and influence of different parameters should be clarified. Such parameters are filler material, feeding rate, welding speed, shielding gas and positioning of filler wire. To gain maximal benefit from feeding the filler wire, the right parameters should be found. This way the loss of elemental components could be avoided.

The welding experiments in this research consisted only of straight joints. The material was in every experiment constant. Future researches should also concentrate in analysing emissions from welds of more complex geometries. Also hybrid joints, such as steel - stainless steel, should be studied. The rate of dilution and its definition in spectral analysis would be useful to determine.

The goal setting for this thesis stated that statistical data and support for the used monitoring system should be determined. This was conducted in series of experiments and

followed by statistical calculations and analysis. The statistical terms, stability, repeatability and sensitivity, were determined. To gain more information of sensitivity of the monitoring setup, more experiments with similar parameters should be made. From the results of this research it can be said that the used spectrometer can detect relatively well elemental changes in the weld, also in small contents.

**REFERENCES**


Ahasi Spectra USA Inc., 2010. *Optical Filters*. [Online] Available at: www.ahasi-spectra.com [Accessed 27 October 2010].

Aragón, C. & Aguilera, J.A., 2008. *Characterization of laser induced plasmas by optical emission spectroscopy: A review of experiments and methods*. Elsevier B.V.

Avantes, 2010. *Spectrometers*. [Online] Available at: www.avantes.com [Accessed 27 October 2010].

Beyer, E., 1985. *Einfluss des laserinduzierten Plasmas beim Schweissen mit CO2-lasern*. Doctoral Thesis. Darmstadt: Technische Universität Darmstadt.

Black, A. & Copley, S., 2010. Laser Technology for Materials Processing. *Advanced Materials & Processes*, Vol 168(No 1), pp.31-32.

Cobine, J.D., 1941. *Gaseous Conductors*. First Edition ed. New York, United States of America: McGraw-Hill Book Company, Inc.

Cremers, D.A. & Radziemski, L.J., 2006. *Handbook of Laser-Induced Breakdown Spectroscopy*. Chichester, West Sussex, England: John Wiley & Sons, Ltd.

Dahotre, N.B. & Harimkar, S.P., 2008. *Laser Fabrication and Machining of Materials*. New York, New York, United States of America: Springer Science.

Dietrich, S., 2009. ISSN 1431-6226 *Sensoriken zur Schwerpunktslagebestimmung der optischen Prozessemissionen baim Laserstrahltiefschweißen*. Doctoral Thesis. Erlangen-Eltersdorf: Meisenbach Verlag Bamberg Friedrich-Alexander-Universität Erlangen-Nürnberg.

Dietrich, E. & Schultze, A., 2002. *Statistische Verfahren zur Maschinen- und Prozessqualifikation*. 4th ed. Munich, Germany: Hanser.

Ehlers, B., 2001. Welding with Diode Lasers. In J.F. Ready, ed. *Handbook of Laser Materials Processing*. 1st ed. Orlando, United States of America: Laser Institute of America. Ch. 10.3.9. pp.348-50.

EN ISO 18273:2007. Welding consumables - Wire electrodes, wires and rods for welding aluminium and aluminium alloys - Classification (ISO 18273:2004). Standard.

EN 573-3:2007. Aluminium and aluminium alloys - Chamical composition and form of wrought products - Part 3: Chemical composition and form of products. Standard.

Galmed, A.H. & Harith, M.A., 2008. Temporal follow up of the LTE conditions in aluminium laser induced plasma at different laser energies. *Applied Physics B, Lasers and Optics*, 91(4), p.652.

Gebhardt, A., 2001. Laser Welding with Filler Wire. In J.F. Ready, ed. *Handbook of Laser Materials Processing*. 1st ed. Orlando, United States of America: Laser Institute of America. Ch. 11.3.8. pp.400-04.

Glasschröder, J., 2010. *Integration von Prozess- und Fabrikplanung im Gesamtkonzept der Digitalen Fabrik*. Master's Thesis. München: Technische Universität München.

Gnanamuthu, D., 2001. Describtion of Penetration Welding. In J.F. Ready, ed. *Handbook of Laser Materials Processing*. 1st ed. Orlando, United States of America: Laser Institute of America. Ch. 11.1. pp.361-63.

Green, L., 2001. Monitoring laser beam performance. *The Fabricator*, 31(2), pp.38-40.

Greses, J., Hilton, P.A., Barlow, C.Y. & Steen, W.M., 2001. Spectroscopic studies of plume/plasma in different gas environments. In *20th International Congress on ICALEO 2001: Applications of Lasers & Electro-Optics*. Jacksonville, 2001.

Haferkamp, H., 2004. Joining. In R. Poprawe, H. Weber & G. Herziger, eds. *Advanced Materials and Technologies · Laser Physics and Applications · Laser Applications*. 1st ed. Springer-Verlag. Ch. 2.4. pp.137-57.

Havrilla, D., 2009. Laser welding update. *Practical Welding Today*, 13(6), pp.10-12.

Ion, J.C., 2005. *Laser Processing of Engineering Materials*. Amsterdam, Netherlands: Elsevier Ltd.

Jäger, M., Humbert, S. & Hamprecht, F.a., 2008. Sputter Tracking for the Automatic Monitoring of Industrial Laser-Welding Processes. *IEEE Transactions on industrial electronics*, 55(5), pp.2177-84.

Kaplan, A., 2009. Metallurgy of Welding and Hardening. In J.M. Dowden, ed. *The Theory of Laser Materials Processing*. 1st ed. Dordrecht, Netherlands: Springer Science+Business Media B.V. pp.217-33.

Katayama, S., Nagayama, H., Mizutani, M. & Kawahito, Y., 2009. Fibre laser welding of aluminium alloy. *Welding International*, 23(10), pp.744-52.

Kugler, T.R., 2001. Fusion Front Penetration. In J.F. Ready, ed. *Handbook of Laser Materials Processing*. 1st ed. Orlando, United States of America: Laser Institute of America. Ch. 10.1.4. p.311.

Kujanpää, V., Salminen, A. & Vihinen, J., 2005. *Lasertyöstö*. 1st ed. Tampere, Finland: Teknologiainfo Teknova Oy.

Laserline, 2010. *High-Power Diode Lasers*. [Online] Available at: http://www.laserline-inc.com/diode-laser-material-processing.php [Accessed 9 December 2010].

Mackwood, A.P. & Crafer, R.C., 2004. *Thermal modelling of laser welding and related processes: a literature review*. Elsevier Ltd.

Mason, R.L., Gunst, R.F. & Hess, J.L., 2003. *Statistical Design and Analysis of Experiments*. 2nd ed. Hoboken, New Jersey, United States of America: John Wiley & Sons Inc.

Mathers, G., 2002. Material standards, designations and alloys. In *The welding of aluminium and its alloys*. 1st ed. Abington Cambridge, England: Woodhead Publishing Limited. pp.35-45.

Mohamed (2), W.T.Y., 2007. *Improved LIBS limit of detection of Be, Mg, Si, Mn, Fe and Cu in aluminum alloy samples using a portable Echelle spectrometer with ICCD camera*. Elsevier Ltd.

Mohamed, W.T.Y., 2007. Fast LIBS Identification of Aluminum Alloys. *Progress in Physics*, 3(2), pp.87-92.

NIST, 2010. *NIST Atomic Spectra Database Lines Form*. [Online] Available at: http://physics.nist.gov/PhysRefData/ASD/lines_form.html [Accessed 30 October 2010].

Ohnesorge, A., 2008. *Bestimmung des Aumischungsgrades beim Laser-Pulver-Auftragschweißen mittels laserinduzierter Plasmaspektroskopie (LIPS)*. Doctoral Thesis. Dresdner: Technische Universität Dresdner.

Paschotta, R., 2010. *Encyclopedia of Laser Physics and Technology*. [Online] Available at: http://www.rp-photonics.com/encyclopedia.html [Accessed 14 May 2010].

Pedrotti, F.L., Pedrotti, L.M. & Pedrotti, L.S., 2007. *Introduction to Optics*. 3rd ed. Upper Saddle River, New Jersey, United States of America: Pearson Education, Inc.

Popov, A.M., Labutin, T.A. & Zorov, N.B., 2009. Application of Laser-Induced Breakdown Spectrometry. *Moscow University Chemistry Bulletin*, 64(6), pp.366-77.

Precitec Group, 2011. *Process Monitoring*. [Online] Available at: http://www.precitec.com/index.html [Accessed 21 February 2011].

Ready, J.F., 2001. Conducion Welding. In J.F. Ready, ed. *Handbook of Laser Materials Processing*. 1st ed. Orlando, United States of America: Laser Institute of America. Ch. 10.0. p.307.

Schittenhelm, H., 2000. *Diagnostik des laserinduzierten Plasmas beim Abtragen und Schweißen*. 1st ed. München, Germany: Herbert Utz Verlag GmbH.

Scitec Instruments, 2008. *M2 Factor (Quality Factor)*. [Online] Available at: http://www.scitec.uk.com/lasers/m2_factor.php [Accessed 17 May 2010].

Sibillano, T., Ancona, A., Berardi, V. & Lugarà, P.M., 2009. A Real-Time Spectroscopic Sensor for Monitoring Lase Welding Process. *Sensor*, vol. 9(5), pp.3376-85.

Skupin, J., 2004. *Nichtlinear dynamisches Modell zum Laserstrahlschweißen von Alminiumlegierung*. Doctoral Thesis. Bremen: Universität Bremen.

Solarz, R.W., 2001. High-Power Diode Lasers for Materials Processing. In J.F. Ready, ed. *Handbook of Laser Materials Processing*. 1st ed. Orlando, United States of America: Laser Institute of America. Ch. 2.5.4. pp.64-66.

Statistics Finland, 2007. *Tilastokeskus - Verkkokoulu*. [Online] Available at: http://www.stat.fi/tup/verkkokoulu/ [Accessed 12 October 2010].

Steen, W.M., 2003. *Laser Material Processing*. 3rd ed. London, England: Springer-Verlag London Limited.

Trautmann, A., 2009. ISBN 978-3-8316-0876-8 *Bifocal Hybrid Laser Welding*. Doctoral Thesis. München: Herbert Utz Verlag Technische Universität München.

Ullmann, C. & Eltze, A., 2001. High Power Diode Lasers: New Possibilities in Welding Techniques. In M. Geiger & A. Otto, eds. *Laser Assisted Net Shape Engineering 3*. 1st ed. Erlangen, Germany: Meisenbach-Verlag Bamberg. pp.637-44.

Wandera, C., 2010. ISBN 978-952-214-973-2 *Performance of high power fibre laser cutting of thick-section steel and medium-section aluminium*. Phd Thesis. Lappeenranta: Digipaino Lappeenranta University of Technology.

Zhai, H. & DebRoy, T., 2003. Macroporosity free aluminum alloy weldments through numerical simulation of keyhole mode laser welding. *Journal of Applied Physics*, 93(12), pp.10089-97.

Zäh, M.F., Gebhard, P., Huber, S. & Ruhstorfer, M., 2008. Bifocal Hybrid Laser Beam Welding and Friction Stir Welding of Aluminium Extrusion Components. In Weinert, K. et al., eds. *Flexible Manufacture of Lightweight Frame Structures*. Zurich, 2008. Trans Tech Publications.

# FIGURES

# TABLES